



**POLITECNICO**  
MILANO 1863

# Attitude Control of a Solar Sail

Written by Enol Vilchez Llamazares

Tutored by James Douglas Biggs

Final Thesis Bachelor's Degree

February 2018

## Content

1.	State of the art .....	7
1.1.	History of the Solar Sail .....	7
1.2.	Current situation of the control of the Solar Sails.....	7
2.	Introduction .....	9
3.	Dynamics of the Solar Sail .....	10
3.1.	Abstract .....	10
3.2.	Reference frame.....	10
3.3.	Euler's Rotational Equations of Motion .....	11
3.3.1.	External torques .....	12
3.4.	Solar Radiation Pressure .....	12
3.4.1.	Solar Radiation Pressure Model .....	12
3.4.2	Solar Radiation Pressure Torque .....	14
3.5.	Euler's Rotational Equations of Motion considering flexible appendages .....	15
4.	Rotational Kinematics of the Solar Sail .....	17
4.1.	Direction Cosine Matrix.....	17
4.2.	Euler Angles.....	18
4.3.	The Euler Parameters or Quaternions .....	19
4.3.1.	Kinematic differential equations with quaternions .....	21
4.4.	Error function – Quaternion Error.....	21
5.	Implemented controls.....	23
5.1.	Quaternion Error proportional control using Reaction Wheels as actuator.....	24
5.1.1.	Study of stability of the control.....	25
5.1.2.	Block diagram .....	25
5.2.	Sliding mode control .....	26
5.2.1.	Implementation of the control.....	27
5.3.	PD control plus a term which considers the flexible dynamics.....	28
5.3.1.	Study of stability.....	29
5.4.	Improvement of the controller; output feedback controllers .....	29
5.5.	Nonlinear state observer control .....	30
5.5.1.	Modelling of the disturbance .....	30
5.5.2.	Implementing the control .....	31
6.	Calculation of the Moments of Inertia of the Solar Sail.....	32
6.1.	Why to calculate them? .....	32

6.2.	Solar Sail model using Solid Works .....	32
6.2.1.	Design of the Solar Sail .....	32
6.2.2.	Calculation of the moments of Inertia .....	35
7.	Study of the effects of flexibility in the Spacecraft .....	37
7.1.	Results for a non-flexible spacecraft.....	37
7.2.	Flexible Spacecraft study.....	38
7.2.1.	First attempt; change the nature of the movement of the flexible appendages	38
7.2.2.	Second attempt; change the magnitude of the movement of the flexible appendages .....	40
7.3.	Results of Flexible Spacecraft.....	41
7.4.	Verdict .....	43
8.	Comparison of the flexible disturbance using different controls .....	45
8.1.	Influence of the modal variables into the flexible disturbance .....	45
8.2.	Action of the controllers in the reduction of the Flexible disturbance .....	45
8.3.	Final comparison and corollary .....	49
9.	Simulation and Results .....	51
9.1.	Results for each control .....	51
9.2.	Graphic results on each control implemented.....	56
9.3.	Ranking of the controllers and final selection.....	75
10.	Conclusions .....	79
11.	Bibliography .....	81
	Annex 1: Quaternion Error proportional control using CMG as actuator.....	83

## List of Figures

Figure 1 . L1 Lagrangian point .....	10
Figure 2 Solar Radiation Pressure Force Diagram .....	14
Figure 3 Point of incidence of the rays of the Sun .....	15
Figure 4 Reference frames .....	17
Figure 5 Block diagram of the Quaternion Error Proportional control .....	26
Figure 6 Sliding mode objective function.....	26
Figure 7 Front view of the solar sail .....	33
Figure 8 Side view of the solar sail .....	33
Figure 9 Control stucture of the solar sail.....	34
Figure 10 Antenna of the Solar Sail .....	34
Figure 11 3D view of the solar sail .....	36
Figure 12 Angular Velocity vs time using Quaternion Error control with non-flexible spacecraft .....	37
Figure 13 Quaternion Error vs time using Quaternion Error control with non-flexible spacecraft .....	37
Figure 14 Control torque vs time using Quaternion Error control with non-flexible spacecraft	38
Figure 15 Angular Velocity vs time using Quaternion Error control with a flexible spacecraft..	41
Figure 16 Quaternion Error vs time using Quaternion Error control with a flexible spacecraft.	42
Figure 17 Control Torque vs time using Quaternion Error control with a flexible spacecraft....	42
Figure 18 Modal Coordinate Variable vs time using Quaternion Error control with a flexible spacecraft.....	43
Figure 19 Total velocity of the flexible appendages vs time using Quaternion Error control with a flexible spacecraft .....	43
Figure 20 Flexible disturbance using Quaternion Error control.....	46
Figure 21 Closer look of the flexible disturbance using Quaternion Error control .....	46
Figure 22 Flexible disturbance using Nonlinear state observer control obtaining data of the angular velocities from a Quaternion Error controller .....	47
Figure 23 Closer look of the flexible disturbance using Nonlinear state observer control obtaining data of the angular velocities from a Quaternion Error controller .....	47
Figure 24 Flexible disturbance using Nonlinear state observer control having an own calculation of the angular velocities .....	47
Figure 25 Closer look for the flexible disturbance using Nonlinear state observer control having an own calculation of the angular velocities.....	47
Figure 26 Flexible disturbance using Flexible control .....	48
Figure 27 Closer look to the flexible disturbance using Flexible control .....	48
Figure 28 Flexible disturbance using Flexible control with output feedback controllers .....	49
Figure 29 Closer look to the flexible disturbance using Flexible control with output feedback controllers .....	49
Figure 30 Block diagram of the simulation .....	51
Figure 31 Angular Velocity vs time with Quaternion Error Control using gains: $k_p=50$ , $k_{qe}=4$ ..	56
Figure 32 Quaternion Error vs time with Quaternion Error Control using gains: $k_p=50$ , $k_{qe}=4$	56
Figure 33 Control Torque vs time with Quaternion Error Control using gains: $k_p=50$ , $k_{qe}=4$ ....	57

Figure 34 Total Velocity of the flexible appendages with Quaternion Error Control using gains  $k_p=50, k_{qe}=4$  ..... 57

Figure 35 Modal state variable vs time with Quaternion Error Control using gains:  $k_p=50, k_{qe}=4$  ..... 57

Figure 36 Precision error vs time with Quaternion Error Control using gains:  $k_p=50, k_{qe}=4$  .... 57

Figure 37 Angular Velocity vs time with vs time with Quaternion Error Control using gains:  $k_p=80, k_{qe}=15$  ..... 58

Figure 38 Quaternion Error vs time with Quaternion Error Control using gains:  $k_p=80, k_{qe}=15$  ..... 58

Figure 39 Control Torque vs time with Quaternion Error Control using gains:  $k_p=80, k_{qe}=15$ .. 58

Figure 40 Total velocity of the flexible appendages vs time with Quaternion Error Control using gains:  $k_p=80, k_{qe}=15$ ..... 59

Figure 41 Modal coordinate variable vs time with Quaternion Error Control using gains:  $k_p=80, k_{qe}=15$ ..... 59

Figure 42 Precision Error vs time with Quaternion Error Control using gains:  $k_p=80, k_{qe}=15$  .. 59

Figure 43 Angular velocity vs time with sliding mode control using gains:  $k_p=50, k_{qe}=4$ ..... 60

Figure 44 Quaternion Error vs time with sliding mode control using gains:  $k_p=50, k_{qe}=4$  ..... 60

Figure 45 Control Torque vs time with sliding mode control using gains:  $k_p=50, k_{qe}=4$  ..... 60

Figure 46 Total velocity of the flexible appendages vs time with sliding mode control using gains:  $k_p=50, k_{qe}=4$ ..... 61

Figure 47 Modal coordinate variable vs time with sliding mode control using gains:  $k_p=50, k_{qe}=4$ ..... 61

Figure 48 Precision error vs time with sliding mode control using gains:  $k_p=50, k_{qe}=4$  ..... 61

Figure 49 Angular velocity vs time with nonlinear state observer control (1) using gains:  $k_p=50, k_{qe}=4$ ..... 62

Figure 50 Quaternion Error vs time with nonlinear state observer control (1) using gains:  $k_p=50, k_{qe}=4$ ..... 62

Figure 51 Control Torque vs time with nonlinear state observer control (1) using gains:  $k_p=50, k_{qe}=4$ ..... 62

Figure 52 Total Velocity of the flexible appendages vs time with nonlinear state observer control (1) using gains:  $k_p=50, k_{qe}=4$  ..... 63

Figure 53 Modal coordinate variable vs time with nonlinear state observer control (1) using gains:  $k_p=50, k_{qe}=4$ ..... 63

Figure 54 Precision Error vs time with nonlinear state observer control (1) using gains:  $k_p=50, k_{qe}=4$ ..... 63

Figure 55 Angular Velocity vs time with Flexible Control using gains:  $k_p=450, k_{qe}=125$  ..... 64

Figure 56 Quaternion Error vs time with Flexible Control using gains:  $k_p=450, k_{qe}=125$ ..... 64

Figure 57 Control Torque vs time with Flexible Control using gains:  $k_p=450, k_{qe}=125$  ..... 64

Figure 58 Total velocity of the flexible appendages vs time with Flexible Control using gains:  $k_p=450, k_{qe}=125$ ..... 64

Figure 59 Modal Coordinate Variable vs time with Flexible Control using gains:  $k_p=450, k_{qe}=125$ ..... 65

Figure 60 Precision Error vs time with Flexible Control using gains:  $k_p=450, k_{qe}=125$ ..... 65

Figure 61 Angular Velocity vs time with Flexible Control Estimation with output feedback controllers using gains:  $k_p=50$ ,  $k_{qe}=4$  ..... 65

Figure 62 Quaternion Error vs time with Flexible Control Estimation with output feedback controllers using gains:  $k_p=50$ ,  $k_{qe}=4$  ..... 66

Figure 63 Control Torque vs time with Flexible Control Estimation with output feedback controllers using gains:  $k_p=50$ ,  $k_{qe}=4$  ..... 66

Figure 64 Total Velocity of the Flexible Appendages vs time with Flexible Control Estimation with output feedback controllers using gains:  $k_p=50$ ,  $k_{qe}=4$  ..... 66

Figure 65 Modal Coordinate Variable vs time with Flexible Control Estimation with output feedback controllers using gains:  $k_p=50$ ,  $k_{qe}=4$  ..... 67

Figure 66 Precision Error vs time with Flexible Control Estimation with output feedback controllers using gains:  $k_p=50$ ,  $k_{qe}=4$  ..... 67

Figure 67 Angular Velocity vs time with Flexible control estimation with output feedback controllers using gains:  $k_p=80$ ,  $k_{qe}=15$  ..... 67

Figure 68 Quaternion Error vs time with Flexible control estimation with output feedback controllers using gains:  $k_p=80$ ,  $k_{qe}=15$  ..... 68

Figure 69 Control Torque vs time with Flexible control estimation with output feedback controllers using gains:  $k_p=80$ ,  $k_{qe}=15$  ..... 68

Figure 70 Total Velocity of the flexible appendages vs time with Flexible control estimation with output feedback controllers using gains:  $k_p=80$ ,  $k_{qe}=15$  ..... 68

Figure 71 Modal Coordinate Variable vs time with Flexible control estimation with output feedback controllers using gains:  $k_p=80$ ,  $k_{qe}=15$  ..... 69

Figure 72 Precision Error vs time with Flexible control estimation with output feedback controllers using gains:  $k_p=80$ ,  $k_{qe}=15$  ..... 69

Figure 73 Angular Velocity vs time with Quaternion Error Control using gains:  $k_p=1200$ ,  $k_{qe}=60$  ..... 70

Figure 74 Quaternion Error vs time with Quaternion Error Control using gains:  $k_p=1200$ ,  $k_{qe}=60$  ..... 70

Figure 75 Control Torque vs time with Quaternion Error Control using gains:  $k_p=1200$ ,  $k_{qe}=60$  ..... 70

Figure 76 Total Velocity of the Flexible Appendages vs time with Quaternion Error Control using gains:  $k_p=1200$ ,  $k_{qe}=60$  ..... 70

Figure 77 Modal Coordinate Variable vs time with Quaternion Error Control using gains:  $k_p=1200$ ,  $k_{qe}=60$  ..... 71

Figure 78 Precision Error vs time with Quaternion Error Control using gains:  $k_p=1200$ ,  $k_{qe}=60$  ..... 71

Figure 79 Angular Velocity vs time with Nonlinear state observer control (2), using gains:  $k_p=1200$ ,  $k_{qe}=60$  ..... 71

Figure 80 Quaternion Error vs time with Nonlinear state observer control (2), using gains:  $k_p=1200$ ,  $k_{qe}=60$  ..... 72

Figure 81 Control Torque vs time with Nonlinear state observer control (2), using gains:  $k_p=1200$ ,  $k_{qe}=60$  ..... 72

Figure 82 Total Velocity of the flexible Appendages vs time with Nonlinear state observer control (2), using gains:  $k_p=1200$ ,  $k_{qe}=60$  ..... 72

Figure 83 Modal Coordinate Variable vs time with Nonlinear state observer control (2), using gains: $k_p=1200$ , $k_{qe}=60$ .....	73
Figure 84 Precision Error vs time with Nonlinear state observer control (2), using gains: $k_p=1200$ , $k_{qe}=60$ .....	73
Figure 85 Angular Velocity vs time with Flexible control estimation with output feedback controllers using gains: $k_p=1200$ , $k_{qe}=60$ .....	73
Figure 86 Quaternion Error vs time with Flexible control estimation with output feedback controllers using gains: $k_p=1200$ , $k_{qe}=60$ .....	74
Figure 87 Control Torque vs time with Flexible control estimation with output feedback controllers using gains: $k_p=1200$ , $k_{qe}=60$ .....	74
Figure 88 Total Velocity of the Flexible Appendages vs time with Flexible control estimation with output feedback controllers using gains: $k_p=1200$ , $k_{qe}=60$ .....	74
Figure 89 Modal Coordinate Variable vs time with Flexible control estimation with output feedback controllers using gains: $k_p=1200$ , $k_{qe}=60$ .....	75
Figure 90 Precision Error vs time with Flexible control estimation with output feedback controllers using gains: $k_p=1200$ , $k_{qe}=60$ .....	75
Figure 91 Block diagram of the Quaternion Error proportional control using CMG as actuator	83

## List of Tables

Table 1 Change of the nature of the movement of the flexible appendages .....	39
Table 2 Change of the magnitude of the movement of the flexible appendages .....	41
Table 3 Rank of the controls in relation with the flexible disturbance performance .....	50
Table 4 Time of convergence and precision performance of each control .....	55
Table 5 Control Torque Requirements Performance of each control.....	55
Table 6 Global Rank of the Performance of each Control.....	77

## 1. State of the art

### 1.1. History of the Solar Sail

From a scientific point of view the dawn of the Solar Sail implementation can be placed in the 1920s. When the Russian scientists Konstantin Tsiolkovsky and Friedrich Arturowisch Zander noted that a very thin sheet in space would be able to achieve high speeds propelled by solar-light pressure. Afterwards, Carl Wiley in 1951 and Richard Garwin in 1958 published the first technical papers about solar sails of the modern era. In fact, Garwin was the first one to use “solar sailing” applied to space vehicles.

Subsequently there were several studies and works related with the solar sail, but the lack of a material light enough impeded the realization of this new idea. Years later, with the discovering of new and stronger materials the idea of solar sailing became stronger. In the 90s and the 00s new important studies were realised by Japan, Europe and US. Specially the Japanese space agency (JAXA) and NASA have given big importance to the solar sail option for space exploration and utilization. Several trials of sails deployment in vacuum chambers were performed by ESA and NASA during the first years of the 21th century. Also, JAXA achieved a successful sail-unfurlment test from a sub-orbital rocket.

All these achievements have become important steps into the development of the concept of the solar sail. But in the year 2010 one success marked a milestone in the progress of the solar sail as an operational in-space propulsion system. JAXA accomplished the unfurling of the IKAROS solar sail technology demonstrator in the interplanetary space between the solar orbits of Earth and Venus. That spacecraft demonstrated that the sail could be used for controlling its own attitude relative to the Sun and for interplanetary propulsion. On the other part, NASA succeed in the launching and unfurling of the Nanosail-D2. This spacecraft was created to demonstrate that the solar sails could be unfurled in low orbits to work as parachute and accelerate the atmospheric re-entry of carrier rockets and obsolete satellites attached to them.

Those events show that it exists a myriad of possible applications of this new technology and the solar sail could be the new base of technology of the near-future spacecrafts.

### 1.2. Current situation of the control of the Solar Sails

Every new spacecraft implemented has to possess a control to perform a proper activity. In the actual spacecrafts traditional methods including reaction wheels and propellant ejection are used to perform the control. However current implementations of the Solar Sails like IKAROS are using cutting-edge control methods.

IKAROS uses a reflective control device (RCD) to perform a control attitude of the solar sail. The basic idea is to change the optical properties electronically, then having different solar radiation pressure torque used to perform the control of the spacecraft. To accomplish this change of the optical properties a peculiar material is used. The sail is recovered by PDLC films, which consist in liquid crystal microdroplets diffused in a polymer matrix. The liquid crystal droplets are optically birefringent while the polymer is an optically isotropic material. If there is not an



electric field, the optical axes of individual bipolar droplets align randomly, thence having different refractive indices across the film.

Apart from the current implementations of the control of solar sails, like IKAROS one, there is a great amount of theoretical studies to find the most appropriate way to control the solar sail. As some examples, in 2007 Bong Wie and David Murphy studied the attitude dynamic modelling and control profoundly considering a solar sail as a rigid body with different attitude control actuators. Also, in 2005 Stephanie Thomas and Michael Paluszek considered the flexible dynamics. Then a passive attitude control criterion for an axisymmetric solar sail with a general SRP model was studied by Xiaosai Hu in 2014. Then Shengping Gong and Junfeng Li in 2014 studied the spin-stabilized control method for a sailcraft in a displaced solar orbit. The stability was studied for the coupled attitude/orbit dynamics.

All these studies show that there is a growing of interest in the control of the solar sails. This new technology must mature, and all those studies are beneficial to provide knowledge and achieve a better performance of this new technology in the near-term future.

## 2. Introduction

Attitude coordinates are a batch of coordinates  $\{x_1, x_2, \dots, x_n\}$  that completely define the orientation of a rigid body in relation with a reference frame. In the case of this study, to completely determine the attitude of the Solar Sail, it has been used a set of three angles (Euler angles: roll, pitch, yaw  $\{\Phi, \Theta, \Psi\}$ ) that describe the attitude of a reference frame  $\beta$  (Body Frame) with respect to an inertial frame  $\mathcal{N}$ .

To have a proper behaviour in the space, every spacecraft must control its own attitude. Therefore, have a knowledge of the attitude of the spacecraft and restrict non-desirable movements that can cause a bad movement of the spacecraft, with the possibility to lose the authority of the attitude of the spacecraft. To avoid this situation, every spacecraft has to own a control calculation and an actuator which provides this control.

The aim of this work is to find a proper control with an appropriate actuator for a conventional squared solar sail. This research will consider different types of control, conventional ones and others up-to-date. Focusing in the benefits that provide the usage of more modern controls. Also, it will be studied the effect that creates the presence of the flexibility using a conventional control. The solar sail is normally a very big spacecraft; therefore, little flexibility of the structure can cause appreciable effects in the solar sail. Finally, this work is aimed to be a background for a future study and behave as a tool to make deeper studies in the future.

This study focuses to find the most beneficial control of a Solar Sail situated in the L1 Lagrange point. Several controls will be implemented in this work to find the most suitable one. From the most generic ones, like the Quaternion Error Control or the Sliding Mode Control, to the most specialized ones, like the PD control plus a term considering flexible appendages with output feedback controllers. A comparison of the performance of each of the controls will be made reaching a final selection of the most proper control.

Furthermore, it will be studied the performance of each control in reducing the effects of the disturbance in the control due to the flexibility. And a selection of the most suitable control will be made.

### 3. Dynamics of the Solar Sail

#### 3.1. Abstract

The dynamics of an object express the behaviour of this object in relation with a reference frame. The movement of a spacecraft changes depending of the point of reference selected. Then the election of a proper reference point, thus a proper reference frame, is crucial to have a knowledge of the behaviour of an object in the space.

#### 3.2. Reference frame

To select a proper reference frame, it is needed to have a first knowledge of the position of the spacecraft during this study. Then the first assumption must be decided; where it will be the spacecraft at each time. In other words, mainly thanks to Kepler, which in which orbit will be the spacecraft.

In this case, it has been selected the L1 Lagrange point in a  $0^{\circ}$  of inclination. This orbit has very nice properties that benefit a lot in particularly the Solar Sail. The L1 point is always between the Sun and the Earth in its same relative position. Therefore, there not exist any possibility of an eclipse of the Earth to the Solar Sail. Of course, other planets, like Mercury or Venus, will make some little eclipses to the Solar Sail, but in this first study it won't be considered. Then it is selected a simple case scenario where the rays of the Sun will impact on the Solar Sail during all the year.

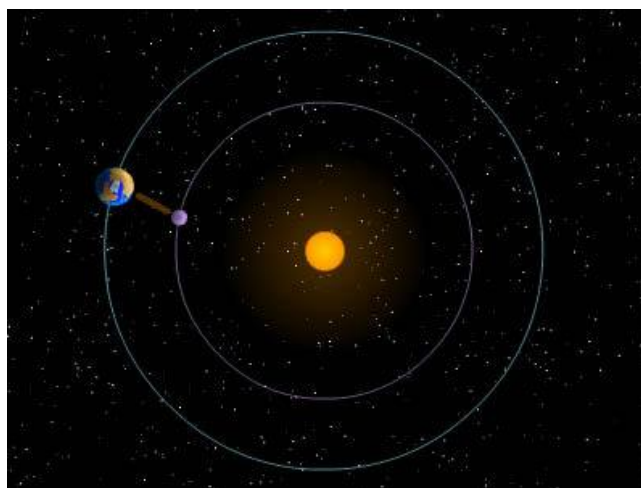


Figure 1 . L1 Lagrangian point

It has been selected an inertial frame as the reference of the body frame. The solar sail will remain in the Lagrangian Point L2, meaning that its motion with respect to the Sun is relatively slow; hence it can be considered that the solar sail is fixed in the Space while it is correcting its attitude. Then the error made using the inertial frame as a reference frame is negligible.

Once the position of the Solar Sail is selected, the next step it will be to which point it will need to be referenced. In this case there are two basic options; the Sun and the Earth as origins of the reference frame. It has been selected the Sun as the origin of the reference frame. Basically, for two reasons, first the sun is in essence the provider of energy of the Solar Sail, then it has way more importance than the Earth. The second one is more important, the relative position of the Sun related with the Solar Sail is mainly the same in the time when the control is implemented (1-week maximum). Then it can be stated that the Sun is fixed in the space during the control of the Solar Sail. Therefore, this assumption gives the possibility to select the **Inertial Reference frame with the Sun as the origin of the centre of reference**. Moreover, considering this reference frame the dynamic equations calculation and the kinematics calculation will be way simpler. Avoiding then changes of reference frames and the errors and complexity that can cause a change of the reference frame.

### 3.3. Euler's Rotational Equations of Motion

The Euler's Rotational Equations of Motion are an ensemble of differential equations that describe the rotational motions of a rigid body with respect to its centre of mass. They are the principal and basic tool to be able to control any spacecraft.

Those equations come from the *principle of conservation of the angular momentum*  $\vec{H}$  of a rigid body respect to its centre of mass. The basic idea is that the angular momentum is conserved (then able to control) if the total external torque acting on the object is zero. For a detailed explanation of the steps made to arrive to the Euler's Rotational Equations of Motion it is recommended to visit the following bibliography [14].

Now there are presented the Euler's Rotational Equations of Motion:

$$J\dot{\vec{\omega}} + \vec{\omega} \times J\vec{\omega} = \vec{M} \quad (1)$$

Then for a principal-axis reference frame the Euler's equation become:

$$J_1\dot{\vec{\omega}}_1 - (J_2 - J_3)\vec{\omega}_2\vec{\omega}_3 = \vec{M}_1 \quad (2)$$

$$J_2\dot{\vec{\omega}}_2 - (J_3 - J_1)\vec{\omega}_3\vec{\omega}_1 = \vec{M}_2 \quad (3)$$

$$J_3\dot{\vec{\omega}}_3 - (J_1 - J_2)\vec{\omega}_1\vec{\omega}_2 = \vec{M}_3 \quad (4)$$

In the equations (2), (3), (4) it has decomposed the Euler's equations of the body frame with respect to the Inertial frame. Therefore, usually the angular velocity  $\vec{\omega}$  is expressed as  $\vec{\omega}_{B/N}$ . Furthermore, those three equations (2), (3), (4) are coupled, nonlinear ordinary differential equations for the angular velocity  $\vec{\omega}_1, \vec{\omega}_2, \vec{\omega}_3$  of a rigid body.  $\vec{M}_1, \vec{M}_2, \vec{M}_3$  are the external torques acting on the body about its centre of mass. And  $J_1, J_2, J_3$  are the principal moments of inertia of the spacecraft referring to the its centre of mass.

### 3.3.1. External torques

The objective of the attitude control is to create a torque to counteract the external torque. In fact, the spacecraft loses its desired attitude because an external force is “pushing” or “pulling” the spacecraft in a non-desired direction.

There are many different torques influencing the spacecraft in the Space. For example, the gravitational attraction of other planets, the magnetic torque disturbance of other planets, solar windmills, solar storms, aerodynamic drag (if the spacecraft is close enough to the Earth) ... But the most persistent disturbance which causes a major torque on the Solar Sail is the Solar Radiation Pressure Force. Other disturbances like the gravitational attraction of the Earth or the Magnetic disturbance have a minor effect on the spacecraft in this particular case. Remember that the Solar Sail is situated in the L1 point. Approximately 1495978 km. The noticeable effects of the magnetic disturbance of the Earth on the spacecraft are when the spacecraft is inside the Van Allen radiation belts. The Van Allen belts exist up to 60000 km above the Earth way below than the position of the Solar Sail, therefore in the situation of the Solar Sail the effects of the magnetic field will be negligible.

On the other hand, the effect of the gravitational attraction of the Earth is counteracted by the effect of gravitational attraction of the Sun in the L1 Lagrange Point. Therefore, there is no need to consider any major perturbation due to gravitational effects.

## 3.4. Solar Radiation Pressure

The Solar Radiation Pressure is the key factor for the implementation of the Solar Sail. It is the essence of the creation of motion of the Solar Sail. But, in the attitude control point of view, the Solar Radiation Pressure is the principal inconvenient, the main disturbance. So, it is indispensable to have a good idea of what is it and how does it affect to the spacecraft.

Imagine an existent sail in the sea. The basic idea of how it is propelled is the action-reaction force. The wind “pushes” the sail. In other words, the particles of air collide the sail and transfer their momentum to the sail. Therefore, giving a force to the sailcraft that permits the movement. Analogously happens to the solar sail concept. The particles of sun (photons) collide into the sail of the spacecraft. Those photons transfer their momentum to the sail, creating a reaction force in the opposite direction of the reflected photons.

In the case of the sailing on the sea it exists a friction force between the sailcraft and the water and the sailcraft and the air that impedes to reach very high velocities. But in the Space, there is mainly non-friction! Thus, for the case of the solar sail it is possible to reach very high velocities. Thanks to the constant solar force exerted by the Sun there is a constant acceleration that increases the velocity drastically within a period of time large enough.

### 3.4.1. Solar Radiation Pressure Model

There are different types of models of the Solar Radiation Pressure. For example, models based on the specular reflection and reflectivity of the material of the sail. In this case it has been

selected a more generic model. It considers a flat Lambertian surface located at 1 astronomical unit from the Sun. Thence it is a quite acceptable model for this study.

In this section the solar sail will be assumed a rigid body because the thrust vector of the solar sail and its control are performed in a very slow way. Then the possible vibrations (because of the actual flexibility of the spacecraft) will be avoided. In the following sections it will be explained the effect of having flexible appendages. But in the model of the solar radiation pressure it won't be necessary.

The Solar Radiation Pressure is caused when the photons impact on the surface. It exists a fraction of the photons that are absorbed by the sail ( $\rho_a$ ), then a fraction specularly reflected ( $\rho_s$ ) and another fraction diffusely reflected ( $\rho_d$ ) having:  $\rho_a + \rho_s + \rho_d = 1$

If the photons are absorbed by the sail, they transfer their momentum to the sail as explained before. That cause a force to the sail, but it exists a loss of energy in the absorption of the photon by the sail. Mainly in form of temperature. On the other case, if the photons are reflected the loss of energy during the impact decreases a lot. Then permitting a bigger transfer of the momentum and then a larger net force to the solar sail.

Usually the values of the coefficient of specular reflection ( $\rho_s$ ) of the photons of an average spacecraft are approximately  $\rho_s = 0.4/0.5$ . Whereas in the case of the solar sail the coefficient of the specular reflection ( $\rho_s$ ) increase up to 0.94/0.95. Theoretically in order to have a maximum force this coefficient should be 1.

The generic expression of Solar Radiation Pressure force acting in a Lambertian surface located at 1 astronomical unit (AU) from the Sun is the following:

$$\vec{F} = PA \left\{ \rho_a (\vec{S} \cdot \vec{n}) \vec{S} + 2\rho_s (\vec{S} \cdot \vec{n})^2 \vec{n} + \rho_d (\vec{S} \cdot \vec{n}) \left( \vec{S} + \frac{2}{3} \vec{n} \right) \right\} \quad (5)$$

Using the eq. (5) it can be simplified into the following form:

$$\vec{F} = PA (\vec{S} \cdot \vec{n}) \left\{ (1 - \rho_s) \vec{S} + \left[ 2\rho_s (\vec{S} \cdot \vec{n}) + \frac{2}{3} \rho_d \right] \vec{n} \right\} \quad (6)$$

Where:

- $P = 4,563 \times 10^{-6} N/m^2$  that is the nominal solar radiation pressure constant at 1 AU from the Sun
- $A$  is the surface area
- $\vec{n}$  is a unit vector normal to the surface
- $\vec{S}$  is a unit vector pointing from the Sun to the surface,  $\vec{S} = \cos\alpha \vec{n} + \sin\alpha \vec{t}$  ;  
Where  $\alpha$  is the sun angle between the normal to the surface and the sunline and  $\vec{t}$  is the transverse unit vector as can be seen in Fig.2:

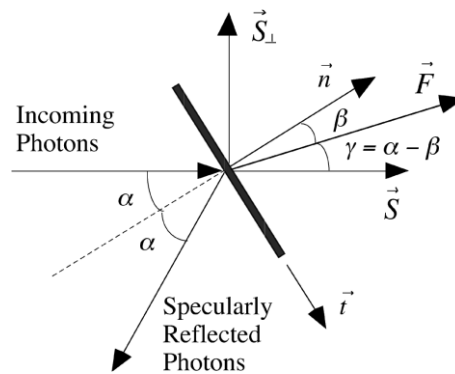


Figure 2 Solar Radiation Pressure Force Diagram

### 3.4.2 Solar Radiation Pressure Torque

The net force of the Solar Radiation Pressure is the major benefactor of the propulsion of the solar sail. Nevertheless, it has drawbacks. The main one is that the photons collide in all the structure and the structure is not completely perpendicular to the sunlines. Then it exists a torque produced that causes a disturbance in the attitude control of the spacecraft.

The torque depends on the distance between the centre of pressure and the point of incidence of the net force. Bigger this distance, larger the torque exerted, thus more control torque needed. If the net force is done exactly in the centre of pressure of the spacecraft, then the torque will be zero.

Also, if the coefficient of absorbance ( $\rho_a$ ) is zero and the centre of pressure is aligned with the centre of mass the unit vector between the centre of pressure and the centre of mass will be in the same direction ( $\vec{S} \cdot \vec{n} = 0$ ). In other words,  $\alpha$  will be zero and the torque will be zero.

In fact, there exist more complex ways to control the attitude of the spacecraft changing the relative position between the CM (Centre of Mass) and the CP (Centre of Pressure) using the idea previously explained.

The expression of the torque is the following:

$$\vec{T} = \vec{r} \times \vec{F} \quad (7)$$

Where

- $\vec{r}$  is the point of incidence
- $\vec{F}$  is the Solar Radiation Pressure Force

To do a first approximation of the torque needed to control it has been selected a distance equal to the 10% of the total length of the sail. Assuming a squared sail of  $40 \times 40 \text{ m}^2$  and assuming that the CP (centre of pressure) is situated in the middle of the sail, the point of incidence will be  $\pm 4 \text{ meters}$  in the vertical direction and  $\pm 4 \text{ meters}$  in the horizontal direction. In the following sketch it can be seen the position of the point of incidence of the sunlines to have a rough approximation of the situation of this point.

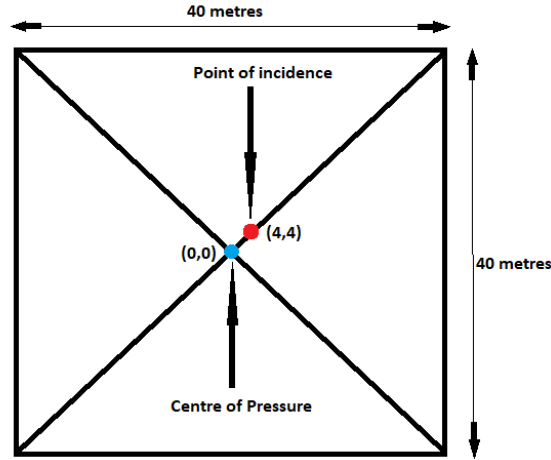


Figure 3 Point of incidence of the rays of the Sun

### 3.5. Euler's Rotational Equations of Motion considering flexible appendages

A real Solar Sail is a flexible object. It is composed by a minimum of four appendages that form the axis of the Solar Sail. Those four appendages are flexible. Therefore, it is necessary to consider the effects of the flexibility when computing the control of the spacecraft.

The Euler's Rotational Equation of Motion can be written under the hypothesis of small elastic deformations (See Bibliography [7]).

$$J\dot{\vec{\omega}} + \delta^T \ddot{\vec{\eta}} = -\vec{\omega} \times (J\vec{\omega} + \delta^T \dot{\vec{\eta}}) + \vec{u} \quad (8)$$

$$\ddot{\vec{\eta}} + C\dot{\vec{\eta}} + K\vec{\eta} = -\delta\dot{\vec{\omega}} \quad (9)$$

Those equations have the angular velocity of the spacecraft and the modal variables as the state variables. In order to be able to compute all the variables they have to be isolated. It is possible to isolate those variables to obtain the dynamics of the flexible spacecraft (See Bibliography [7]).

$$\dot{\vec{\omega}} = J_{mb}^{-1} [-\vec{\omega} \times (J_{mb}\vec{\omega} + \delta^T \vec{\psi}) + \delta^T (C\vec{\psi} + K\vec{\eta} - C\delta\vec{\omega}) + \vec{u}] \quad (10)$$

$$\dot{\vec{\eta}} = \vec{\psi} - \delta\vec{\omega} \quad (11)$$

$$\dot{\vec{\psi}} = -(C\vec{\psi} + K\vec{\eta} - C\delta\vec{\omega}) \quad (12)$$

Having:

$$J_{mb} = J - \delta^T \delta \quad (13)$$

$$\vec{\psi} = \dot{\vec{\eta}} + \delta\vec{\omega} \quad (14)$$



With  $\vec{\omega}$  (angular velocity of the spacecraft),  $\vec{\eta}$  (modal coordinate vector) and  $\vec{\psi}$  (total velocity of the flexible appendages) as the state variables of the problem.

Then:

- $C = \text{diag}\{2\xi_i\vec{\omega}_{ni}, i = 1, \dots, N\}$  = damping matrix

- $K = \text{diag}\{\vec{\omega}_{ni}^2, i = 1, \dots, N\}$  = stiffness matrix

- $N$ =number of elastic modes considered

- $\xi_i$ = damping associated at each elastic mode

- $\vec{\omega}_{ni}$ = natural frequency of each elastic mode

- $J$  is the matrix of inertia considering the spacecraft as a rigid body

-  $\delta$  is the coupling matrix between the flexible and rigid dynamics

- $J_{mb}$  is the main body inertia matrix

As a main difference between this flexible case and the rigid body case is the adding of the modal variables ( $\vec{\eta}$  and  $\vec{\psi}$ ). The first one  $\vec{\eta}$  is the modal coordinate vector whose derivative is the modal velocity  $\dot{\vec{\eta}}$ . It is a non-direct measuring concept; this variable is very related with the difference between the total velocity of the flexible appendages  $\vec{\psi}$  (which corresponds to the second modal variable added) and the global angular velocity of the flexible spacecraft. As a first idea, the objective is to achieve those modal variables to become zero. Then the sailcraft won't have any movement due to its flexibility and will perform a simpler global movement. That means a simpler way to control its attitude and a better knowledge of each position and inclination at any time.

Referring to the explained before,  $N$  represents the complexity of the movement of the flexible appendages. As  $N$  increases, the movement of the flexible appendages becomes more complex. Then the dimensions of the damping matrix and the stiffness matrix increase. This increase of dimensions will suppose an increase of the difficulty to model the control. To model a simple control, it has been selected to have only 1 elastic mode considered. Due to the fact that it has been proved, by several trials of the simulator, that the values of the angular velocities don't change a lot increasing  $N$  and then the complexity of the movement itself. The change of angular velocity is more sensible to the magnitude of the modal variables ( $\vec{\psi}$  and  $\vec{\eta}$ ) and not the quantity of different modal variables existent.

## 4. Rotational Kinematics of the Solar Sail

The kinematics of a spacecraft define the actual inclination of the spacecraft in any time. Without the implementing of rotational kinematics, it is impossible to control the attitude of any spacecraft. The concept of rotational kinematics is purely mathematical. Here it will be explained the key concepts of rotational kinematics to be able to control the attitude of a spacecraft. For a more complete explanation of rotational kinematics, to have a knowledge of where do the matrices, concepts and equations come from it is recommended to see the bibliography [14] in the chapter of Rotational Kinematics.

### 4.1. Direction Cosine Matrix

Imagine two reference frames, each one based in a set of three orthogonal vectors. The frame N, based on the set of vectors  $\{\vec{n}_1, \vec{n}_2, \vec{n}_3\}$  and the frame B, based on the set of vectors  $\{\vec{b}_1, \vec{b}_2, \vec{b}_3\}$ .

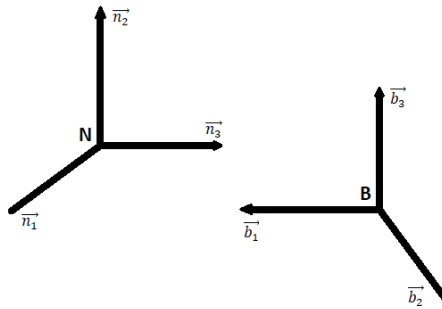


Figure 4 Reference frames

To express the vectors of the reference B in terms of the vectors of the reference N it must be done in the following way:

$$\vec{b}_1 = C_{11}\vec{a}_1 + C_{12}\vec{a}_2 + C_{13}\vec{a}_3 \quad (15)$$

$$\vec{b}_2 = C_{21}\vec{a}_1 + C_{22}\vec{a}_2 + C_{23}\vec{a}_3 \quad (16)$$

$$\vec{b}_3 = C_{31}\vec{a}_1 + C_{32}\vec{a}_2 + C_{33}\vec{a}_3 \quad (17)$$

Those three equations can be expressed in matrix notation as follows:

$$\begin{bmatrix} \vec{b}_1 \\ \vec{b}_2 \\ \vec{b}_3 \end{bmatrix} = \begin{bmatrix} C_{11} & C_{12} & C_{13} \\ C_{21} & C_{22} & C_{23} \\ C_{31} & C_{32} & C_{33} \end{bmatrix} \begin{bmatrix} \vec{a}_1 \\ \vec{a}_2 \\ \vec{a}_3 \end{bmatrix} = C^{N/B} \begin{bmatrix} \vec{a}_1 \\ \vec{a}_2 \\ \vec{a}_3 \end{bmatrix} \quad (18)$$

Where the matrix  $C^{N/B}$  is the direction cosine matrix. It describes the relative orientation of the reference B with the reference N. This matrix is a key aspect to know the actual inclination of the solar sail in the desired reference frame. For example, the direction cosine matrix will allow to know the attitude in the inertial frame from the calculations done in the body frame. Moreover, this direction cosine matrix is an orthonormal matrix, thus its inverse is equal to its transpose and the multiplication between the actual matrix by the transpose gives the identity matrix as the result:

$$C^{-1} = C^T \quad (19)$$

$$CC^T = I \quad (20)$$

Those properties will simplify a lot the future calculations of the attitude.

#### 4.2. Euler Angles

To change the orientation from one reference frame to the other it is trivial that the object must rotate. In fact, that is the information that gives the direction cosine matrix, the rotation effectuated from one reference frame to another.

Euler's eigenaxis rotation theorem states that if a rigid body rotates about an axis that is fixed in the body and stationary in an inertial reference frame, the rigid body can change its attitude from any given orientation to any other orientation. This axis of rotation is called the Euler axis. Furthermore, any rotation can be decomposed into the multiplication of three trivial rotations. So, having three Euler axes with three Euler angles effectuated, each one orthonormal to the others. Each trivial rotation expressed within a matrix as follows:

$$A_1(\psi) = \begin{bmatrix} 1 & 0 & 0 \\ 0 & \cos\psi & \sin\psi \\ 0 & -\sin\psi & \cos\psi \end{bmatrix}, A_2(\theta) = \begin{bmatrix} \cos\theta & 0 & -\sin\theta \\ 0 & 1 & 0 \\ \sin\theta & 0 & \cos\theta \end{bmatrix}, A_3(\phi) = \begin{bmatrix} \cos\phi & \sin\phi & 0 \\ -\sin\phi & \cos\phi & 0 \\ 0 & 0 & 1 \end{bmatrix} \quad (21)$$

There are 12 ways to do any rotation within the Euler angles. Depending on the order selected of the Euler angles to rotate it will exist one sequence or another. Therefore, it exists twelve different direction cosine matrices that express the same rotation. In this case of study, it has been selected the sequence 123, where the first factor is the  $A_1(\psi)$ , the second factor is  $A_2(\theta)$  and the third one is  $A_3(\phi)$ . So, having the expression of the direction cosine matrix as follows:

$$A^{B/N} = A_{123} = A_1(\psi) * A_2(\theta) * A_3(\phi) \quad (22)$$

$$= \begin{bmatrix} \cos\psi\cos\theta & \cos\psi\sin\theta\sin\phi + \sin\psi\cos\phi & -\cos\psi\sin\theta\cos\phi + \sin\psi\sin\phi \\ -\sin\psi\cos\theta & -\sin\psi\sin\theta\sin\phi + \cos\psi\cos\phi & -\sin\psi\sin\theta\cos\phi + \cos\psi\sin\phi \\ \sin\theta & -\cos\theta\sin\phi & \cos\theta\cos\phi \end{bmatrix}$$

Kinematic differential equations

Applying the direction cosine matrix concept but now with angular velocities it is possible to derive the kinematic rotational equations of motion. It is possible to know the derivative of the

direction cosine matrix applying the following formula. For a more detailed explanation it is recommended to visit the bibliography [14].

$$\dot{A}_{B/N} = -[\vec{\omega}_{B/N}]^{\wedge} A_{B/N} \quad (23)$$

$A_{B/N}$  is the direction cosine matrix and  $[\vec{\omega}_{B/N}]^{\wedge}$  are the angular velocities of the object expressed in a matrix on skew symmetric form. That means that the matrix will have the following shape:

$$[\vec{\omega}_{B/N}]^{\wedge} = \begin{bmatrix} 0 & -\omega_3 & \omega_2 \\ \omega_3 & 0 & -\omega_1 \\ -\omega_2 & \omega_1 & 0 \end{bmatrix} \quad (24)$$

Applying the eq.23 selecting a particular  $A_{B/N}$  with a singular sequence is it possible to derive the kinematic differential equations after doing some algebraic steps. For example, the kinematic differential equations derived from the sequence 312 in a matrixial form is the following:

$$\begin{bmatrix} \dot{\psi} \\ \dot{\theta} \\ \dot{\phi} \end{bmatrix} = \frac{1}{\cos\theta} \begin{bmatrix} \cos\theta & \sin\psi\sin\theta & \cos\psi\sin\theta \\ 0 & \cos\psi\cos\theta & -\sin\psi\cos\theta \\ 0 & \sin\psi & \cos\psi \end{bmatrix} \begin{bmatrix} \omega_1 \\ \omega_2 \\ \omega_3 \end{bmatrix} \quad (25)$$

At this point, the kinematics and the dynamics connect. Thanks to the dynamics it is possible to calculate the kinematics of a future iteration. Then, to numerically integrate the Euler angles thus be able to know the future values of the attitude it is only necessary to know the actual values of attitude and angular velocities of the object.

However, this formulation has a problem. The existence of singularities. There are some values of the Euler angles that can crash the simulation. For example, in this particular case if  $\theta$  is 0, it will produce that the first factor will go to a singularity  $\rightarrow \theta = 0 \rightarrow \frac{1}{\cos\theta} = \frac{1}{0}$

To avoid those singularities, it is necessary to implement a new system of numbers. The quaternions.

### 4.3. The Euler Parameters or Quaternions

The Quaternions are a mathematical system of numbers in a four-dimensional form. They were introduced by William Rowan Hamilton in 1843. There is not a direct visualization of quaternions. But they have some properties that help a lot to do the control of an object. This system of numbers is robust against singularities and other problems happened in the previous case.

The quaternions or Euler parameters  $\{q_1, q_2, q_3, q_4\}$  are defined as follows:

$$q_1 = e_1 \sin\left(\frac{\theta}{2}\right) \quad (26)$$

$$q_2 = e_2 \sin\left(\frac{\theta}{2}\right) \quad (27)$$

$$q_3 = e_3 \sin\left(\frac{\theta}{2}\right) \quad (28)$$

$$q_4 = \cos\left(\frac{\theta}{2}\right) \quad (29)$$

Where  $\{e_1, e_2, e_3\}$  are the Euler eigenaxis vector. Each component corresponds to the axis of the rotation of one of the three trivial rotations that are made when performing a rotation. As the three axes are orthonormal it can be stated the subsequent property:

$$e_1^2 + e_2^2 + e_3^2 = 1 \quad (30)$$

Then if eq.30 is implemented, therefore:

$$q_1^2 + q_2^2 + q_3^2 + q_4^2 = 1 \quad (31)$$

The four quaternion variables are constrained by the previous equation. To assure that the quaternions work in a proper way the equation (31) must be always satisfied. Usually if the initial conditions of the quaternions satisfy this condition, the condition will be satisfied during all the simulation. For example, a typical initial condition for initialize quaternions is the following:  $\{q_1(0) = 0, q_2(0) = \frac{1}{\sqrt{3}}, q_3(0) = \frac{1}{\sqrt{3}}, q_4(0) = \frac{1}{\sqrt{3}}\}$ .

It must keep in mind that the quaternions have different properties than vectors. For example, the quaternion multiplication is not intuitive. However, those properties are not needed to be considered while doing the control. But it is useful to be aware that the quaternions are not as simple as vectors for future implementations.

It is feasible to express the direction cosine matrix in terms of the quaternions just by substituting the Euler angles by the quaternions, applying the equation (31) and the following trigonometric identities:

$$\sin^2 \theta + \cos^2 \theta = 1 \quad (32)$$

$$\sin \theta = 2 \sin\left(\frac{\theta}{2}\right) \cos\left(\frac{\theta}{2}\right) \quad (33)$$

$$\cos \theta = \cos^2\left(\frac{\theta}{2}\right) - \sin^2\left(\frac{\theta}{2}\right) = 2 \cos^2\left(\frac{\theta}{2}\right) - 1 = 1 - \sin^2\left(\frac{\theta}{2}\right) \quad (34)$$

Then, having the parametrization of the direction cosine matrix in terms of quaternions:

$$A^{B/N} = \begin{bmatrix} 1 - 2(q_2^2 + q_3^2) & 2(q_1q_2 + q_3q_4) & 2(q_1q_3 - q_2q_4) \\ 2(q_2q_1 - q_3q_4) & 1 - 2(q_1^2 + q_3^2) & 2(q_2q_3 + q_1q_4) \\ 2(q_3q_1 + q_2q_4) & 2(q_3q_2 - q_1q_4) & 1 - 2(q_1^2 + q_2^2) \end{bmatrix} \quad (35)$$

#### 4.3.1. Kinematic differential equations with quaternions

Once the direction cosine matrix using quaternions it is known, it is possible to formulate the kinematic differential equations using quaternions. Basically, the eq.23 must be implemented to obtain the derivatives of the quaternions. Thus, being able to numerically integrate the quaternions and be able to know their future values with the actual ones.

Then, implementing the eq.23 the following big expression is reached:

$$\dot{A}_{B/N} = -[\vec{\omega}_{B/N}]^{\wedge} A_{B/N} = \begin{bmatrix} 0 & -\omega_3 & \omega_2 \\ \omega_3 & 0 & -\omega_1 \\ -\omega_2 & \omega_1 & 0 \end{bmatrix} \cdot \begin{bmatrix} 1 - 2(q_2^2 + q_3^2) & 2(q_1q_2 + q_3q_4) & 2(q_1q_3 - q_2q_4) \\ 2(q_2q_1 - q_3q_4) & 1 - 2(q_1^2 + q_3^2) & 2(q_2q_3 + q_1q_4) \\ 2(q_3q_1 + q_2q_4) & 2(q_3q_2 - q_1q_4) & 1 - 2(q_1^2 + q_2^2) \end{bmatrix} \quad (36)$$

After doing some simplifications and considering the constrain of the quaternions (31) it is possible to achieve the following equations:

$$\omega_1 = 2(\dot{q}_1q_4 + \dot{q}_2q_3 - \dot{q}_3q_2 - \dot{q}_4q_1) \quad (37)$$

$$\omega_2 = 2(\dot{q}_2q_4 + \dot{q}_3q_1 - \dot{q}_1q_3 - \dot{q}_4q_2) \quad (38)$$

$$\omega_3 = 2(\dot{q}_3q_4 + \dot{q}_1q_2 - \dot{q}_2q_1 - \dot{q}_4q_3) \quad (39)$$

Therefore, writing the previous equation in a matrix form and isolating the derivatives of the quaternions the following expression is obtained:

$$\begin{bmatrix} \dot{q}_1 \\ \dot{q}_2 \\ \dot{q}_3 \\ \dot{q}_4 \end{bmatrix} = \frac{1}{2} \begin{pmatrix} 0 & \omega_3 & -\omega_2 & \omega_1 \\ -\omega_3 & 0 & \omega_1 & \omega_2 \\ \omega_2 & -\omega_1 & 0 & \omega_3 \\ -\omega_1 & -\omega_2 & -\omega_3 & 0 \end{pmatrix} \begin{bmatrix} q_1 \\ q_2 \\ q_3 \\ q_4 \end{bmatrix} \quad (40)$$

It can be seen that the future quaternions depend on the current quaternions and the current angular velocities. With this formulation there is no danger to have any singularity. The problem with possible existing singularities in (25) is solved. However, it is not a such direct method that the previous one. Due to the fact there is not a way to see the quaternions in a three-dimensional situation.

#### 4.4. Error function – Quaternion Error

To do the control of the spacecraft the idea of the quaternion error has to be implemented. In the previous case, by numerical integration it is possible to know the current inclination of the spacecraft. But if the objective is to control the spacecraft it is needed to implement the quaternion error. The quaternion error is a column vector of four components, the four quaternion errors. This vector is used in the control. If the control works properly it will reduce the first three components up to zero and the fourth one up to one, always obeying the constraint (31).

The quaternion error can be calculated in the following way:

$$A_e = A_{B/N} A_C^T \quad (41)$$

$$\begin{bmatrix} q_{1e} \\ q_{2e} \\ q_{3e} \\ q_{4e} \end{bmatrix} = \begin{pmatrix} q_{4c} & q_{3c} & -q_{2c} & -q_{1c} \\ -q_{3c} & q_{4c} & q_{1c} & -q_{2c} \\ q_{2c} & -q_{1c} & q_{4c} & -q_{3c} \\ q_{1c} & q_{2c} & q_{3c} & q_{4c} \end{pmatrix} \begin{bmatrix} q_1 \\ q_2 \\ q_3 \\ q_4 \end{bmatrix} \quad (42)$$

Where:

$$\vec{q}_c = \text{commanded quaternion} = \begin{bmatrix} q_{1c} \\ q_{2c} \\ q_{3c} \\ q_{4c} \end{bmatrix} = \begin{bmatrix} 0 \\ 0 \\ 0 \\ \pm 1 \end{bmatrix} \quad (43)$$

The commanded quaternion roughly speaking tells the objective of the control, for example if the objective is to fix a desired attitude, the commanded quaternion will be fixed to  $[0 \ 0 \ 0 \ \pm 1]$ . Or if the objective is to follow some other object, the commanded quaternion will change in time.

-If  $\vec{q}_c = [0 \ 0 \ 0 \ +1]$  then the control law will be  $\vec{u} = -C\vec{\omega} - K\vec{q}_e$

-If  $\vec{q}_c = [0 \ 0 \ 0 \ -1]$  then the control law will be  $\vec{u} = -C\vec{\omega} + K\vec{q}_e$

But physically both commanded quaternions are the same.

In the following chapters there will be explained the control laws implemented in this study.

## 5. Implemented controls

In this thesis it has been implemented four types of control to make the study of the performance of each one of those:

-The first control implemented has been the **Quaternion Error proportional control**. It has been used to compare the response to the control between the rigid body solar sail case and the flexible solar sail case. Two types actuators have been implemented, reaction wheels and CMG.

This type of control has been implemented before in other studies. The main pro that allows this type of control is that achieves the precision quickly. It is one of the most well-known controls implemented in many controls.

For example, the quaternion error proportional control has been used in controlling a quadrotor, where the quickness of the control is crucial to have a good behaviour of the object. In the [1] there is a deeper explanation of this control.

In the specific field of Solar Sails this control has been implemented before. Particularly a pitch-control logic of the sun-pointing mode attitude control of a sailcraft using reaction wheels. This control has been studied by the researcher Bong Wie. A profounder explanation of this control in Solar Sails can be examined in his paper [2].

-The second control corresponds to the **sliding mode control**.

The sliding mode control is another typical control implemented in spacecrafts. It has been widely by the academics. The study of this control has been made of a generic satellite in the presence of Solar Radiation Pressure but can be translated into the implementation of a Solar Sail.

More specifically talking it has been studied an adaptive fault tolerant nonlinear control based on the sliding mode theory to control the attitude using Solar Radiation Pressure. In this case the actuator is a pair of solar flaps that provide the required control torque. The flaps rotate to achieve be able to generate the torque required by Solar Radiation Pressure. In the bibliography [3] it can be found a deeper explanation of this control and a prove of the robustness of the control in the presence of external disturbances as well as a possible failure of the main actuator, the flaps.

Moreover, in the field of the theory of the sliding mode control it can be found in other publications. For instance, there is a paper that explains the attitude control using solar radiation pressure based on non-linear sliding mode control. It is based in a closed loop control law for appropriately rotating solar flaps whose rotation angle is continuously adjusted by the control laws. It has been stated that is robust against uncertainties and has a proper effectiveness with initial attitude tracking errors. For a deeper explanation it is recommended to visit the bibliography [4].

-The third one is a **PD control plus** a term which considers the **flexible dynamics**.

There have been some studies about a control considering flexible dynamics. However, there is not that amount of research done in this type of control as the previous controls. This type of control is very innovative and still needs some time to settle. Nevertheless, this controlling can



provide a more efficient control and this fact could be very beneficial for the control implementation.

There exist a study of the performance and stability validation for a large flexible Solar Sail. This study examines a squared solar sail with a moving mass and quadrant rotation primary actuators with pulsed plasma thrusts at the tips of the sail as a backup attitude control. It studies how the flexible effects of the structure, as torsion and bending of the masts could affect the function of the control actuators. Hence affecting their thrust vector magnitude and direction. For a more detail explanation it is desirable to see the bibliography [5]. It is a complete stability study; however, it considers the spacecraft in a LEO orbit. Having so a different selection of the variables in the problem. But the actual way of controlling the spacecraft can be extrapolated in the case of this study.

There exist studies [6] of a nonlinear attitude control for satellites with flexible appendages dated since the 80s. Moreover, there exist one recent study that has served at a model for the performance of a PD control of a Solar Sail taking into account flexible appendages, used in this work. That study [7], is a proposal of the usage of a dynamic controller for a generic spacecraft with flexible appendages and based on attitude measurements. Therefore, ensuring asymptotic control in a rest-to-rest manoeuvres even when the accelerometer sensors fail and there is non-available angular velocity for the feedback.

Then an adaptation of that control for a generic spacecraft has been done to do create the PD control considering flexible appendages for a Solar Sail, proposed in this work.

-The fourth one is a **non-linear state observer control**.

Regarding the non-linear state observer control there is not any study of implementation in a Solar Sail found. However, based on the theory, this control can allow an asymptotical stability that can benefit its implementation.

### 5.1. Quaternion Error proportional control using Reaction Wheels as actuator

The Quaternion Error proportional control is a linear state feedback control. It is one of the simplest controls that can be implemented. This control is based in the sum of two terms; the quaternion term, and the angular velocities term. Each one multiplied by a proportional (one fixed scalar). It has the following form:

$$\vec{u} = -K\vec{q}_e - C\vec{\omega} \quad (44)$$

Where:

-The K and C are scalars

-  $\vec{q}_e$  are the quaternion errors: it is a vector of three components  $[q_{e_1}, q_{e_2}, q_{e_3}]$ . The way to calculate this vector is explained in the Quaternions subsection inside the Kinematics section.

-  $\vec{\omega}$  are the angular velocities of the spacecraft respect to the body frame: it is a vector of three components  $[\vec{\omega}_1, \vec{\omega}_2, \vec{\omega}_3]$  where the first component corresponds to the rotation of the

spacecraft around the x axis of the body frame, the second component is the rotation around the y axis and the third around the z axis. Each one is orthonormal regarding the others.

### 5.1.1. Study of stability of the control

This control ensures asymptotical stability for the rigid body and the flexible body. This can be stated in the following explanation, for a more complete explanation it is interesting to visit the bibliography [7].

Deriving along the trajectories of the rigid motion and the Quaternion Error proportional control law with K and C as positive scalars:

$$\dot{\vec{\omega}} = J(-\vec{\omega} \times J\vec{\omega} + \vec{u}) \quad (45)$$

$$\dot{\vec{q}}_e = -\frac{1}{2}\vec{\omega}^T \vec{q}_e \quad (46)$$

$$\vec{u} = -K\vec{q}_e - C\vec{\omega} \quad (47)$$

Where:

$$\vec{q}_e = \begin{bmatrix} q_1 \\ q_2 \\ q_3 \end{bmatrix} \quad (48)$$

It can be calculated the following Lyapunov function candidate:

$$V = K[(q_4 - 1)^2 + \vec{q}_e^T \vec{q}_e] + \left(\frac{1}{2}\right) \vec{\omega}^T J \vec{\omega} \quad (49)$$

Where:

$$q_4 = \vec{q}(4) \quad (50)$$

Whose derivative is the following:

$$\dot{V} = K\vec{q}_e^T \dot{\vec{q}}_e + \vec{\omega}^T (-\vec{\omega} \times J_{mb}\vec{\omega} + \vec{u}) = -K\vec{\omega}^T \vec{\omega} \leq 0 \quad (51)$$

As the Lyapunov function candidate is continuously differentiable and positive with a negative derivative, using the LaSalle theorem a global asymptotic stability can be stated. The derivative of the Lyapunov function is lower than zero, then exists a tendency of decreasing the variance of the values up to a fixed value, therefore the values converge.

### 5.1.2. Block diagram

At the following image a block diagram it is exposed to show how the DCM proportional control is implemented:

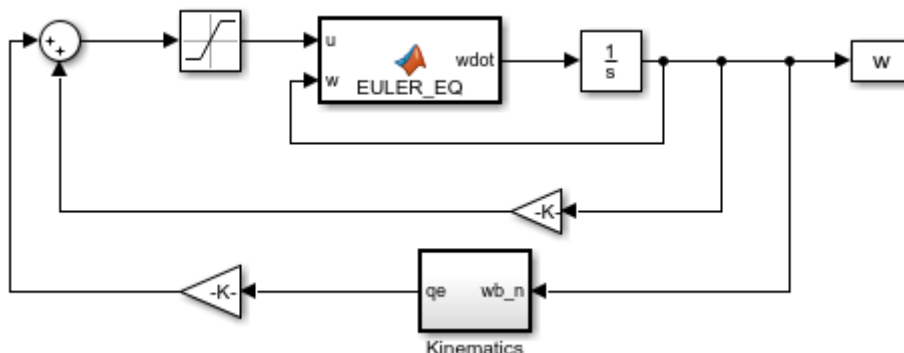



Figure 5 Block diagram of the Quaternion Error Proportional control

Where  corresponds to a saturation block. Basically, it is a limiter of  $u$ . The control is limited because physically constrained by the maximum torque that real control device (inertia wheel, reaction wheel, etc.) can give. In this case it is 0.2 Nm.

In the Annex1 it will be explained the other possible actuator that will be implemented, the CMG.

### 5.2. Sliding mode control

The sliding mode control is a nonlinear state feedback control. In broad terms there is an objective function ( $S$ ) which must converge to 0. This objective function is a straight line which depends on the errors and their derivative that can exist in the control of the system. The following equation defines the objective function and has the following graphical shape:

$$\vec{S} = ke + \dot{e} \tag{52}$$

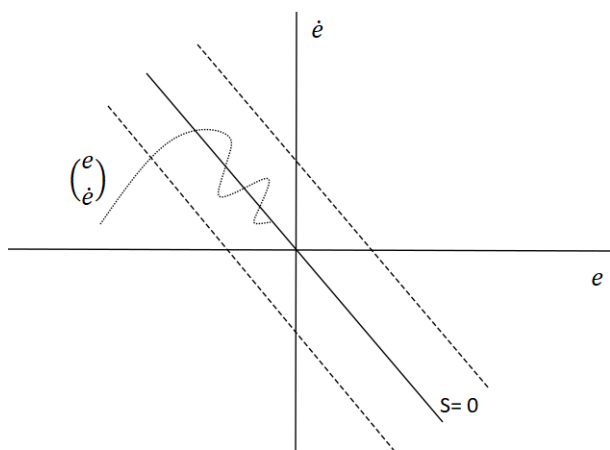


Figure 6 Sliding mode objective function

Then, in order to assure asymptotic control:

$$\dot{e} = -ke \quad (53)$$

Where  $e$  is the error committed and  $\dot{e}$  is the derivative of this error.

In this case of study, the control objective function is related with the angular velocity therefore if the  $S$  converges to 0, the angular velocities will also converge. Then the system will stabilize.

The control equation for a generic sliding mode control is the following:

$$\vec{u} = T_{maxim} * sgn(\vec{S}) \quad (54)$$

In this case of study, the  $\vec{S}$  corresponds to a PD controller.

#### 5.2.1. Implementation of the control

The block diagram of the control in the sliding mode is exactly the same as the Quaternion Error control. There is only a new adding term to the calculation of the control for the next iteration of the simulation. In the control block it is added a conditional situation (if function). If the  $u$  of the previous step is below to zero, the new  $u$  will have a negative sign, the other two remaining case are done in an analogue way.

The  $T_{maxim}$  previously indicated in the (54) corresponds to the maximum torque that the control device can produce. In this situation will we 0.2 Nm.

Basically, this control will work as an on/off mode control. Where in the on mode will have a maximum torque achievable by the control device and in the off mode the control will be 0.

### 5.3. PD control plus a term which considers the flexible dynamics

It is a state feedback PD control. Then it works the same way as the Quaternion Error control. Nevertheless, the main difference between this control and the Quaternion Error control is the addend of the sum in the control law. While in the Quaternion Error control has the first addend as a proportional multiplied by the quaternion error (See [7]), in the PD control accounting flexible dynamics the first addend is a matrix F multiplied by a vector a.

The matrix F takes into account the physical properties of the solar sail. Then the vector "a" contains the quaternion error, the modal coordinate vector and the total velocity of the flexible appendages. It is worth to indicate that both matrix F and vector "a" depend on the number of the elastic modes selected. If the number of elastic modes increases, the complexity of the movement of the flexible appendages will also increase. As the complexity of the movement increases, the complexity of the system and its complexity of the simulation increases drastically.

In this case of study, it has been selected only 1 elastic mode for practical reasons. One elastic mode it is enough to see the difference between the non-flexible case and the flexible case. That is sufficient for the purpose of this study. With one elastic mode the matrix F has a dimension of 5x5 and the vector "a" has a dimension of 5x1.

The control law will be the following:

$$\vec{u} = -F\vec{a} - k_d\vec{\omega} \quad (55)$$

$$F = \left[ k_p I, \delta^T \left\{ \begin{bmatrix} K \\ C \end{bmatrix} - P_1 \begin{bmatrix} I \\ -C \end{bmatrix} \right\}^T \right] \quad (56)$$

$$\vec{a} = \begin{bmatrix} \vec{q}_e \\ \vec{\eta} \\ \vec{\psi} \end{bmatrix} \quad (57)$$

Where:

- I is the identity matrix (in this case 1x1)
- $k_p$  is a constant value
- $\delta$  is the coupling matrix between the flexible and rigid dynamics
- $K = \text{diag}\{\vec{\omega}_{ni}^2, i = 1, \dots, N\}$  where N are the number of the elastic modes, in this case N=1
- $C = \text{diag}\{2\xi_i\vec{\omega}_{ni}, i = 1, \dots, N\}$  where N are the number of the elastic modes, in this case N=1
- $\vec{q}_e$  is the quaternion error
- $\vec{\eta}$  is the modal coordinate vector
- $\vec{\psi}$  is the total velocity of the flexible appendages
- $P_1$  is a positive definite matrix calculated as the solution of

$$P_1 \begin{bmatrix} 0 & I \\ -K & -C \end{bmatrix} + \begin{bmatrix} 0 & I \\ -K & -C \end{bmatrix}^T P_1 = -2Q_1 \quad (58)$$

Where  $Q_1$  is a fixed matrix, in this case it has been selected the identity matrix of a dimension  $1 \times 1$ .

### 5.3.1. Study of stability

With this control an asymptotic stability it is achieved. To visualise the prove of the achievement of asymptotic stability it is recommended to see the Bibliography [7]. However, this control doesn't ensure that the final value of the control will be correct. This is due to the lack of the modal measurements. Without the possibility to measure the modal coordinate vector thus the final result completely depends of the initial conditions. The initial values of the modal variables  $\eta$  and  $\psi$  are calculated based on a model of the structure therefore it cannot assure that the initial conditions are acceptable.

## 5.4. Improvement of the controller; output feedback controllers

With the previous controller it is not possible to assure proper results due to the lack of measurement of the modal variables. Therefore, it has been created an extension of this controller that permits calculate the control only measuring the attitude and the angular velocity.

This extension of the control is based on the estimation of the modal variables  $(\hat{\eta}, \hat{\psi})$ . Then the errors of the modal variables are introduced:

$$e_\eta = \vec{\eta} - \hat{\eta} \quad (59)$$

$$e_\psi = \vec{\psi} - \hat{\psi} \quad (60)$$

Those errors are not used into the implementation of the controller. But they are used to prove that the control will be asymptotically stable. If the reader wants to delve into the calculation of the Lyapunov function of the system and the application of LaSalle theorem to prove the stability it is worth considering going to the bibliography [7].

Finally, the dynamic controller with the extension of output feedback controllers will have the following formulation:

$$\begin{bmatrix} \dot{\hat{\eta}} \\ \dot{\hat{\psi}} \end{bmatrix} = \begin{bmatrix} 0 & I \\ -K & -C \end{bmatrix} \begin{bmatrix} \hat{\eta} \\ \hat{\psi} \end{bmatrix} - \begin{bmatrix} I \\ -C \end{bmatrix} \delta \vec{\omega} + P_2^{-1} \begin{bmatrix} K \\ C \end{bmatrix} - P_1 \begin{bmatrix} I \\ -C \end{bmatrix} \delta \vec{\omega} \quad (61)$$

$$\vec{u} = -F \begin{bmatrix} \vec{q}_e \\ \hat{\eta} \\ \hat{\psi} \end{bmatrix} - k_d \vec{\omega} \quad (62)$$

Where  $P_2$  has been calculated as the solution of the following equation:

$$P_2 \begin{bmatrix} 0 & I \\ -K & -C \end{bmatrix} + \begin{bmatrix} 0 & I \\ -K & -C \end{bmatrix}^T P_2 = -2Q_2 \quad (63)$$

With  $Q_2$  as a fixed matrix, in this case it has a dimension of  $1 \times 1$ .

With this model of control, it can be proved that the errors of the estimation of the modal variable tend to zero because the system is asymptotically stable. Then, if the system is asymptotically stable, at the end of the manoeuvre the  $w$  and  $q$  will also tend to zero. And if the  $w$  tends to 0, therefore there isn't any velocity of the object; hence the modal variables will tend to zero.

With this explanation it can be stated that doing the estimation of the modal variables helps to have a more precise knowing of the system and a better transient, but they are not indispensable to state the asymptotic stability of the system. The solar sail can be stabilized without the extension, but it is highly recommended to use the extension to have a proper stabilization of the spacecraft.

## 5.5. Nonlinear state observer control

This is a nonlinear control used in the cases when does not exist a way to model a part of the control. Or there is not any possibility to do the measurements of some parameters of the control.

The basic idea of this controller is to model the unknown parameters of the control as disturbances. These disturbances are estimated by previous values starting from some initial known values. This control allows an asymptotically stability of the system without the need of external measurements. This controller and the previous one, the PD controller with a term which considers the flexible dynamics with output feedback controllers, are based on the same idea.

### 5.5.1. Modelling of the disturbance

First, here are presented the dynamic equations of the solar sail considering a flexible appendage:

$$J\dot{\vec{\omega}} + \delta^T \ddot{\vec{\eta}} = -\vec{\omega} \times (J\vec{\omega} + \delta^T \dot{\vec{\eta}}) + \vec{u} \quad (64)$$

$$\ddot{\vec{\eta}} + C\dot{\vec{\eta}} + K\vec{\eta} = -\delta\vec{\omega} \quad (65)$$

From these equations the addends that cannot be directly measured are isolated, then those terms will be the corresponding disturbance:

$$\dot{\vec{\omega}} = J^{-1}(-\vec{\omega} \times J\vec{\omega}) + J^{-1}\vec{u} - J^{-1}\vec{\omega} \times \delta^T \dot{\vec{\eta}} - J^{-1}\delta^T \ddot{\vec{\eta}} \quad (66)$$

This equation is the typical dynamic equation plus a disturbance addend:

$$\dot{\vec{\omega}} = J^{-1}(-\vec{\omega} \times J\vec{\omega}) + J^{-1}\vec{u} + \vec{d} \quad (67)$$

Where  $d$  is the disturbance term and is the following:

$$\vec{d} = -J^{-1}\vec{\omega} \times \delta^T \dot{\vec{\eta}} - J^{-1}\delta^T \ddot{\vec{\eta}} \quad (68)$$

In this case the disturbance term is constituted by the modal variables which cannot be measured in the reality.

### 5.5.2. Implementing the control

Once the disturbance is isolated from the system then the next step is to estimate this disturbance. Basically, the disturbance is modelled as the error between the estimation of the angular velocity and the real angular velocity of the spacecraft. Therefore, the following equations will be implemented to consider this disturbance on the system:

$$\dot{\hat{\omega}} = J^{-1}(-\hat{\omega} \times J\hat{\omega}) + J^{-1}\vec{u} + \hat{d} + L_1(\vec{\omega} - \hat{\omega}) \quad (69)$$

$$\dot{\hat{d}} = L_2(\vec{\omega} - \hat{\omega}) \quad (70)$$

Considering:  $\hat{\omega}(0) = \vec{\omega}(0)$  and  $\hat{d}(0) = 0$

As it is possible to measure the actual angular velocity of the spacecraft and estimating the angular velocity  $\hat{\omega}$  of the future time. It is possible to do an estimation of the disturbance as a simple subtraction of the actual angular velocity minus the estimated angular velocity multiplied by a matrix  $L_2$  that it has to be tuned to do a proper estimation.

Then this disturbance estimation is added in the control law thus controlling properly the spacecraft having in mind all the existing disturbances in the problem.

$$\vec{u} = -k_1\vec{q}_e - k_2\vec{\omega} - \hat{d} \quad (71)$$

With this control an asymptotic stability can be achieved if the tuning of the error matrices  $L_1$  and  $L_2$  is good enough.



## 6. Calculation of the Moments of Inertia of the Solar Sail

### 6.1. Why to calculate them?

The principal moments of Inertia are one of the principal parameters to control a spacecraft. Roughly speaking, they define how easy or difficult is to rotate the object in the three-principal axis of the object. Usually the matrix of Inertia of an object is a 3x3 matrix whose diagonal are the three moments of inertia of the three-principal axis.

Dealing with the control of an object whose matrix of inertia is in the order of units is different than dealing with the control of an object whose matrix of inertia is in the order of thousands of units. The needed torque will be much higher.

Therefore, to do a realistic simulation of the control, it is needed to calculate the actual moments of inertia of the spacecraft. In this case the Solar Sail.

### 6.2. Solar Sail model using Solid Works

In order to calculate the principal moments of inertia of the Solar Sail it has been selected to use Solid Works. Solid Works is a solid modelling computer aided design (CAD) computer program. One of its capacities is to calculate the moments of inertia of a designed object.

#### 6.2.1. Design of the Solar Sail

This Solar Sail will be composed by three main parts: the sail, the control structure and the antenna. Each one performing basic and necessary tasks of the spacecraft. The sail provides the thrust to the global structure. The control structure logically provides the control. Finally, the antenna provides the communications of the spacecraft.

##### 6.2.1.1. *The Sail*

The Solar Sail can have different shapes (squared, disc or heliogyro) to perform different tasks. In this particular case, with the sail orbiting around the Sun it has been selected a squared shape. To have enough pushing solar pressure to perform its activity it has been selected to have a squared sail of 40x40 metres. That is a really big area, thus it is necessary to have a very thin sail, thus avoiding a very heavy object. If the sail is so heavy, the solar pressure force won't be strong enough to maintain the object in the orbit. Then, the thickness chosen has been 6 micrometres ( $6 \cdot 10^{-6}$ metres).

The following figure represents the front view of the Solar Sail.

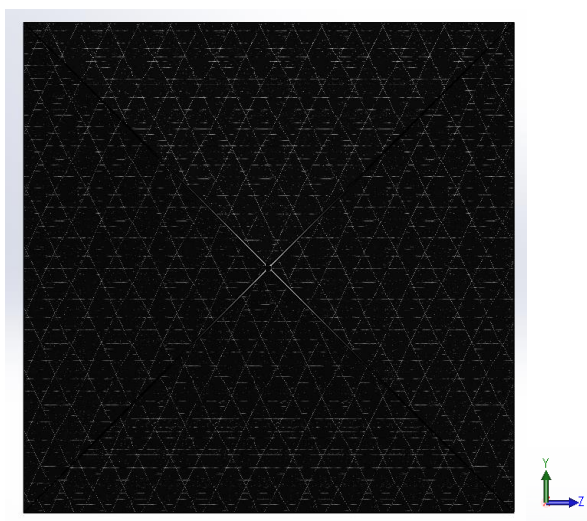


Figure 7 Front view of the solar sail

The sail is not completely plane, it has a little inclination through the centre. The main objective of this inclination is to focalize the photons to the centre of pressure, due to the material is high reflective. An analogue idea is a sink with water, as the inclination increases, more amount of water per second will fall in the centre. But in this case, the reflected photons coming from the Sun will be likely conducted to the centre of the sail, where is the centre of pressure. Therefore, theoretically having an improvement of the force created by the solar radiation pressure and less solar radiation pressure disturbance.

The next figure is the profile view of the solar sail. It can provide an idea to the reader about this defined inclination.

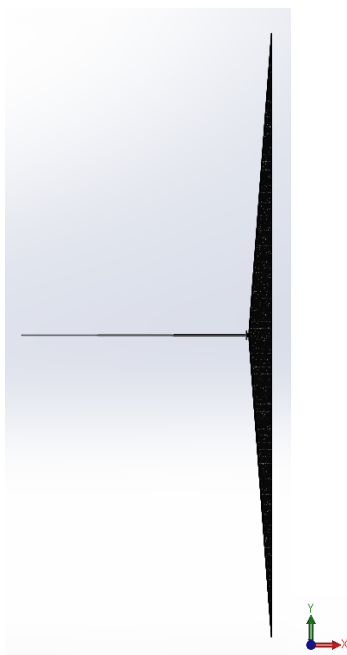


Figure 8 Side view of the solar sail

#### 6.2.1.2. *The control structure*

The control structure is the place where all the control actuators are situated, usually Reaction Wheels or CMGs. Then other components with take a secondary role, like radiators. In this study it will be considered the simplest structure, then having an approximation of the mass and the volume that occupy all the existing components of the actual spacecraft.

The control structure will be based on a nucleus with a shape of a cube whose dimensions are  $\{0.16 \times 0.24 \times 0.24\}$  meters plus four radiators each one measuring  $\{0.01 \times 0.24 \times 0.17\}$  metres, all of them situated in the corner of the nucleus so it can be folded when it is necessary.

The following figure shows the shape of the control structure previously explained:

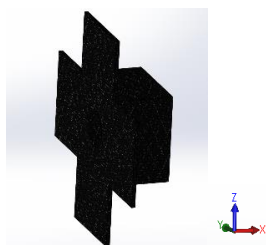


Figure 9 Control structure of the solar sail

#### 6.2.1.3. *The antenna*

The antenna is the key parameter to perform the communication. In this case it is required to perform a high directive antenna. The main reason is that the spacecraft is situated very far away from the Earth, therefore the gain of the antenna must be high enough to assure a proper sending of the signal.

The antenna will be based on 3 cylinders. The first one with a diameter of 0.1 metres and a longitude of 5 metres. The second one with a diameter of 0.05 metres and a longitude of 5 metres. And the third one with a diameter of 0.025 metres and a longitude of 5 metres.

The following figure shows the shape of the antenna previously explained:

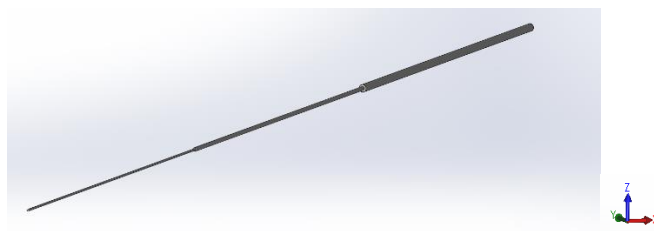


Figure 10 Antenna of the Solar Sail

## 6.2.2. Calculation of the moments of Inertia

Once the object is created it is possible to use Solid Works program to calculate the moments of inertia and other aspects of the Solar Sail. There is a button named "Physical Properties" that automatically calculates the total mass, the volume, area and the moments of inertia of the spacecraft.

### 6.2.2.1. Selection of the materials

But, first must be selected the material of each structure to know its density and then be able to calculate all the variables described before. Solid Works provides a great variety of options of materials that can be selected. Nevertheless, the actual materials that are used nowadays for the Solar Sails are not still implemented by Solid Works. Therefore, the materials used have been the ones whose density is the most fitted to the actual used. Their reflectivity properties are not considered, only their density to have an approximate calculation of the structure and its moments of inertia. It is necessary to recall that the materials that will be mentioned won't be used in the reality, only its density will be desirable to do a first approach of the moments of inertia. For the studies that will continue this one it is highly desirable to select actual materials used. But for this first approach, this selection is accurate enough.

For the sail itself and the control structure it has been selected the composite material Hexcel AS4C (3000 filaments) whose density is  $1780 \text{ kg/m}^3$ . For the antenna it has been selected the generic fiberglass A, whose density is  $2440 \text{ kg/m}^3$ .

These materials selected are in the same level of magnitude of the actual ones nowadays being implemented, for example the Kapton, used in the actuals Solar Sails has a density of  $1420 \text{ kg/m}^3$  that does not differ a big amount to the composite material selected in this study.

Accordingly, with the materials selected the physical properties has been calculated and are the following:

-Total mass: 315.53 kg

-Total volume:  $0.16 \text{ m}^3$

-Total surface area:  $3195.79 \text{ m}^2$

-Matrix of moments of inertia, obtained in the centre of mass and aligned with respect to the resulting coordinate system:

$$I = \begin{bmatrix} 4559.79 & 0.00 & -37.51 \\ 0.00 & 5184.04 & 0.00 \\ -37.51 & 0.00 & 5183.05 \end{bmatrix} \text{ kg} \cdot \text{m}^2$$

To seek of simplicity to do the control calculations it has been selected to use only the three principal moments of inertia  $I_{xx}, I_{yy}, I_{zz}$  because the secondary moments of inertia are not very high and can be neglected. Having so, the following matrix of Inertia:

$$I = \begin{bmatrix} 4559.79 & 0.00 & 0.00 \\ 0.00 & 5184.04 & 0.00 \\ 0.00 & 0.00 & 5183.05 \end{bmatrix} kg \cdot m^2$$

In the following figure it can be seen the 3D representation of the Solar Sail. With the purpose that the user can have a complete idea of the shape of the Solar Sail that it is desired to be implemented. One clarification, the antenna is pointing towards the Earth, that is why in this case is in the space on the negative x axis.

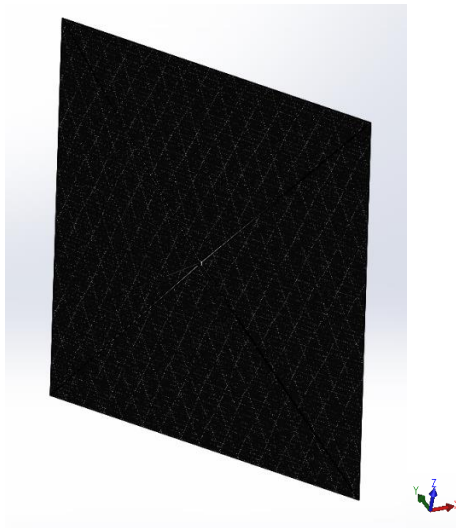


Figure 11 3D view of the solar sail

## 7. Study of the effects of flexibility in the Spacecraft

As the Solar Sail is a flexible spacecraft it is necessary to consider the effects of the flexibility that can occur into the attitude control of the spacecraft. This study is a comparison of the behaviour of the spacecraft using two different controls with different configurations. The first control is a Quaternion Error control. The second one is a Quaternion Error control but considering flexible appendages. Both controls are theoretically explained before (44). To do a proper and a coherent comparison it has been selected the same actuator and the same control gains for both situations. The used actuator will be the Reaction Wheel. And the control gains  $k_p, k_e$  will be fixed as  $k_p = 50$  and  $k_e = 4$ . It is worth remembering the simple Quaternion Error control law:

$$\vec{u} = -k_p \vec{\omega} - k_e \vec{q}_e \quad (72)$$

### 7.1. Results for a non-flexible spacecraft

The following three figures are obtained for a non-flexible spacecraft implementing a Quaternion Error control with reaction wheels. Also selecting the previous values of control gains and performing a rest to rest manoeuvre.

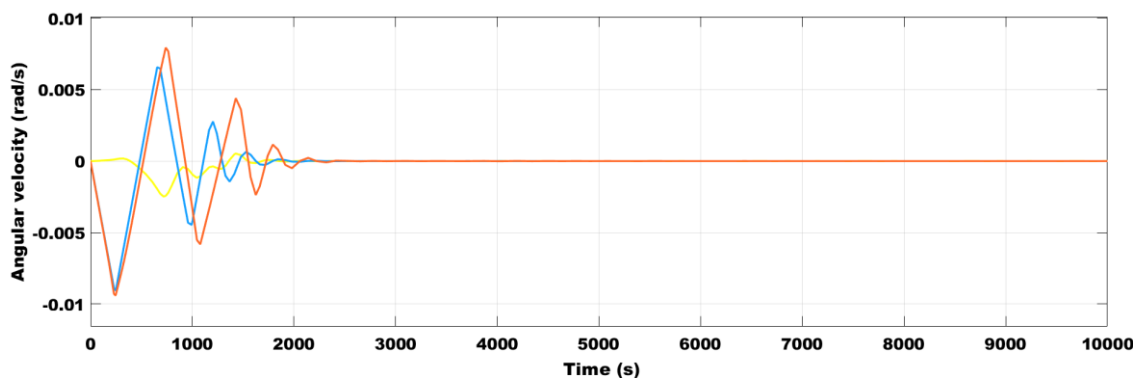


Figure 12 Angular Velocity vs time using Quaternion Error control with non-flexible spacecraft

In the case of the angular velocity it exists a convergence of the three angular velocities up 0 within a time of 2650 seconds. The final precision of the angular velocities is in the order of magnitude of  $10^{-6}$  rad/s.

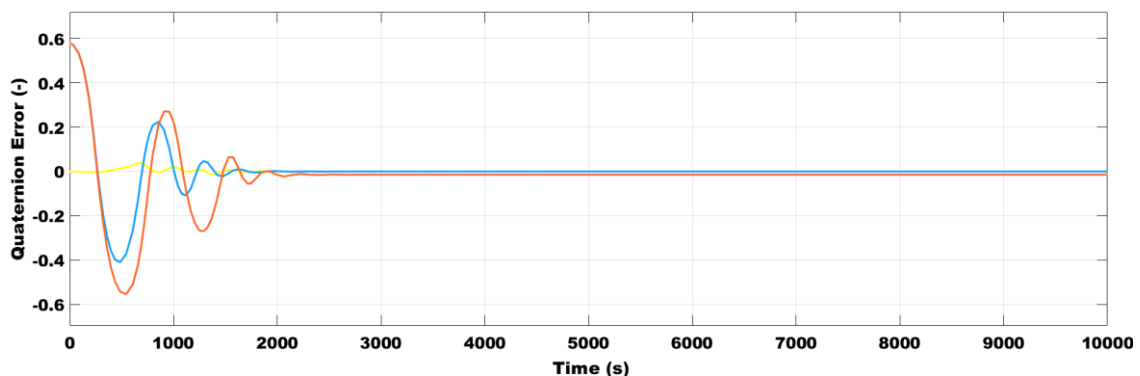


Figure 13 Quaternion Error vs time using Quaternion Error control with non-flexible spacecraft

Considering the Quaternion Error, a convergence of the three quaternion errors is obtained in 2500 seconds. The third quaternion error converges to  $-0.01445$ , having a fixed error of  $0.01445$ . The other two quaternions errors converge to zero.

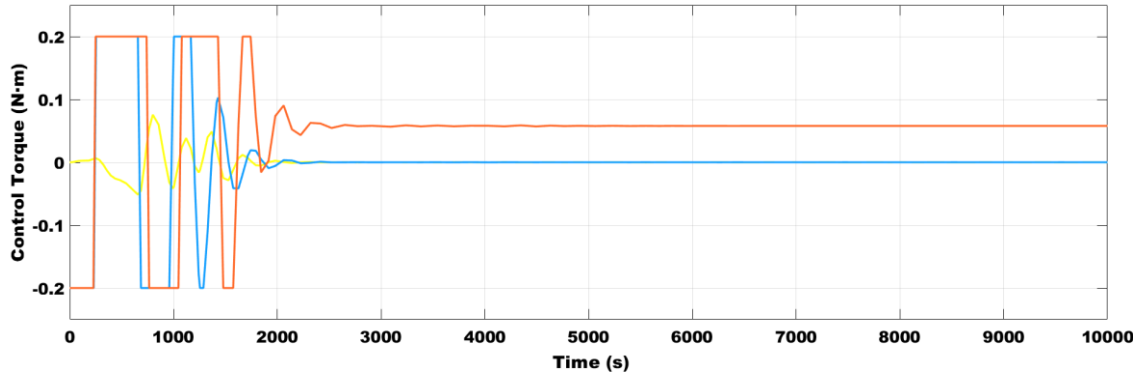


Figure 14 Control torque vs time using Quaternion Error control with non-flexible spacecraft

Considering the control torque, maximum values of the control torque are reached for the third component of the control torque until 1742 seconds. In the case of the second control torque those maximum values are reached until 1288 seconds.

## 7.2. Flexible Spacecraft study

There are some new variables that take an important role in the consideration of adding flexible appendages in the spacecraft. There are two new state variables when the addition of flexible appendages is considered. The modal coordinate variable and the total velocity of the flexible appendages. Both are explained in the previous chapters, but basically, they express the magnitude of the movement of the flexible appendages and its complexity. Then there are other variables that are added to the control, the natural frequency and the damping ratio. Those two last are fixed values during the simulation and express the nature of the movement. Depend on the value of the damping factor, an overdamped, underdamped or critically damped response will be achieved.

Therefore, there are two ways of changing the conditions of flexibility. Or changing the nature of the movement, then shifting the natural frequencies and the damping factor. Or changing the magnitude of the movement, thus shifting the initial values of the modal coordinate variable and the total velocity of the flexible appendages.

### 7.2.1. First attempt; change the nature of the movement of the flexible appendages

First, it has been fixed an initial modal coordinate variable equal to zero and a velocity of the flexible appendages equal to  $0.005$  m/s. Then it has been selected different values of natural frequencies and damping ratios. In the following table it will be expressed the results obtained.

Natural frequency (rad/s)	Damping Ratio	Observations
0.74	0.004	No significant changes in $\omega$ vs time and $q_e$ vs time plots
5.69	0.017	No significant changes in $\omega$ vs time and $q_e$ vs time plots
70	0.3	No significant changes in $\omega$ vs time and $q_e$ vs time plots
1000	0 (Critically damped)	Simulation time increases 1000%, there is a big change at time= 2000s, the $\omega$ , modal coordinate variable and the total velocity of flexible appendages doesn't converge.
1000	2 (Overdamped)	No significant changes in $\omega$ vs time and $q_e$ vs time plots  The progression of the modal coordinate variable changes, with a final convergence with an uncertainty of $10^{-6}$
1000	0.4 (Underdamped)	No significant changes in $\omega$ vs time and $q_e$ vs time plots  The progression of the modal coordinate variable changes, with a final convergence with an uncertainty of $10^{-7}$
400	0.4	No significant changes in $\omega$ vs time and $q_e$ vs time plots  The progression of the modal coordinate variable changes, with a final convergence with an uncertainty of $10^{-6}$ Much quicker response

Table 1 Change of the nature of the movement of the flexible appendages

As can be seen in the previous table, the natural frequency and the damping ratio do not take a very big role in the change of the behaviour of the system if the initial values of the modal coordinate variable and the total velocity of the flexible appendages is near to zero. The tendency of the  $\omega, q_e, \eta, \psi$  versus time is practically invariable considering the change of the natural frequency and damping ratio. Only when the natural frequency is high enough (larger than 1000 rad/s with a critically damped oscillation), the system turns unstable.



### 7.2.2. Second attempt; change the magnitude of the movement of the flexible appendages

In this case the natural frequency has been fixed with a value of 5.69 rad/s and a damping ratio of 0.017. Therefore, the nature of the movement will be always the same, but in this case, its magnitude will vary. To vary the magnitude of the movement it is necessary to change the initial values of the modal coordinate variable ( $\mu$ ) and the total velocity of the flexible appendages ( $\psi$ ). In the following table it will be expressed all the results obtained.

<i>initial</i> $\mu(-)$	<i>initial</i> $\psi\left(\frac{m}{s}\right)$	Observations
0	0	No significant changes in the tendency of $\omega, q_e, \mu, \psi$ versus time
5	0	No significant changes in the tendency of $q_e$ versus time Increase of the frequency of the change of $\omega_1, \omega_2$ , the values change more rapidly. Their final convergence has a precision of $10^{-3}$
5	5	<b>In relation with the previous case:</b> -Increase of magnitude of $\omega_1$ -Increase of magnitude and frequency of change of $q_{e1}$ with a final convergence -Same tendency of $q_{e2}$ but with more oscillations in the transient -Same tendency of $q_{e3}$ than without flexible appendages No significant changes in the tendency of $\mu, \psi$ versus time
0	5	-Increase of magnitude and frequency of change of $q_{e1}$ with a final convergence -Increase of magnitude and frequency of change of $q_{e2}$ with a final convergence - $q_{e3}$ remains the same -Increase of magnitude and frequency of change of $\omega$ with a final convergence. Final precision of $\omega_1 = 1.2 \cdot 10^{-4} \frac{rad}{s}$ ,

		$\omega_2 = 2 \cdot 10^{-4} \frac{rad}{s}, \omega_3 = 5.7 \cdot 10^{-3} \frac{rad}{s}$
0	2.5	<p><b>In relation with the previous case:</b></p> <p>-Same behaviour of <math>\omega</math>, with an improvement of precision of <math>\omega_2 = 9 \cdot 10^{-5} \frac{rad}{s}</math></p> <p>-Same behaviour of <math>q_e</math> but with a decrease of oscillations.</p>
0	1.25	Nearly the same performance than without flexible appendages. Non-a visible change adding flexible appendages.

Table 2 Change of the magnitude of the movement of the flexible appendages

As can be perceived in the previous table, there are some visible changes between the flexible and the non-flexible case when the initial velocity of the flexible appendages is higher than 1.5 m/s ( $\psi(0) \geq 1.5 \frac{m}{s}$ ) with a fixed initial modal state variable of zero ( $\mu(0) = 0$ ).

If the initial velocity of the flexible appendages increases, using the same control, the error committed will be greater. More particularly if the initial value of the velocity doubles, the error will increment a factor of 10 approximately. Especially the final precision error of  $\omega_2$ , which is that variable that has behaved more dependent of the initial velocity of the flexible appendages.

### 7.3. Results of Flexible Spacecraft

In order to have a more visual comparison it has been selected one option of all the particular cases that have been implemented to do the study of the change of the responses. In this case it has been selected the Quaternion Error Control using Reaction Wheels as actuators. The initial conditions of the modal variables are the following:

- $\omega_n = 5.69 \frac{rad}{s}$
- *damping ratio* =  $\xi = 0.017$
- Initial modal coordinate variable =  $\mu(0) = 0$
- Initial total velocity of flexible appendages =  $\psi(0) = 2.5 \frac{m}{s}$

Having the following responses:

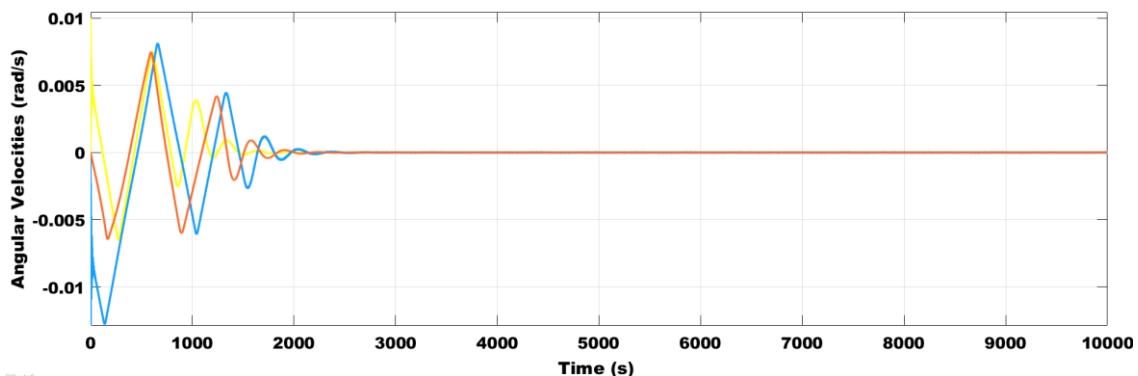


Figure 15 Angular Velocity vs time using Quaternion Error control with a flexible spacecraft

The convergence is accomplished in the same time. There is a substantial increase of the magnitude of the oscillations during the transient of  $\omega_1, \omega_2$ . Also there is a reduction of the final precision of the three angular velocities:

$$\text{precision } \omega_1 \text{ in nonflexible} = 2.3 \cdot 10^{-6} \rightarrow \text{precision } \omega_1 \text{ in flexible} = 1.2 \cdot 10^{-4}$$

$$\text{precision } \omega_2 \text{ in nonflexible} = 1.8 \cdot 10^{-7} \rightarrow \text{precision } \omega_2 \text{ in flexible} = 2 \cdot 10^{-4}$$

$$\text{precision } \omega_3 \text{ in nonflexible} = 7.5 \cdot 10^{-9} \rightarrow \text{precision } \omega_3 \text{ in flexible} = 5.7 \cdot 10^{-8}$$

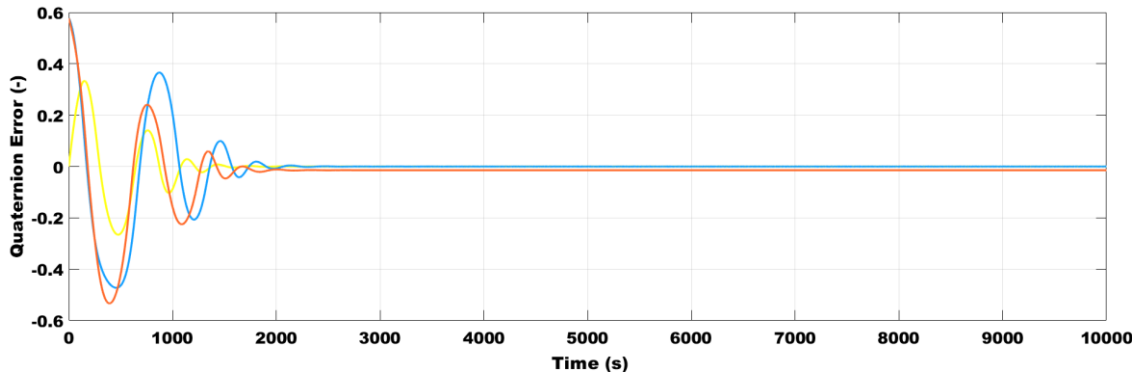


Figure 16 Quaternion Error vs time using Quaternion Error control with a flexible spacecraft

In the case of the quaternion error there is a great increase of the magnitude of the  $q_{e1}, q_{e2}$  during the transient. However all the quaternion errors converge in the same time and the final precision is the same than the non-flexible case.

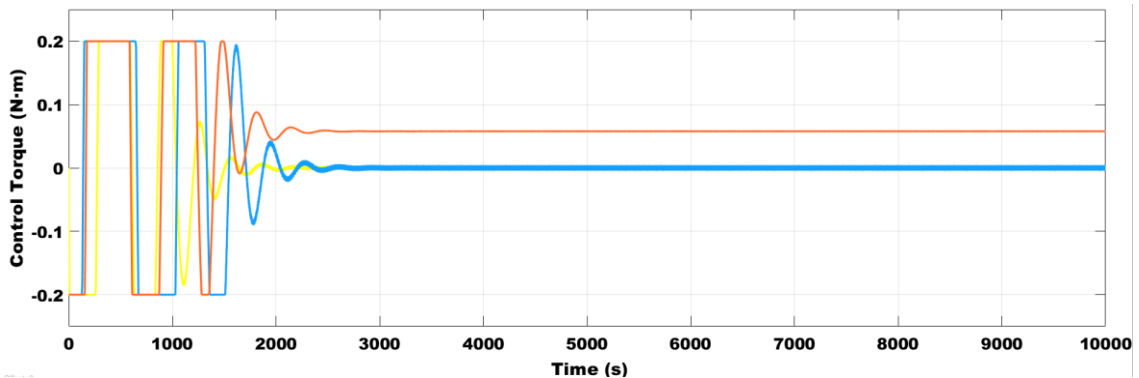


Figure 17 Control Torque vs time using Quaternion Error control with a flexible spacecraft

The control torque for the flexible case has the same behaviour than the non-flexible case. However the final control  $u_1, u_2$  for the flexible case has an oscillative behaviour whose maximums are between  $\pm 3.5 \cdot 10^{-3} N \cdot m$

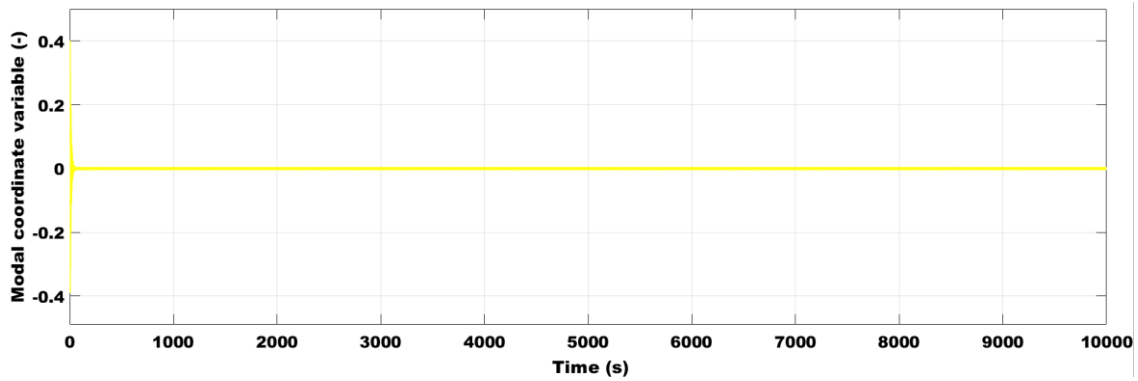


Figure 18 Modal Coordinate Variable vs time using Quaternion Error control with a flexible spacecraft

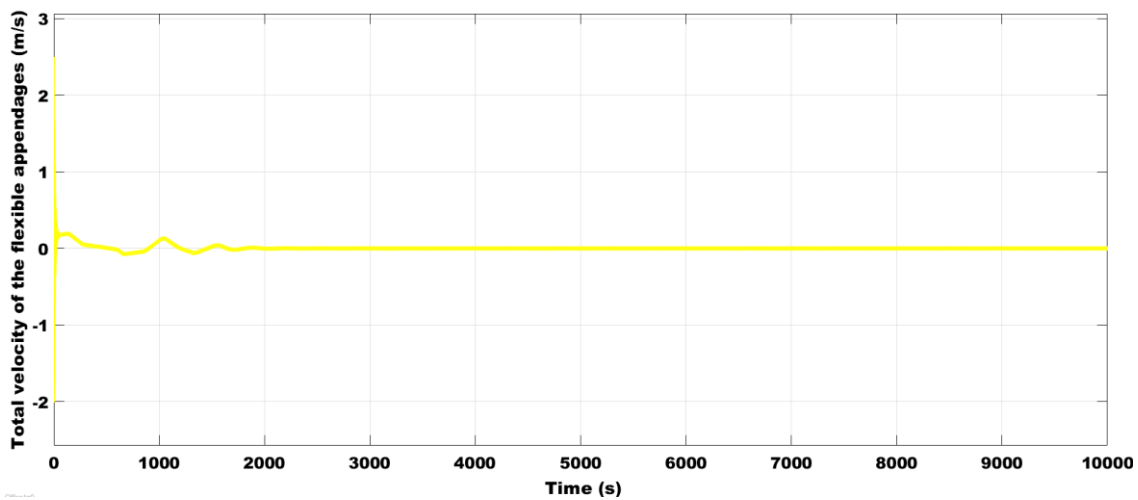


Figure 19 Total velocity of the flexible appendages vs time using Quaternion Error control with a flexible spacecraft

In the case of the tendency of the modal variables showed above they tend to 0. They converge, therefore there is a stabilization of the spacecraft with flexible appendages. Those results are coherent because the other three variables  $\vec{\omega}$ ,  $\vec{q}_e$  and  $\vec{u}$  also tend to stabilise.

#### 7.4. Verdict

There is a reduction of the performance of the control when it is considered the effects of flexibility. The precision of the angular velocity decreases. And the transient response becomes more abrupt. Nevertheless, a stability it is achieved if the control is tuned in a proper way with acceptable initial conditions of the modal variables. Moreover, the time needed to stabilize is very similar.

In the reality, the spacecraft will perform a more extreme manoeuvre to stabilize, but it will finally stabilize. The control needed to realize this manoeuvre won't be as easy as expect and its magnitude won't be fixed, it will oscillate during time.

This study show that it is necessary to consider the effects of the flexibility in the control and in the system. Because if those effects are not considered, the results obtained won't show the reality of the behaviour of the spacecraft. The controller will think that the spacecraft is well controlled, while the previous results show that the behaviour, mainly during the transient, changes.

To avoid these problems, it will be necessary to perform a control that takes into consideration the effects of the flexibility. And, to create a background, a calculation of the dynamics considering flexible appendages.

## 8. Comparison of the flexible disturbance using different controls

The main difference between an average control of a spacecraft and this specific control is that it is taken into consideration the presence of flexible appendages, flexibility, in the spacecraft. Therefore, there are some components that on a normal control are not considered. Those components that consider the effects of flexibility can be modelled as a disturbance.

The objective of the control will be decrease this disturbance up to zero. Therefore those “flexible terms” won't cause difficulties and inconvenient on the movement of the spacecraft.

This Flexible disturbance torque can be mathematically isolated from the Flexible dynamic equations of the spacecraft (10), (11), (12). Having the following final expression:

$$\dot{\vec{\omega}} = J_{mb}^{-1}[-\vec{\omega} \times (J_{mb}\vec{\omega} + \delta^T \vec{\psi}) + \delta^T (C\vec{\psi} + K\vec{\eta} - C\delta\vec{\omega}) + \vec{u}] \quad (73)$$

Where the flexible disturbance is:

$$\vec{d}_{flex} = J_{mb}^{-1}[(-\vec{\omega} \times \delta^T \vec{\psi}) + \delta^T (C\vec{\psi} + K\vec{\eta} - C\delta\vec{\omega})] \quad (74)$$

In comparison with the other disturbance, the Solar Radiation Pressure torque, it has the same order of magnitude. Nevertheless, this flexible disturbance tends to converge up to zero if the control is used in a proper way. While the Solar Radiation Pressure torque does not tend to zero in any case because depends on external factors (mainly the Sun).

### 8.1. Influence of the modal variables into the flexible disturbance

There are four modal state variables accounting in the control, the natural frequency of the movement, the damping ratio, the modal state variable and the velocity of the flexible appendages. Doing several attempts with one particular control it has been noticed that as the initial value of the velocity of the flexible appendages, the natural frequency and the damping ratio of the movement of those flexible appendages increase, the peaks of the of the flexible disturbance increase in quantity and magnitude.

Hence, if the complexity and the magnitude of the flexible movement increases, then the flexible disturbance becomes less smooth and more unstable.

### 8.2. Action of the controllers in the reduction of the Flexible disturbance

In this chapter there is a study of the comparison of how each one of the controls implemented deal with the flexible disturbance.

(The **first plot** of each control is a **global view** of the disturbance, the **second** one is the an **ampliation** to see its convergence error)

**There are the same initial conditions and gains for all cases**, to do a coherent comparison:

$$\omega_n = 5.69 \frac{rad}{s} ; \xi = 0.017 ; \psi(0) = 2.5 \frac{m}{s} ; \eta(0) = 0 ; gains: k_d = 60, h_e = 0.9$$

Flexible disturbance using Quaternion Error control

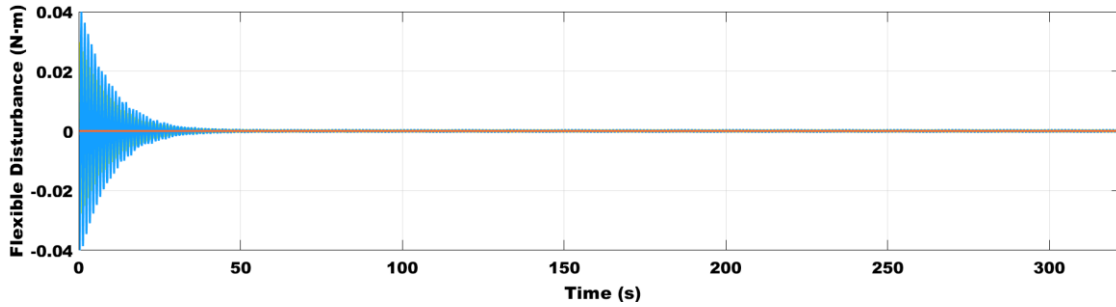


Figure 20 Flexible disturbance using Quaternion Error control

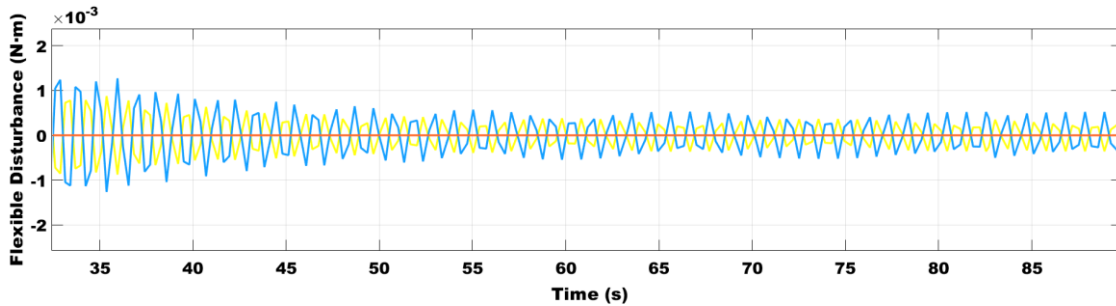


Figure 21 Closer look of the flexible disturbance using Quaternion Error control

Using the Quaternion Error control, the flexible disturbance decreases very rapidly, in approximately 45 seconds achieves its convergence. However, the x and y components of the disturbance have a sinusoidal nature of an amplitude of  $3,7 \cdot 10^{-4} N \cdot m$  for the disturbance in the x axis, and  $5 \cdot 10^{-4} N \cdot m$  for the disturbance in the y axis. Having that final sinusoidal convergence is not desirable because it can cause problems on the control.

Flexible disturbance using Nonlinear state observer control obtaining data of the angular velocities from a Quaternion Error controller

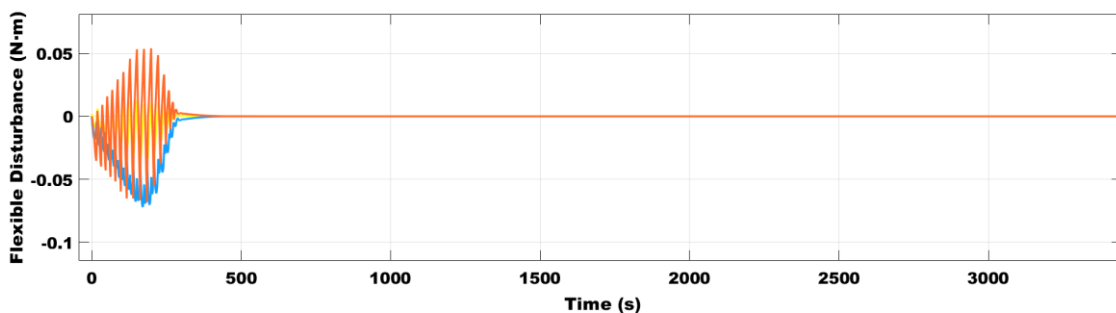


Figure 22 Flexible disturbance using Nonlinear state observer control obtaining data of the angular velocities from a Quaternion Error controller

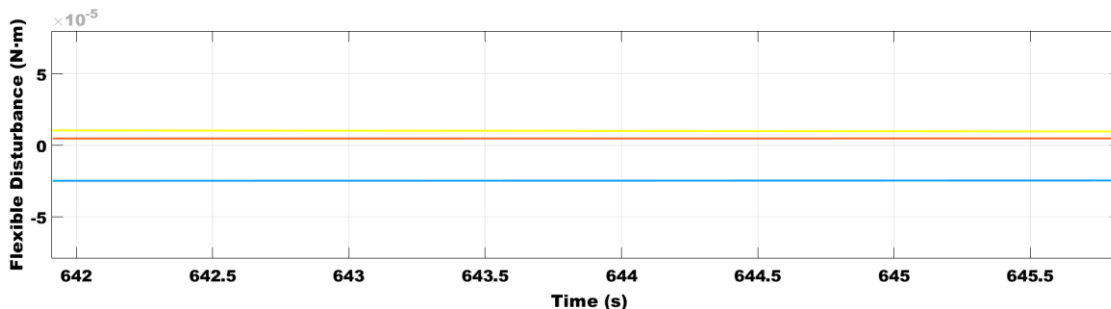


Figure 23 Closer look of the flexible disturbance using Nonlinear state observer control obtaining data of the angular velocities from a Quaternion Error controller

In this case the convergence is achieved in a larger amount of time than the Quaternion Error control. Approximately the convergence is achieved in 520 seconds. Once the convergence is achieved the errors are constant one the order of magnitude less than the Quaternion Error control.

Flexible disturbance using Nonlinear state observer control having an own calculation of the angular velocities

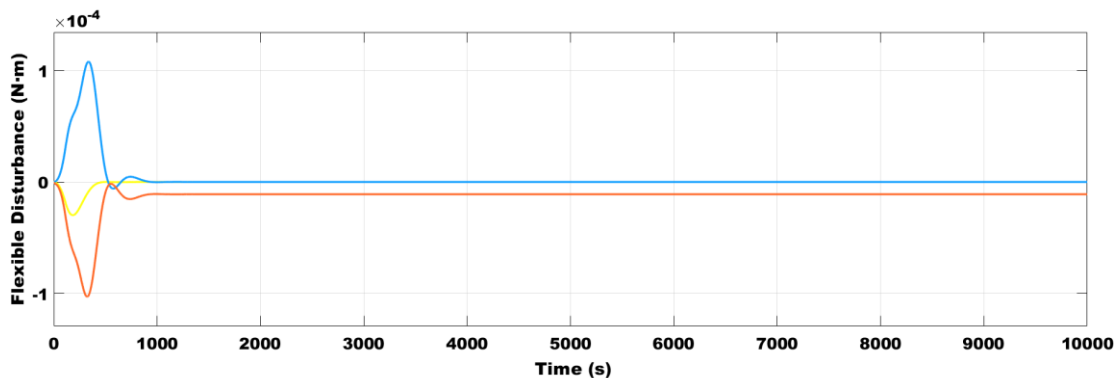


Figure 24 Flexible disturbance using Nonlinear state observer control having an own calculation of the angular velocities

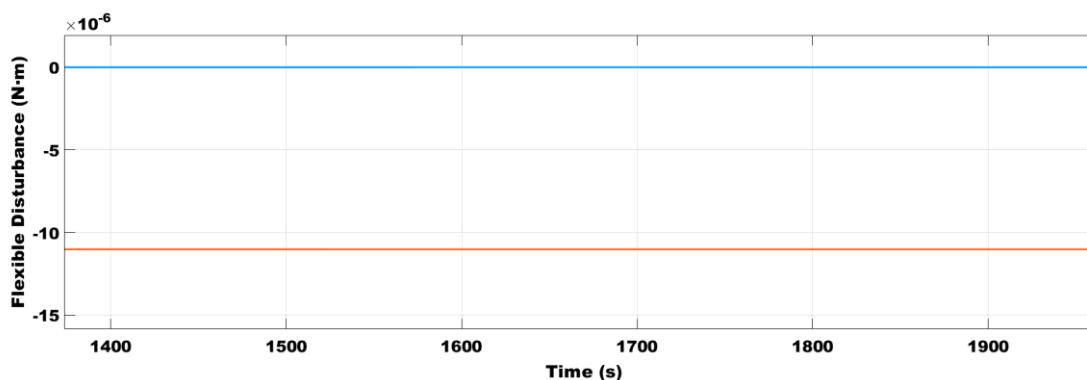


Figure 25 Closer look for the flexible disturbance using Nonlinear state observer control having an own calculation of the angular velocities



Using this control, the convergence needs 900 seconds to converge, then the time of convergence increases. However, the error at the convergence decreases, only having an error in the z component of the flexible disturbance. Theoretically this control is governed by the same equations than the previous one. However, this control calculates its own angular velocity. Then in theory it is a very good control, but its real implementation is way more complex than the other controllers.

#### Flexible disturbance using Flexible control

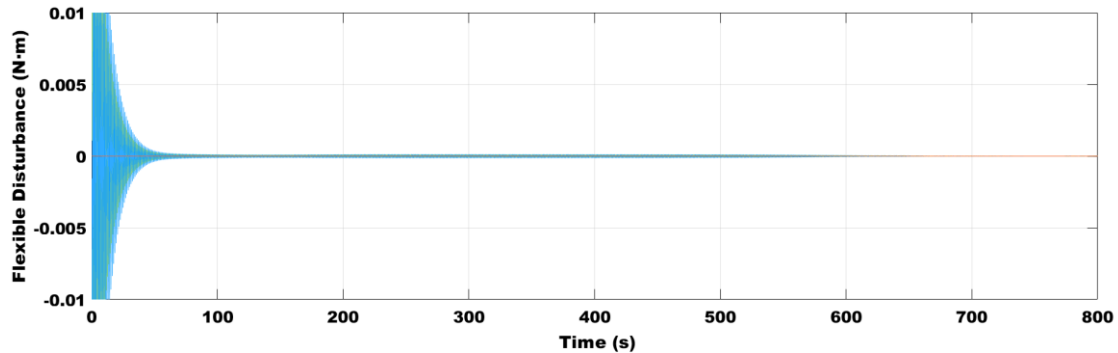


Figure 26 Flexible disturbance using Flexible control

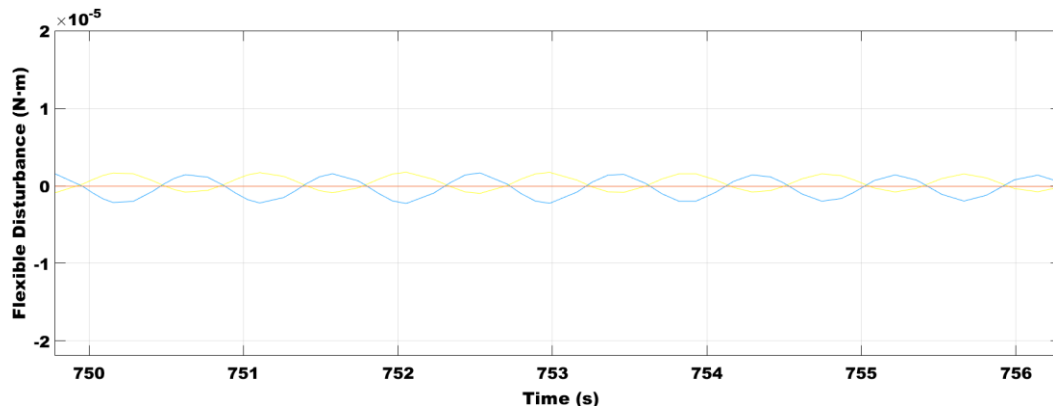


Figure 27 Closer look to the flexible disturbance using Flexible control

The implementation of the flexible control has some advantages and disadvantages. The error committed diminishes. However, this error has a sinusoidal nature of an amplitude of  $1.75 \cdot 10^{-6} N \cdot m$  for the x component of the Flexible disturbance and an amplitude of  $2.25 \cdot 10^{-6} N \cdot m$  for the y component of the Flexible disturbance. On the other hand, the time to achieve the convergence increases up to 750 seconds.

### Flexible disturbance using Flexible control with output feedback controllers

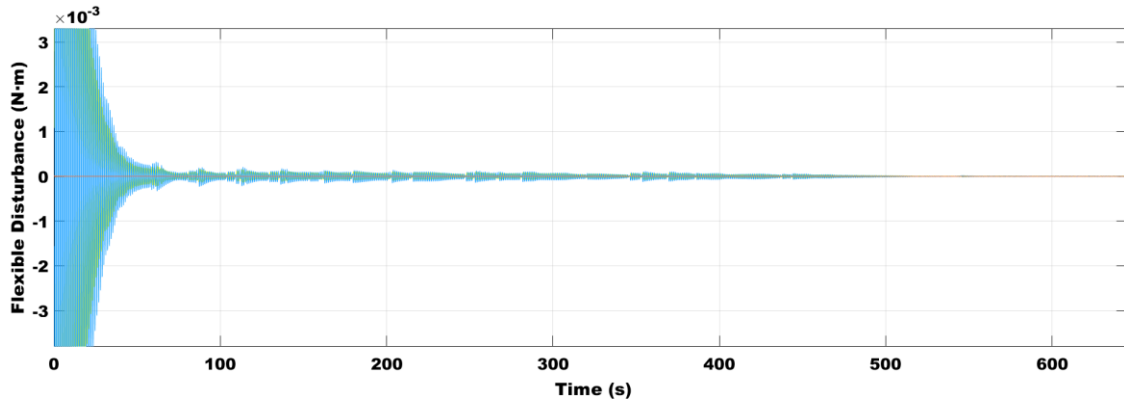


Figure 28 Flexible disturbance using Flexible control with output feedback controllers

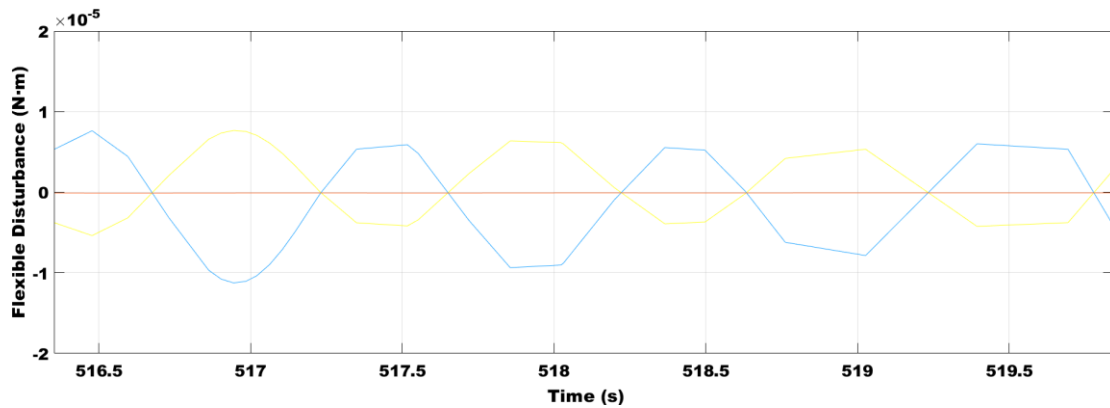


Figure 29 Closer look to the flexible disturbance using Flexible control with output feedback controllers

In this final case, the progression of the disturbance works in the same way than in the previous case, the flexible control. Nevertheless, with two differences, the time of convergence and the error at its convergence.

Using the Flexible control with output feedback controllers a convergence it achieved within 520 seconds and the error at the convergence has a sinusoidal nature whose amplitude is  $12.2 \cdot 10^{-6} N \cdot m$  for the x component of the Flexible disturbance and an amplitude of  $6.5 \cdot 10^{-6} N \cdot m$  for the y component of the Flexible disturbance.

### 8.3. Final comparison and corollary

To do a complete comparison of all the cases effectuated it has been decided to rank all the controllers considering two variables. The first one is the time of convergence of the Flexible disturbance torque. The second one is the error committed at the convergence. All the results are noted in the following table.

Type of control	Rank in time of convergence	Rank in error at the convergence
Quaternion Error control	1	5
Nonlinear State Observer (1)	2	4
Nonlinear State Observer (2)	5	2
Flexible control	4	1
Flexible control with output feedback controllers	3	3

*Table 3 Rank of the controls in relation with the flexible disturbance performance*

(1). Nonlinear state observer control obtaining data of the angular velocities from a Quaternion Error controller

(2). Nonlinear state observer control having an own calculation of the angular velocities

Considering the two variables to do the comparison look that the most balanced controller to deal with the Flexible disturbance is the Flexible control with output feedback controllers. Other controllers, like Quaternion Error have a very good performance in the time of convergence but a very bad one in the error at the convergence.

Other controls, like the Nonlinear State Observer provide very accurate results. Notwithstanding, there is the total lack of knowledge of the Flexible disturbance, because in the implementation of this control the modal variables are not used. This lack of knowledge of the flexible movement in the control can cause that in a real case the tuning of the estimators of the Nonlinear State won't be accurate enough and won't provide a good response. In this case the perform is very accurate but is not possible to assure that this control will have that good responses in other situations.

Therefore, it can be state that the Flexible control using output feedback controllers is the most appropriate to deal with the flexible disturbance due to its liability. Theoretically it assures a final convergence, and that is a key factor to select the proper control. Also, as it works with the modal variables it is possible to understand how them interfere the control and have a knowledge of how to solve warning situations. It need more time to converge but is has more accurate knowledge of the disturbance and an error sufficiently low to avoid possible problems in the implementation of the control of the spacecraft, our implemented Solar Sail.

## 9. Simulation and Results

All the controls explained in the theory chapter can be simulated numerically using Simulink. This program can solve numerically the needed torque and all the other parameters that are considered in the control.

The idea to do a simulation of the control in Simulink is to divide the global simulator into several blocks, each one with a specific function. The first block is the Dynamics block, the second one is the Kinematics block and the third one is the Control block. Inside the Dynamics block is situated also the external disturbance torque block, in this case the Solar Radiation Pressure torque.

All these blocks are interacting with each other working together to do the control of the spacecraft. The next diagram shows how those blocks interact with each other.

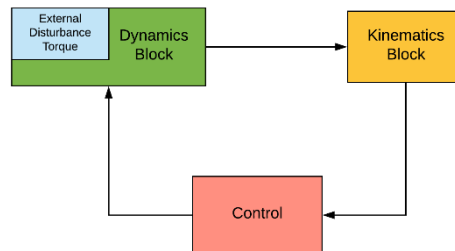


Figure 30 Block diagram of the simulation

Basically, the dynamics block provides the angular velocity of the body respect to the inertial frame  $\vec{\omega}_{b/N}$ . Then the kinematics block is feed with this  $\vec{\omega}_{b/N}$  to be able to calculate the quaternion error  $\vec{q}_e$  and the direction cosine matrix  $A_{b/N}$ . With the  $\omega_{b/N}$  and  $q_e$  the control block can calculate the control torque  $\vec{u}$  to do the control of the spacecraft, required in the Dynamics block. Then the direction cosine matrix  $A_{b/N}$  is required in the External disturbance block to calculate the pointing vector of the spacecraft towards the Sun  $\vec{x}_p$ . This  $\vec{x}_p$  is needed to calculate the Solar Radiation Pressure disturbance torque that is considered in the Dynamics block.

Afterwards, this idea can be putted in practise in the program Simulink and performing all the blocks. Once all the blocks are performed in Simulink it is possible to numerically integrate the equations of each block and obtain the results.

### 9.1. Results for each control

Once the simulation it is done it has been decided to present in tables the results obtained to subsequently do a comparison of the global performance of each control.

In these tables of results, it has been decided to note the following variables to have a complete knowledge of the performance of each control and be able to do a complete and coherent comparison, considering all the decided situations:

- Gain of the angular velocity used  $k_p$
- Gain of the quaternion error used  $k_e$
- Time of convergence of the angular velocity  $\vec{\omega}$  and its final convergence error
- Time of convergence of the quaternion error  $\vec{q}_e$  and its final convergence error
- Time of convergence of the modal state variable  $\eta$  and its final convergence error
- Time of convergence of the total velocity of the flexible appendages  $\vec{\psi}$  and its final convergence error
- Final precision error  $\phi$  in ° degrees.
- Time with a maximum torque required  $t_{u_{maximum}}$
- Torque requiring constant during the implementation  $\tau$  in  $N^2 \cdot m^2$

Where:

$$\tau = \int_{t_o}^{t_f} (u_1^2 + u_2^2 + u_3^2) dt \quad (75)$$

- Torque requiring constant per second  $\gamma$  in  $\frac{N^2 \cdot m^2}{s}$ . That is the torque required constant divided by number of seconds that the control has been implemented.

The last three variables provide information of the expense of torque needed to perform each control.

In all the following cases the initial modal variables are selected to be the same. Also, the Solar Sail will perform a rest to rest manoeuvre in all cases. With the aim of having the same initial situation in all cases and then be able to do a coherent and fair comparison.

Therefore:

- The natural frequency of the flexible movement  $\vec{\omega}_n$  is fixed as 5.69 rad/s, its damping ratio  $\xi$  fixed as 0.017.
- The initial value of the modal state variable  $\vec{\eta}(0) = 0$ .
- The initial value of the total velocity of the flexible appendages  $\vec{\psi}(0) = 2.5 \text{ m/s}$
- The initial value of the angular velocity of the spacecraft,  $\vec{\omega}(0) = [0, 0, 0] \text{ rad/s}$

To have a more pleasant view it has been decided to use two different tables. The first one will consider the gains, the time of convergence of  $\vec{\omega}$ ,  $\vec{q}_e$ ,  $\eta$ ,  $\vec{\psi}$  with their errors at the convergence and the final precision error  $\phi$  for each control performed. The second one will consider the

gains, the time with maximum torque required  $t_{u_{maximum}}$ , the torque requiring constant  $\tau$  and the torque requiring constant per second  $\gamma$ .

Finally, here is presented the performed tables considering all the previous conditions:

Type of control	$k_p$	$k_{q_e}$	Time of convergence (s)				Final Precision Error
			$\vec{\omega}$ (rad/s)	$\vec{q}_e$ (-)	$\eta$ (-)	$\vec{\psi}$ (m/s)	$\phi$ ( $^\circ$ degrees)
Quaternion Error Control	50	4	3000 $w_1 \rightarrow \pm 6 \cdot 10^{-5}$ $w_2 \rightarrow \pm 9 \cdot 10^{-5}$ $w_3 \rightarrow \pm 3 \cdot 10^{-8}$	2530 $q_{e1} \rightarrow \pm 6 \cdot 10^{-6}$ $q_{e2} \rightarrow \pm 1 \cdot 10^{-6}$ $q_{e3} \rightarrow -0.01452$	80 $\pm 0.005$	2000 $\pm 0.027$ High freq.	1.654
Sliding Mode Control	50	4	520 $w_1 \rightarrow dev + 6 \cdot 10^{-5}$ $\pm 6 \cdot 10^{-5}$ $w_2 \rightarrow dev - 6 \cdot 10^{-5}$ $\pm 6 \cdot 10^{-5}$ $w_3 \rightarrow dev - 10 \cdot 10^{-5}$ $\pm 5 \cdot 10^{-6}$	Do not converge	90 $\pm 0.005$	500 $\pm 0.025$	82
Nonlinear State Observer (1)	50	4	2600 $w_1 \rightarrow \pm 2.7 \cdot 10^{-7}$ $w_2 \rightarrow \pm 13 \cdot 10^{-7}$ $w_3 \rightarrow \pm 9 \cdot 10^{-6}$	2440 $q_{e1} \rightarrow \pm 3.1 \cdot 10^{-5}$ $q_{e2} \rightarrow \pm 2.27 \cdot 10^{-4}$ $q_{e3} \rightarrow dev - 0.0145$	68 $\pm 5 \cdot 10^{-5}$	1680 $\pm 0.00335$	1.657
Nonlinear State Observer (2)	50	4	3200 $w_1 \rightarrow \pm 4.852 \cdot 10^{-8}$ $w_2 \rightarrow \pm 2.652 \cdot 10^{-7}$ $w_3 \rightarrow \pm 7.093 \cdot 10^{-7}$	2800 $q_{e1} \rightarrow \pm 4.69 \cdot 10^{-7}$ $q_{e2} \pm 2.463 \cdot 10^{-6}$ $q_{e3} dev - 0.01445$	75 $\pm 4.1 \cdot 10^{-3}$	1950 $\pm 0.0237$	1.6566
					2400	1300	

Flexible Control	50	4	Do not converge	Do not converge	$\pm 1 \cdot 10^{-3}$	$\pm 6 \cdot 10^{-3}$	---
Flexible Control with Output Feedback controllers	50	4	$1.65 \cdot 10^4$ $w_1 \rightarrow dev + 5.13 \cdot 10^{-6}$ $w_2 \rightarrow dev - 1 \cdot 10^{-9}$ $w_3 dev - 8.268 \cdot 10^{-6}$	$8.55 \cdot 10^3$ $q_{e1} dev - 8.59 \cdot 10^{-4}$ $q_{e2} dev + 1.43 \cdot 10^{-3}$ $q_{e3} dev - 0.01445$	$+1.637 \cdot 10^{-10}$	$+1.243 \cdot 10^{-4}$	1.6589
Flexible Control	450	125	4700 $w_1 \rightarrow dev - 1.5 \cdot 10^{-5}$ $\pm 1.5 \cdot 10^{-5}$ $w_2 \rightarrow dev - 1 \cdot 10^{-5}$ $\pm 2 \cdot 10^{-5}$ $w_3 \rightarrow dev - 15 \cdot 10^{-8}$	4800 $q_{e1} \rightarrow \pm 3.49 \cdot 10^{-4}$ $q_{e2} \rightarrow \pm 2.19 \cdot 10^{-4}$ $q_{e3} \rightarrow \pm 4.55 \cdot 10^{-4}$	870 $\pm 2.2 \cdot 10^{-3}$	1600 $\pm 6.6 \cdot 10^{-3}$	0.054
Flexible Control with Output Feedback controllers	80	15	3540 $w_1 \rightarrow dev + 3.32 \cdot 10^{-6}$ $w_2 \rightarrow dev + 5.32 \cdot 10^{-6}$ $w_3 \rightarrow dev - 5.83 \cdot 10^{-7}$	9000 $q_{e1} dev + 2.13 \cdot 10^{-3}$ $q_{e2} dev - 3.51 \cdot 10^{-3}$ $q_{e3} dev + 3.85 \cdot 10^{-3}$	213 <i>dev</i> $-9.55 \cdot 10^{-10}$	225 <i>dev</i> $+3.55 \cdot 10^{-3}$	0.595
Quaternion Error Control	80	15	4300 $w_1 \rightarrow \pm 6 \cdot 10^{-5}$ $w_2 \rightarrow \pm 1 \cdot 10^{-4}$ $w_3 \rightarrow \pm 1.83 \cdot 10^{-7}$	4350 $q_{e1} \rightarrow \pm 5.065 \cdot 10^{-6}$ $q_{e2} dev - 7.39 \cdot 10^{-6}$ $q_{e3} dev - 3.86 \cdot 10^{-3}$	60 $\pm 5 \cdot 10^{-3}$	3910 $\pm 0.02696$	0.4418
Flexible Control with Output Feedback controllers	1200	60	6050 $w_1 dev + 1.612 \cdot 10^{-6}$ $w_2 \rightarrow dev - 2.65 \cdot 10^{-6}$ $w_3 \rightarrow dev + 7.2 \cdot 10^{-9}$	7000 $q_{e1} - 3.395 \cdot 10^{-4}$ $q_{e2} + 6.381 \cdot 10^{-4}$ $q_{e3} \rightarrow -9.64 \cdot 10^{-4}$	210 $\pm 1.33 \cdot 10^{-6}$	350 <i>dev</i> $+6.14 \cdot 10^{-3}$	0.133
Quaternion Error Control	1200	60	1200 $w_1 \rightarrow osc + 4.93 \cdot 10^{-5}$ $-5.6 \cdot 10^{-5}$ $w_2 \rightarrow \pm 8 \cdot 10^{-5}$ $w_3 \rightarrow dev + 4.7 \cdot 10^{-9}$	1250 $q_{e1} \rightarrow \pm 4.33 \cdot 10^{-6}$ $q_{e2} \rightarrow \pm 7.02 \cdot 10^{-6}$ $q_{e3} dev - 9.64 \cdot 10^{-4}$	90 $\pm 5 \cdot 10^{-3}$	1050 <i>osc</i> $+0.025$ $-0.038$	Oscillate to achieve it 0.110

Nonlinear State Observer (2)	1200	60	1280	1250	75	910	0.11044
			$w_1 \rightarrow \sim 0$ $w_2 \rightarrow \sim 0$ $w_3 \rightarrow dev + 3.39 \cdot 10^{-13}$	$q_{e1} dev + 3.75 \cdot 10^{-8}$ $q_{e2} dev + 7.36 \cdot 10^{-8}$ $q_{e3} dev - 9.64 \cdot 10^{-4}$	$\pm 4.33 \cdot 10^{-3}$	$\pm 0.0241$	

Table 4 Time of convergence and precision performance of each control

Type of control	$k_p$	$k_{q_e}$	$t_{u_{maximum}}$ (s)	$\tau$ ( $N^2 \cdot m^2$ )	$\gamma$ ( $\frac{N^2 \cdot m^2}{s}$ )
Quaternion Error Control	50	4	1650	768986.812	76.891
Sliding Mode Control	50	4	10000 (All time)	237972.2	23.795
Nonlinear State Observer (1)	50	4	1712	1704087.591	170.392
Nonlinear State Observer (2)	50	4	1713	721875.273	72.180
Flexible Control	50	4	10000 (All time)	8217100.940	821.628
Flexible Control with Output Feedback controllers	50	4	990	566077.860	56.602
Flexible Control	450	125	10000 (All time)	8641341.755	864.048
Flexible Control with Output Feedback controllers	80	15	2575	1035861.910	103.576
Quaternion Error Control	80	15	3753	1843707.916	184.352
Flexible Control with Output Feedback controllers	1200	60	557	453522.880	45.348
Quaternion Error Control	1200	60	1016.4	1101525.968	110.142
Nonlinear State Observer (2)	1200	60	1008	546577.020	54.652

Table 5 Control Torque Requirements Performance of each control

(1). Nonlinear state observer control obtaining data of the angular velocities from a Quaternion Error controller

(2). Nonlinear state observer control having an own calculation of the angular velocities



### 9.2. Graphic results on each control implemented

To give the reader a better knowledge about the performance of each control and to be able to know how the spacecraft will behave during the transient until the convergence time it is desirable to present the plots of the angular velocity  $\vec{\omega}$ , the quaternion error  $\vec{q}_e$ , the control torque  $\vec{u}$ , the modal coordinate variable  $\eta$ , the total velocity of the flexible appendages  $\vec{\psi}$ , and the precision error versus time.

In all cases the time of simulation will be 10000 seconds. All the results of the tables before are obtained from the following plots.

#### Quaternion Error Control using gains: $k_p = 50, k_{q_e} = 4$

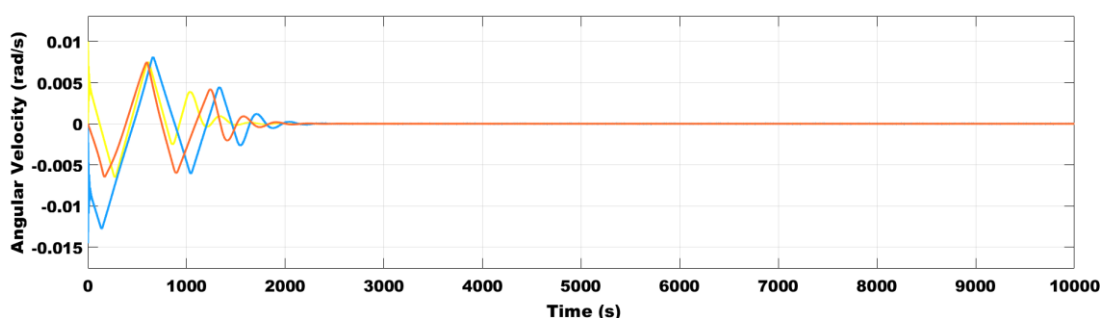


Figure 31 Angular Velocity vs time with Quaternion Error Control using gains:  $k_p=50, k_{q_e}=4$

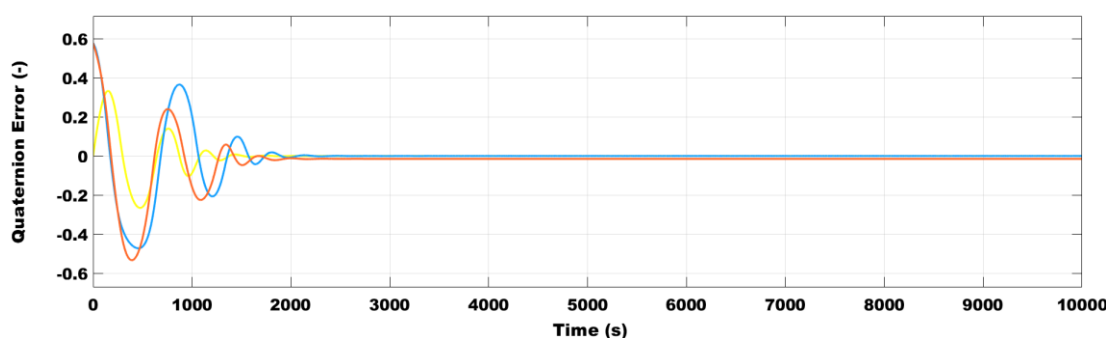


Figure 32 Quaternion Error vs time with Quaternion Error Control using gains:  $k_p=50, k_{q_e}=4$

In the Angular Velocity plot and the quaternion error plot there is an underdamped tendency to achieve the convergence. The frequency of the oscillation is not very high. Therefore it seems physically achievable to arrive to the convergence.

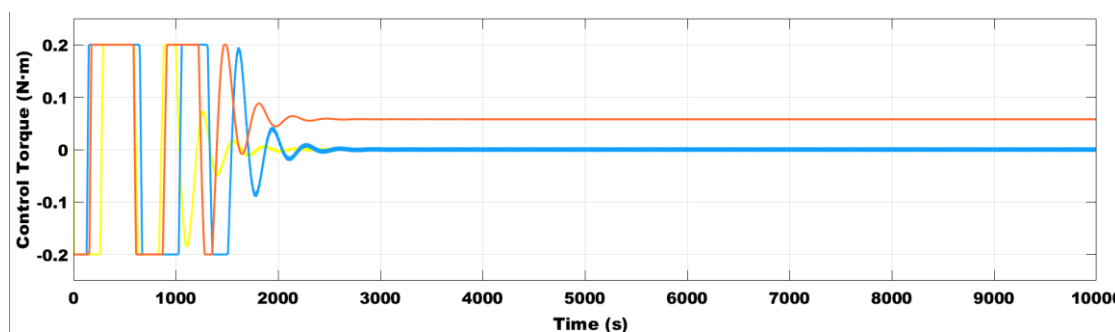


Figure 33 Control Torque vs time with Quaternion Error Control using gains:  $k_p=50$ ,  $k_{qe}=4$

In the case of the control there are some abrupt changes of the control torque and a final sinusoidal behaviour of the y component of the control that can cause struggles in the implementation of the control torque.

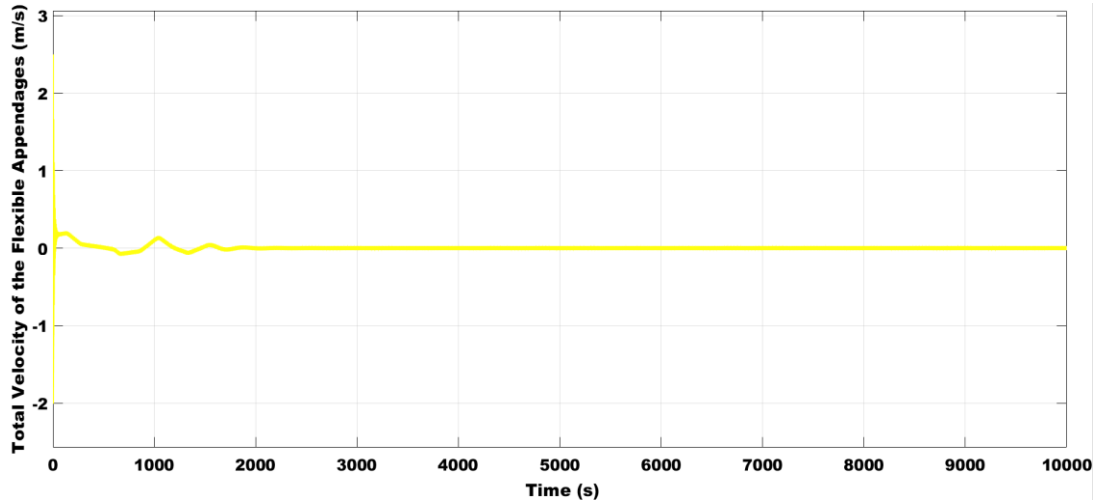


Figure 34 Total Velocity of the flexible appendages with Quaternion Error Control using gains  $k_p=50$ ,  $k_{qe}=4$

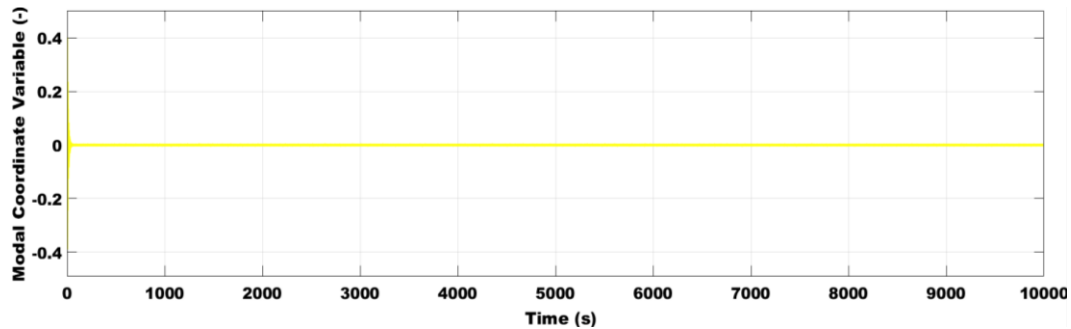


Figure 35 Modal state variable vs time with Quaternion Error Control using gains:  $k_p=50$ ,  $k_{qe}=4$

In the case of the tendency of the total velocity of the flexible appendages and the modal coordinate variable there is a very quick transient to achieve the convergence. In particular, in the total velocity of the flexible appendages plot there is a quite irregular behaviour during the first 2000 seconds, having some peaks but with a little amplitude. Those peaks are not desirable to cause great complications in performing this control.

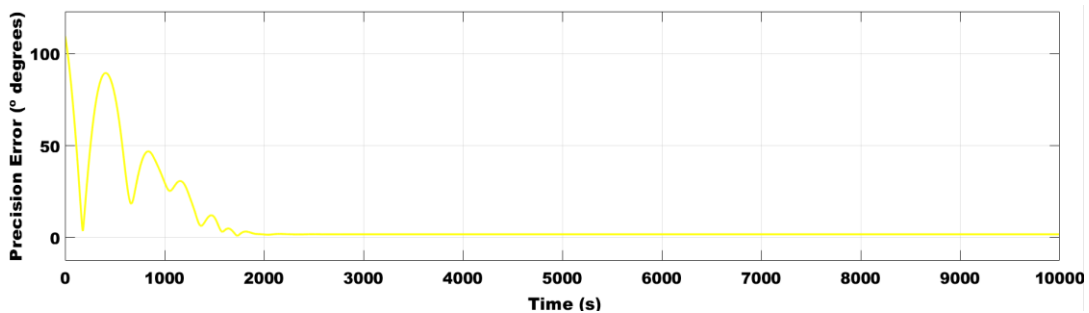


Figure 36 Precision error vs time with Quaternion Error Control using gains:  $k_p=50$ ,  $k_{qe}=4$

Considering the precision error, the transient to achieve the convergence is quite irregular. There are very big changes in the control at the first moments of its action. This big difference in the error can cause struggles in the real performance of the control.

### Quaternion error Control using gains: $k_p = 80, k_{q_e} = 15$

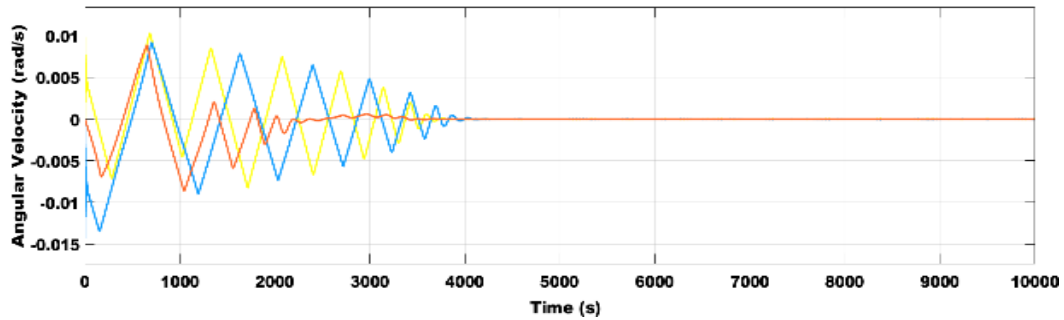


Figure 37 Angular Velocity vs time with vs time with Quaternion Error Control using gains:  $k_p=80, k_{q_e}=15$

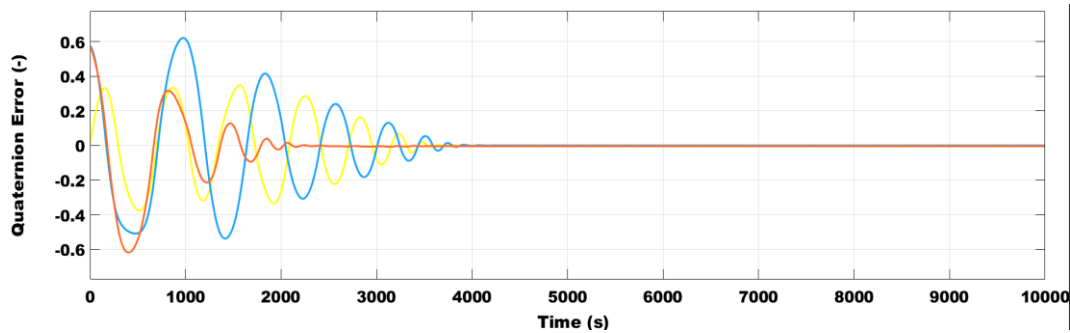


Figure 38 Quaternion Error vs time with Quaternion Error Control using gains:  $k_p=80, k_{q_e}=15$

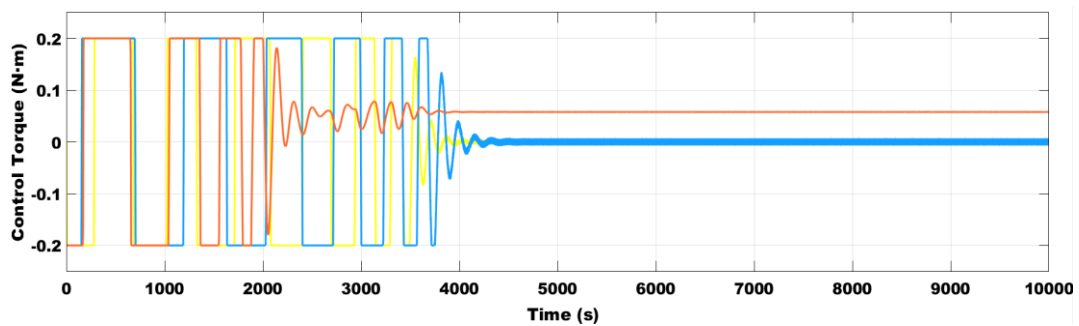


Figure 39 Control Torque vs time with Quaternion Error Control using gains:  $k_p=80, k_{q_e}=15$

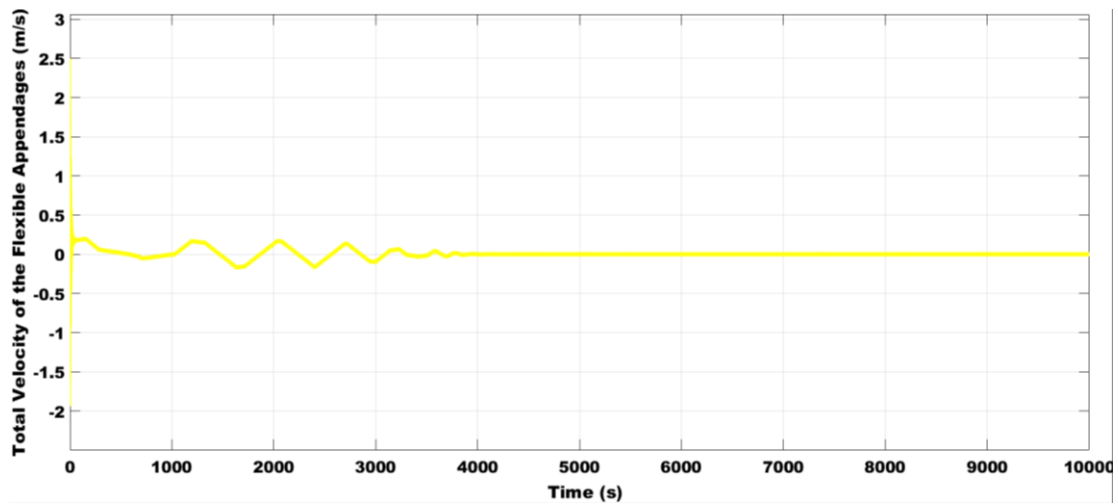


Figure 40 Total velocity of the flexible appendages vs time with Quaternion Error Control using gains:  $k_p=80, k_{qe}=15$

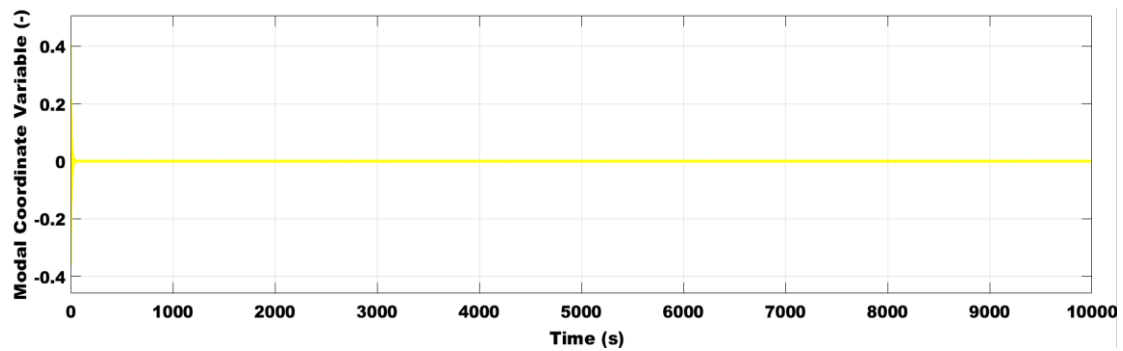


Figure 41 Modal coordinate variable vs time with Quaternion Error Control using gains:  $k_p=80, k_{qe}=15$

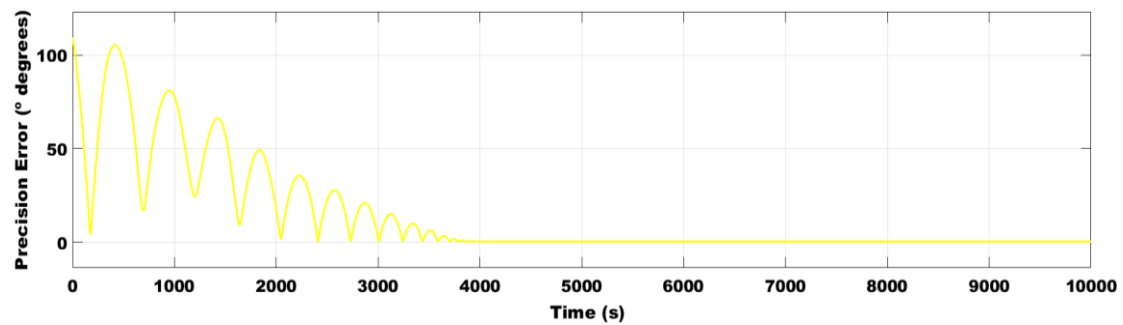


Figure 42 Precision Error vs time with Quaternion Error Control using gains:  $k_p=80, k_{qe}=15$

In comparison with the previous case, if the gains increase, the number of oscillations to achieve the convergence also increase. The time when the maximum control torque is required also increases. However, the transient has the same progression as the previous case, the quaternion control using gains  $k_p = 50, k_{qe} = 4$ . Furthermore, the final error at the convergence decreases. Therefore, the final precision is better but the movement to achieve this final stable state becomes more complex.

Sliding mode control using gains:  $k_p = 50, k_{q_e} = 4$

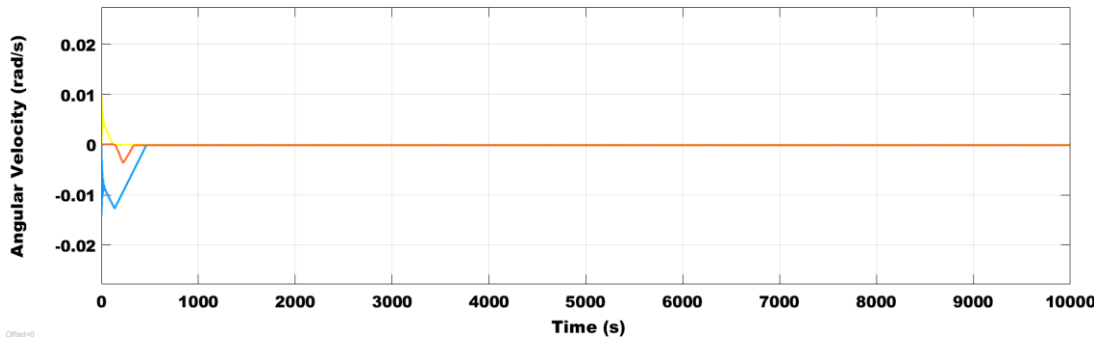


Figure 43 Angular velocity vs time with sliding mode control using gains:  $k_p=50, k_{q_e}=4$

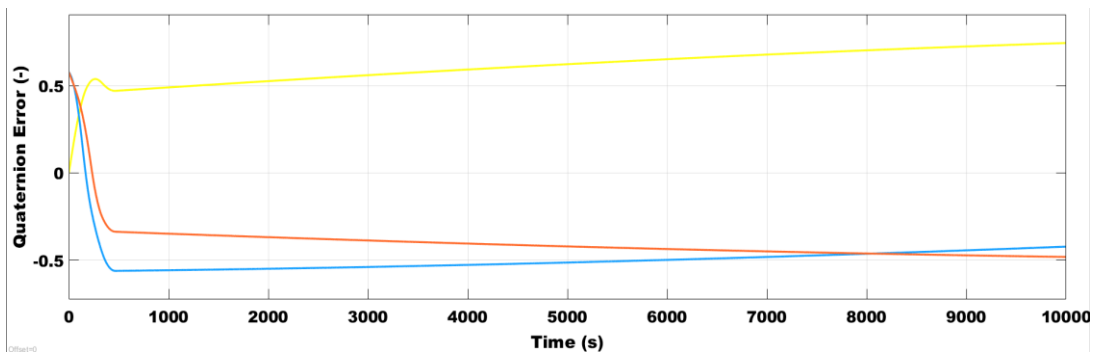


Figure 44 Quaternion Error vs time with sliding mode control using gains:  $k_p=50, k_{q_e}=4$

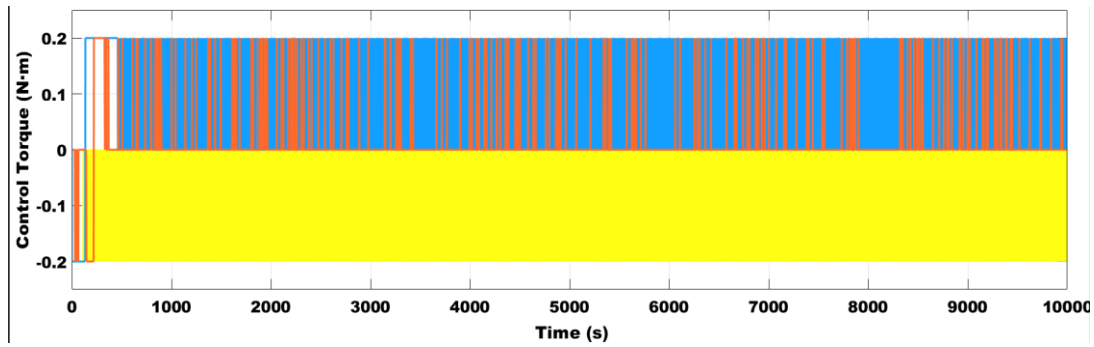


Figure 45 Control Torque vs time with sliding mode control using gains:  $k_p=50, k_{q_e}=4$

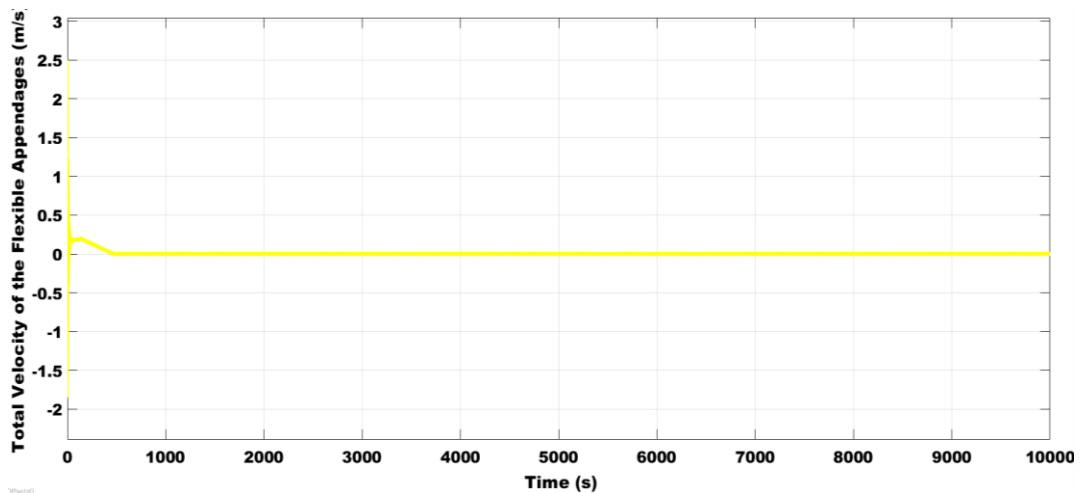


Figure 46 Total velocity of the flexible appendages vs time with sliding mode control using gains:  $k_p=50$ ,  $k_{qe}=4$

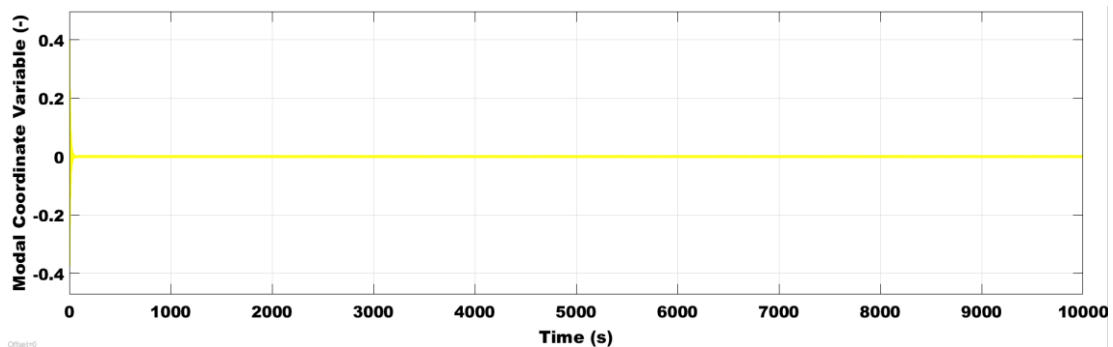


Figure 47 Modal coordinate variable vs time with sliding mode control using gains:  $k_p=50$ ,  $k_{qe}=4$

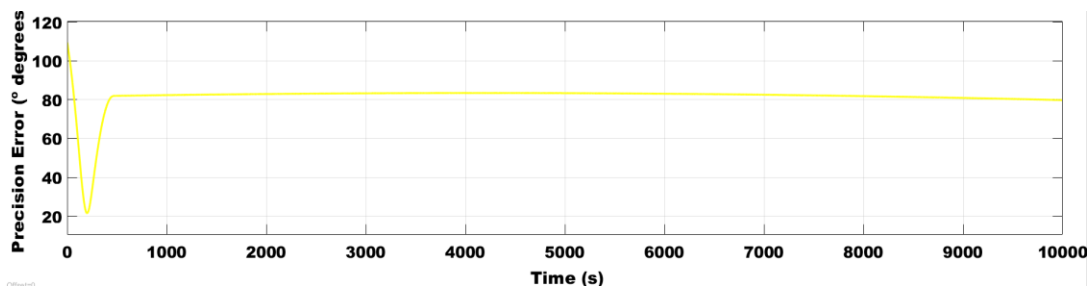


Figure 48 Precision error vs time with sliding mode control using gains:  $k_p=50$ ,  $k_{qe}=4$

A final stabilization is not achieved using this type of control. This aspect can be easily noted regarding the plots of quaternion error and precision error, the final values are not zero or do not tend to zero. That shows that a final stabilization is not achieved. Nevertheless, in terms of angular velocity there is a great transient response using this control. The total velocity of the flexible appendages and the modal coordinate variable progress in the same way than using the quaternion error control. Moreover, the required control torque seems unfeasible. There is a need of using the maximum torque during all the implementation. Theoretically the required total torque in global during all the implementing time is not really high but implementing this type of control in the reality it seems not possible that the thrusters (the actual actuator of the sliding mode control) would work that amount of time continuously.

**Nonlinear state observer control (1) using gains:  $k_p = 50, k_{q_e} = 4$**

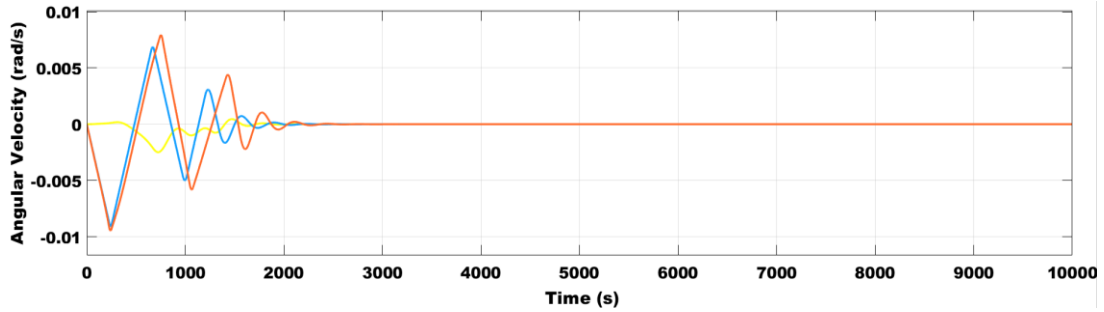


Figure 49 Angular velocity vs time with nonlinear state observer control (1) using gains:  $k_p=50, k_{q_e}=4$

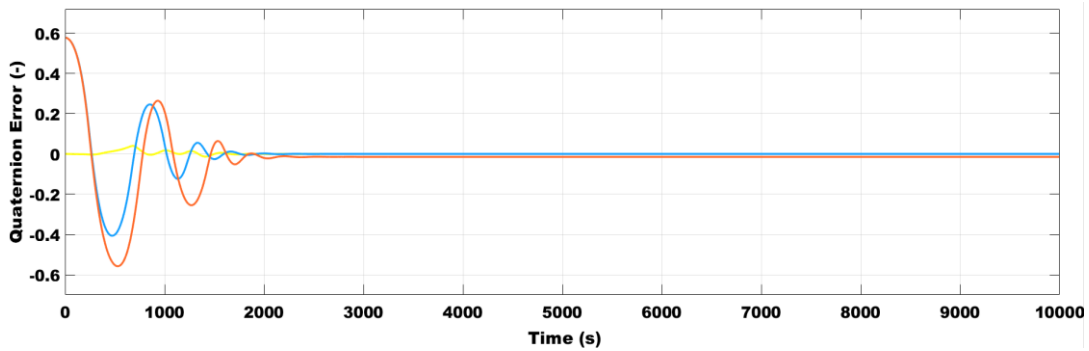


Figure 50 Quaternion Error vs time with nonlinear state observer control (1) using gains:  $k_p=50, k_{q_e}=4$

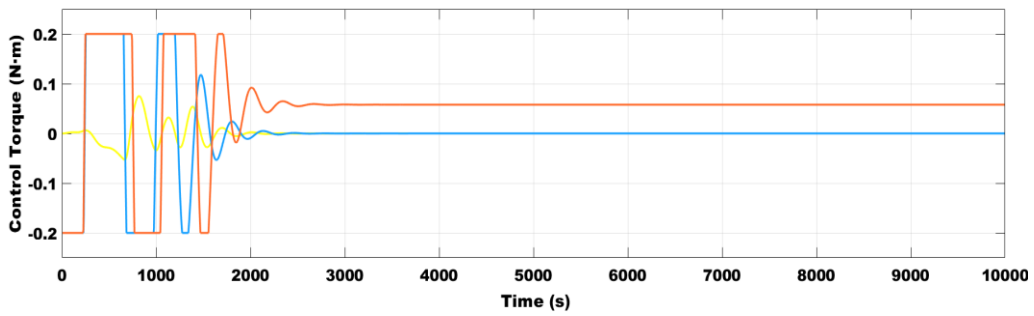


Figure 51 Control Torque vs time with nonlinear state observer control (1) using gains:  $k_p=50, k_{q_e}=4$

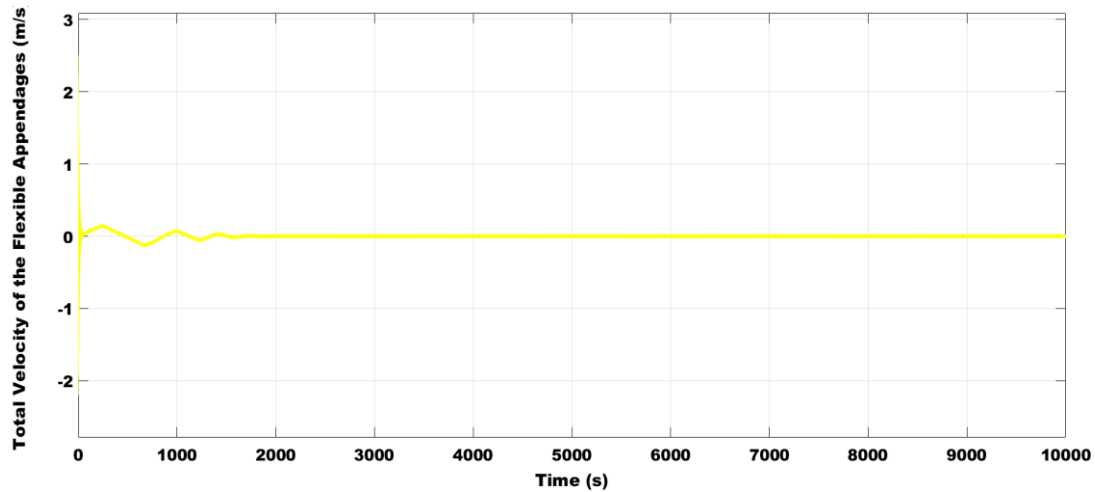


Figure 52 Total Velocity of the flexible appendages vs time with nonlinear state observer control (1) using gains:  $k_p=50, k_{qe}=4$

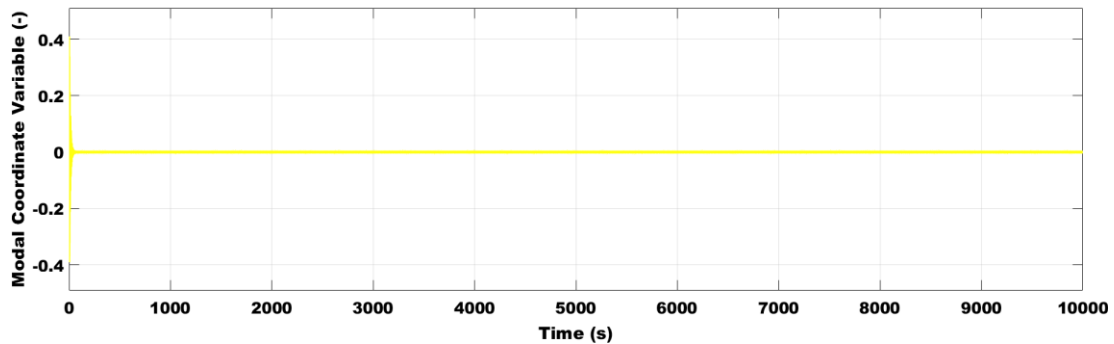


Figure 53 Modal coordinate variable vs time with nonlinear state observer control (1) using gains:  $k_p=50, k_{qe}=4$

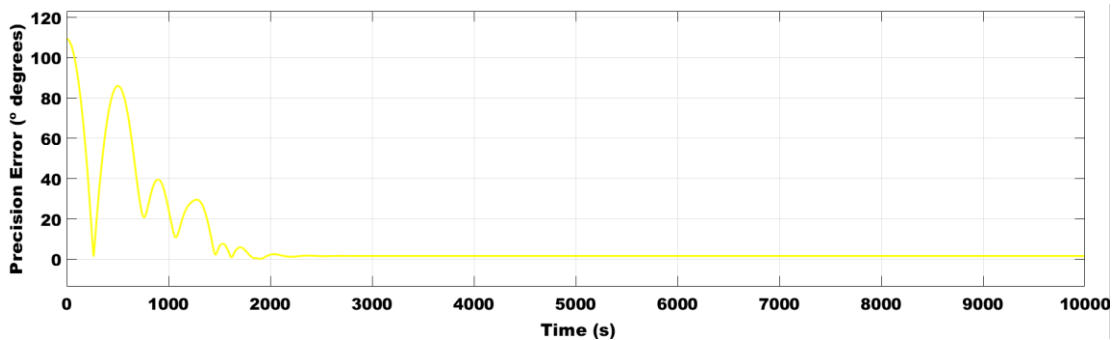


Figure 54 Precision Error vs time with nonlinear state observer control (1) using gains:  $k_p=50, k_{qe}=4$

Considering only the progression of the variables during the transient, the nonlinear state observer (1) has approximately the same evolution than the quaternion error control. Nevertheless the final convergence error decreases, that is a crucial aspect to consider in the comparison. Particularly, the first component of the angular velocity and the first component of the component of the quaternion error has a less oscillative nature. The amplitude of its oscillation is way lower than the other two components and has a smoother progression.



**Flexible Control using gains:  $k_p = 450, k_{q_e} = 125$**

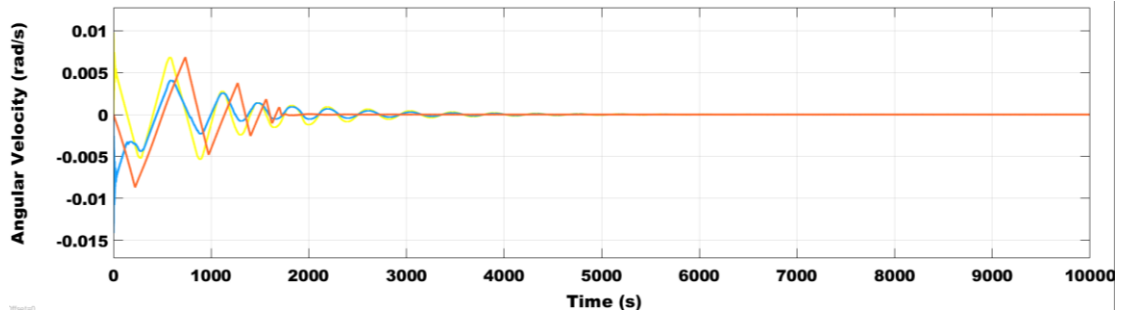


Figure 55 Angular Velocity vs time with Flexible Control using gains:  $k_p=450, k_{q_e}=125$

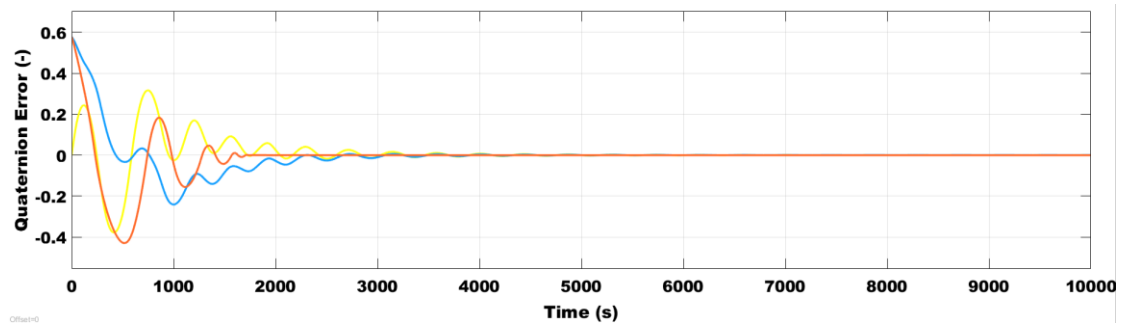


Figure 56 Quaternion Error vs time with Flexible Control using gains:  $k_p=450, k_{q_e}=125$

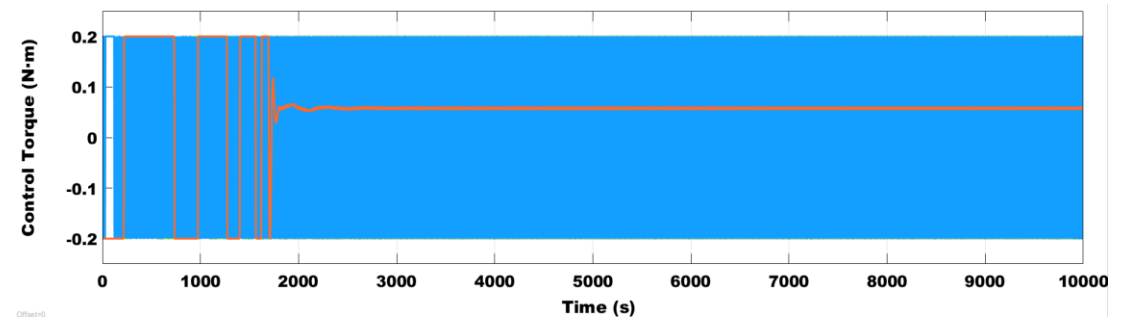


Figure 57 Control Torque vs time with Flexible Control using gains:  $k_p=450, k_{q_e}=125$

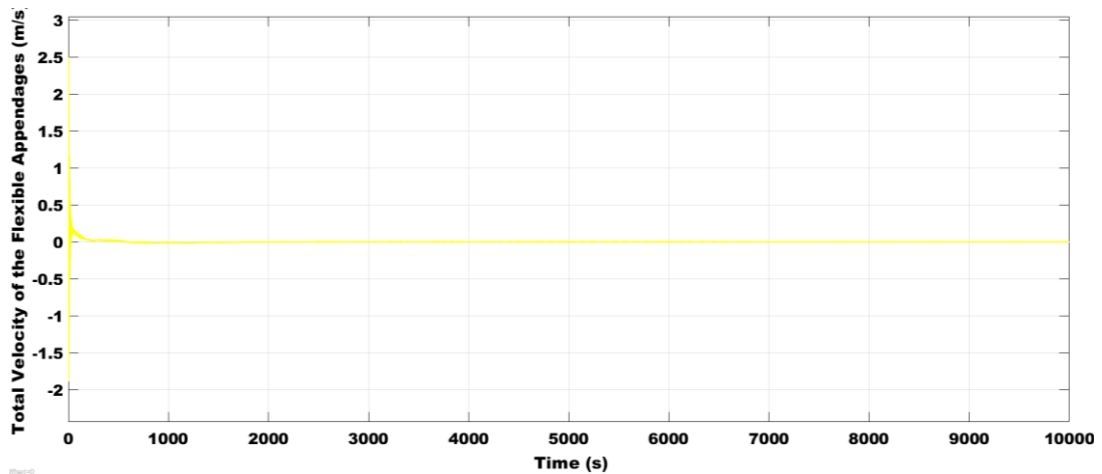


Figure 58 Total velocity of the flexible appendages vs time with Flexible Control using gains:  $k_p=450, k_{q_e}=125$

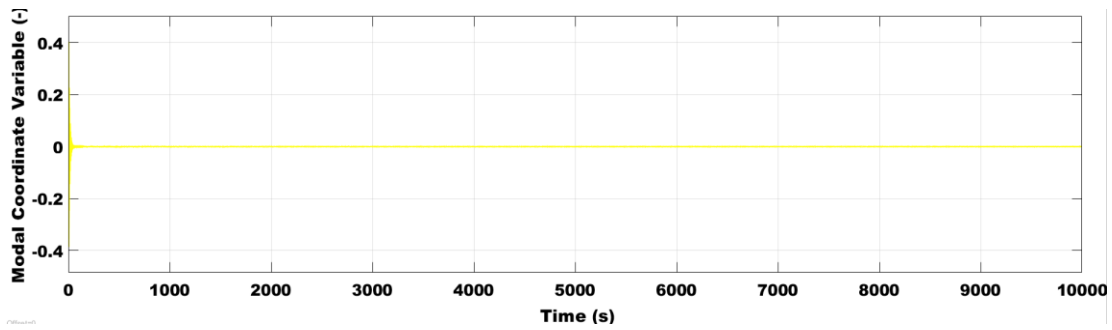


Figure 59 Modal Coordinate Variable vs time with Flexible Control using gains:  $k_p=450, k_{qe}=125$

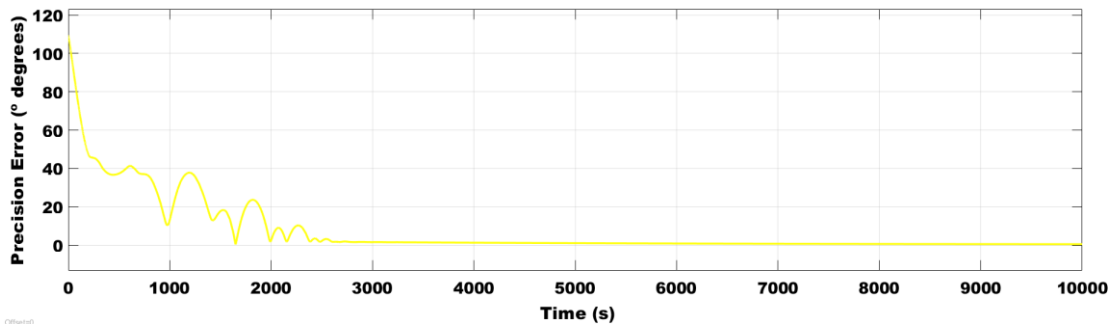


Figure 60 Precision Error vs time with Flexible Control using gains:  $k_p=450, k_{qe}=125$

The flexible control has a slightly different response of the transient regarding the angular velocity and the quaternion error plot. Usually the three components of the angular velocity and the quaternion error have a similar tendency during the transient. In this case the three components have an independent response than the others. This aspect reduces the probability of coupling of the response. Nevertheless this aspect will not cause a major consequence of the implementation of the control.

**Flexible control Estimation with output feedback controllers using gains:  $k_p = 50, k_{qe} = 4$**

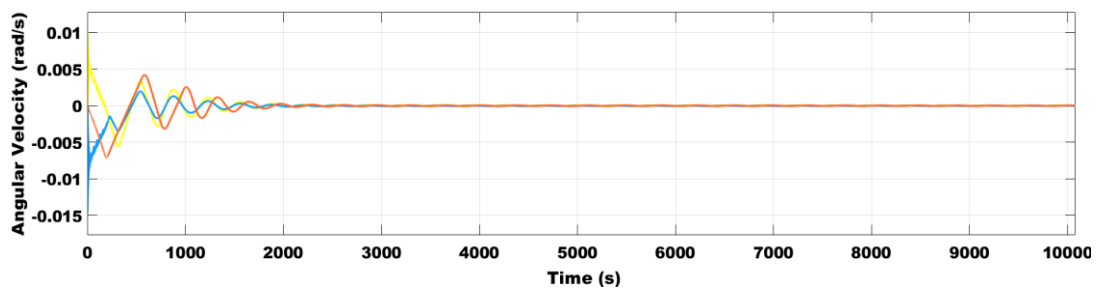


Figure 61 Angular Velocity vs time with Flexible Control Estimation with output feedback controllers using gains:  $k_p=50, k_{qe}=4$

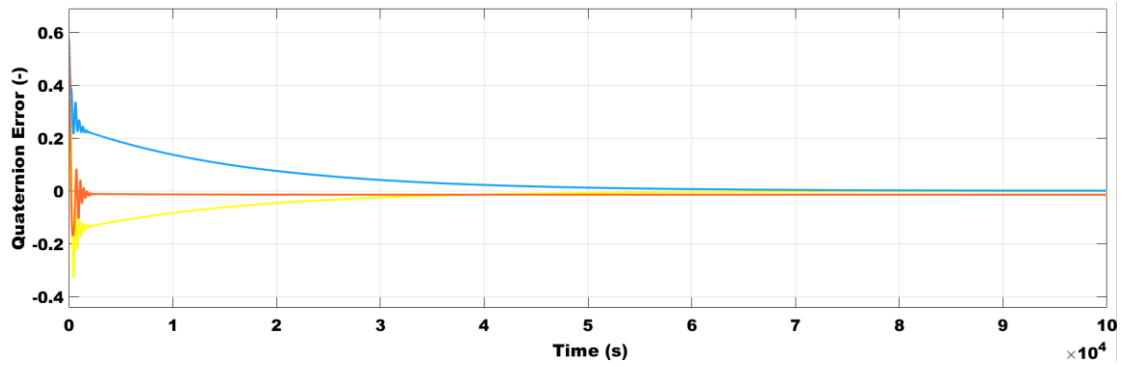


Figure 62 Quaternion Error vs time with Flexible Control Estimation with output feedback controllers using gains:  $k_p=50, k_{qe}=4$

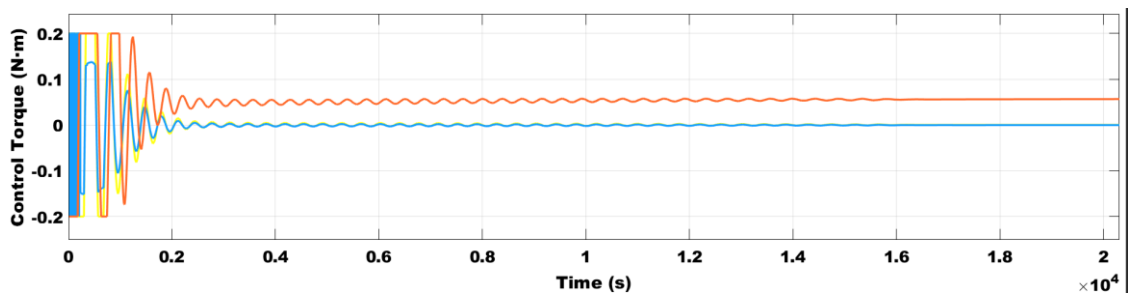


Figure 63 Control Torque vs time with Flexible Control Estimation with output feedback controllers using gains:  $k_p=50, k_{qe}=4$

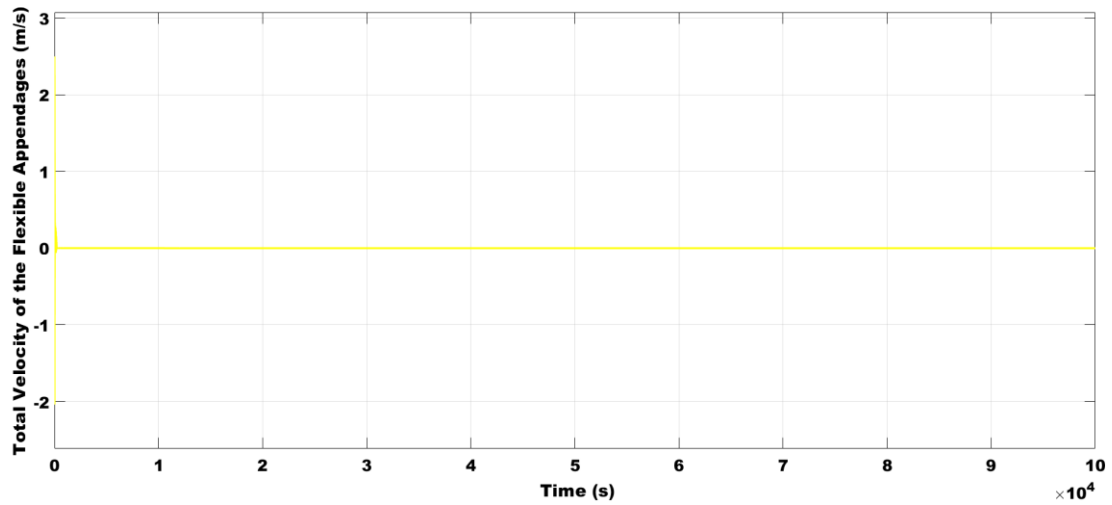


Figure 64 Total Velocity of the Flexible Appendages vs time with Flexible Control Estimation with output feedback controllers using gains:  $k_p=50, k_{qe}=4$

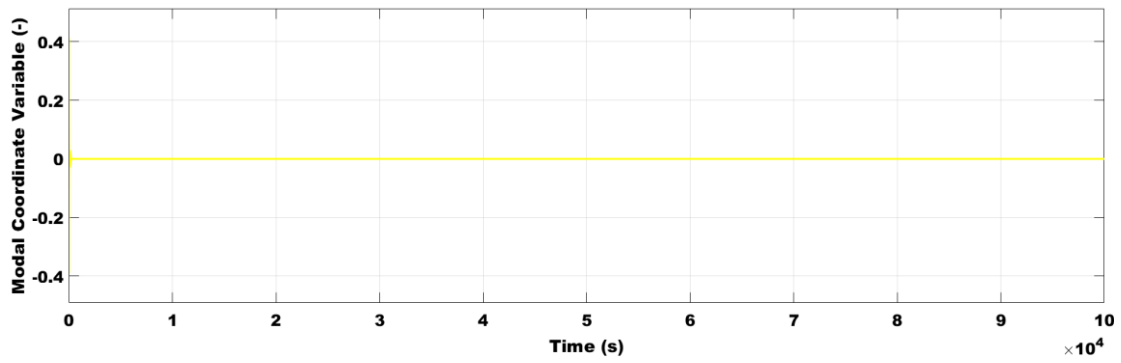


Figure 65 Modal Coordinate Variable vs time with Flexible Control Estimation with output feedback controllers using gains:  $k_p=50, k_{q_e}=4$

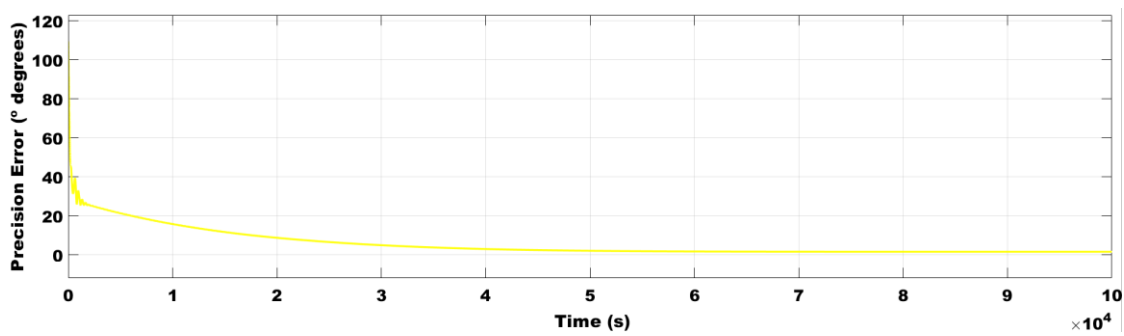


Figure 66 Precision Error vs time with Flexible Control Estimation with output feedback controllers using gains:  $k_p=50, k_{q_e}=4$

This control with these selected gains provide a really smooth response of the main part of the transient of the quaternion error and the precision error. Also, the number of oscillations to achieve the convergence of the angular velocity reduce. Those two aspects are very desirable in the implementation of the control. However, the required torque has an oscillating nature. This can cause inconvenient and complexity on the real implementation of the control.

**Flexible control estimation with output feedback controllers using gains:  $k_p = 80, k_{q_e} = 15$**

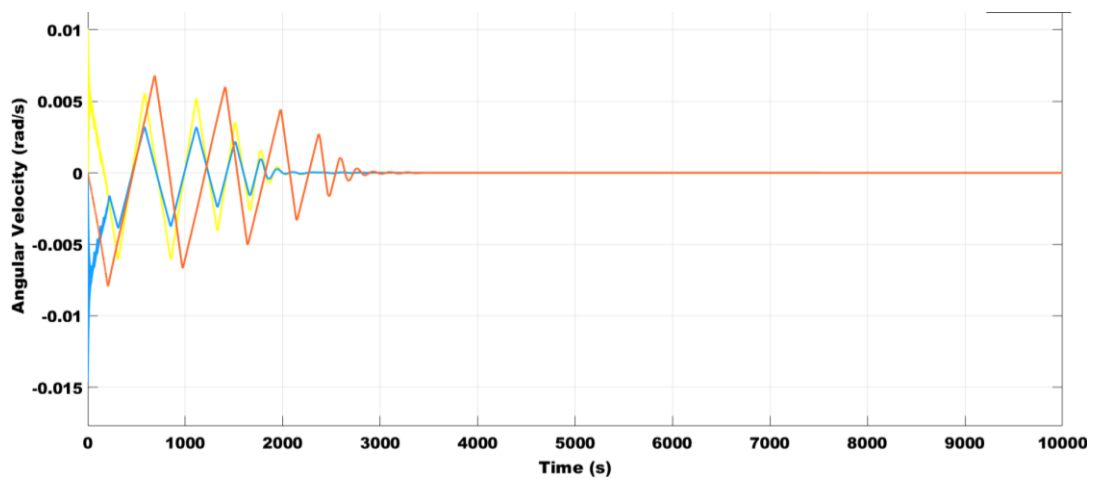


Figure 67 Angular Velocity vs time with Flexible control estimation with output feedback controllers using gains:  $k_p=80, k_{q_e}=15$

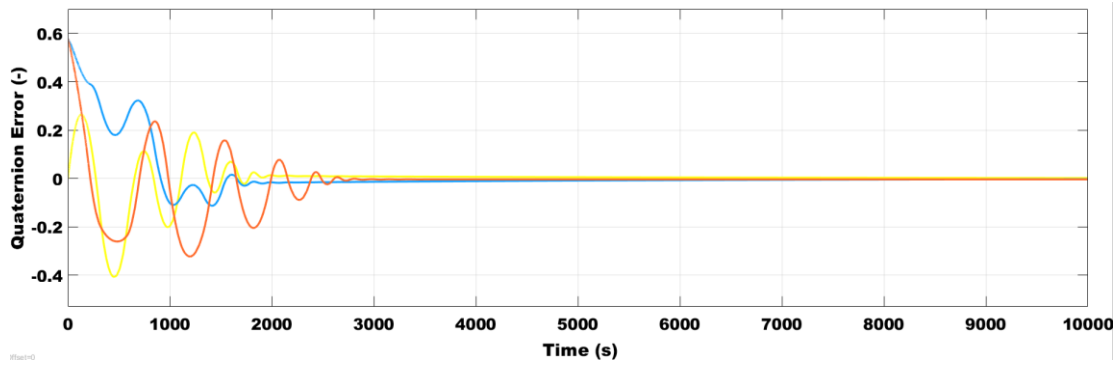


Figure 68 Quaternion Error vs time with Flexible control estimation with output feedback controllers using gains:  $k_p=80, k_{qe}=15$

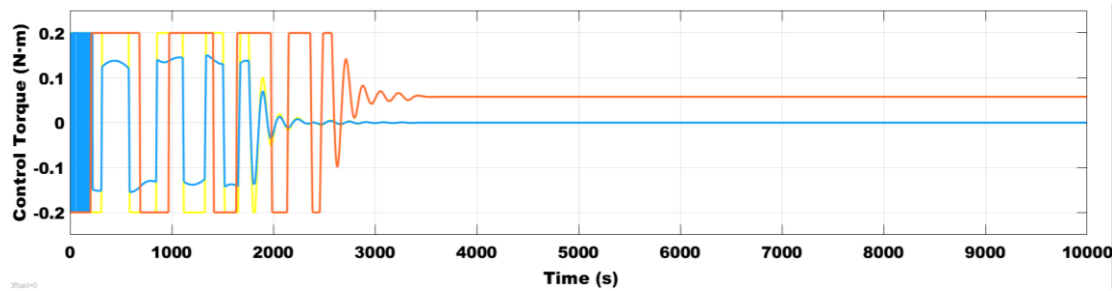


Figure 69 Control Torque vs time with Flexible control estimation with output feedback controllers using gains:  $k_p=80, k_{qe}=15$

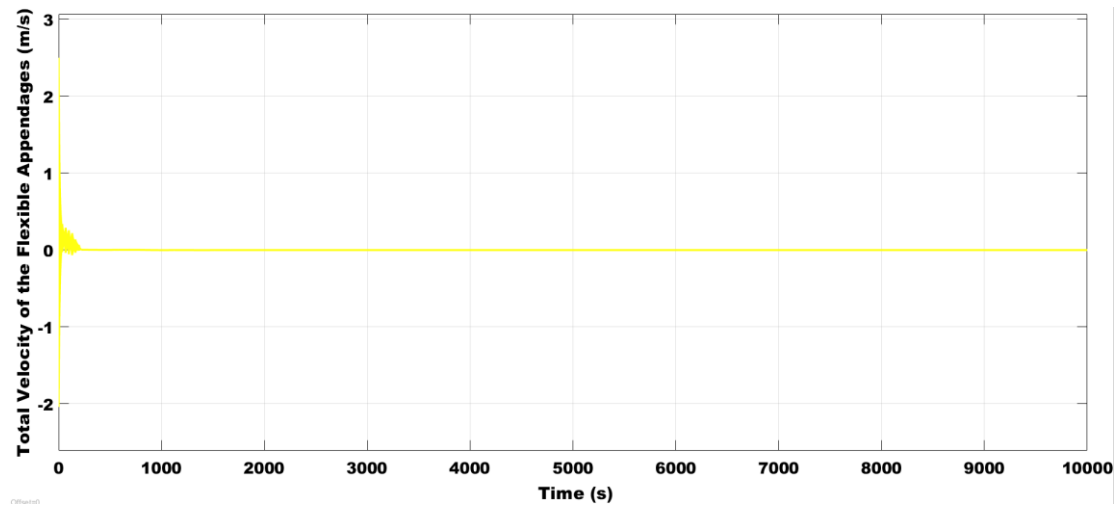


Figure 70 Total Velocity of the flexible appendages vs time with Flexible control estimation with output feedback controllers using gains:  $k_p=80, k_{qe}=15$

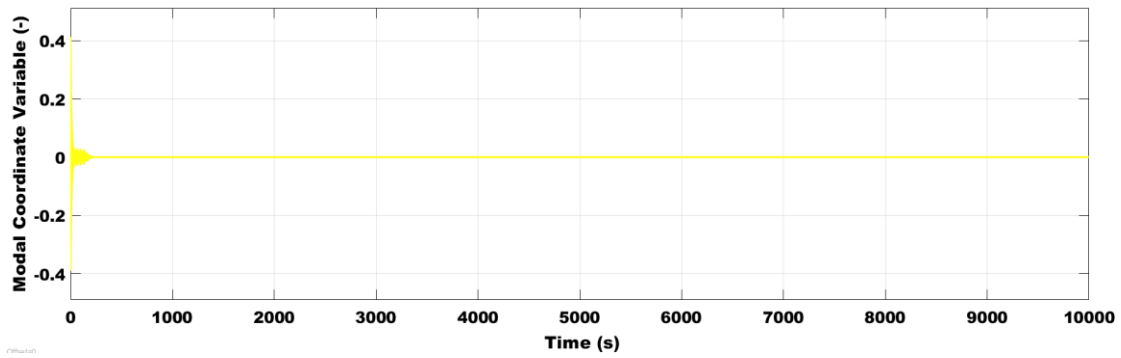


Figure 71 Modal Coordinate Variable vs time with Flexible control estimation with output feedback controllers using gains:  $k_p=80, k_{q_e}=15$

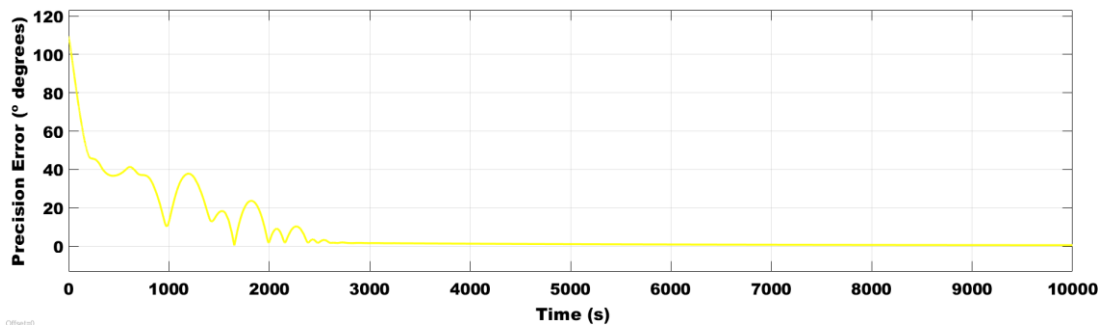


Figure 72 Precision Error vs time with Flexible control estimation with output feedback controllers using gains:  $k_p=80, k_{q_e}=15$

Increasing the gains of the flexible control with output feedback controllers cause a big change in the transient of the variables. Specially in the angular velocity, the quaternion error and the precision error. The quantity and amplitude of the oscillations increase, losing the smooth tendency accomplished in the previous case. The time when maximum torque is required increases.

The modal state variable and the total velocity of the flexible appendages tendency do not suffer a major change. The convergence is still achieved in a very quick way.

The final error in the convergence of most of the state variables decreases. This fact is really desirable considering the possible implementation of the control. Also the oscillating nature of the control torque required vanishes, simplifying the implementation of the control.

**Quaternion Error Control using gains:  $k_p = 1200, k_{q_e} = 60$**

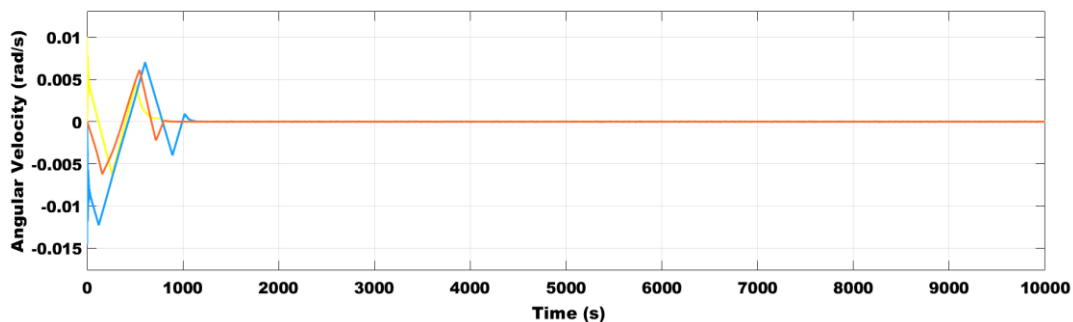


Figure 73 Angular Velocity vs time with Quaternion Error Control using gains:  $k_p=1200$ ,  $k_{qe}=60$

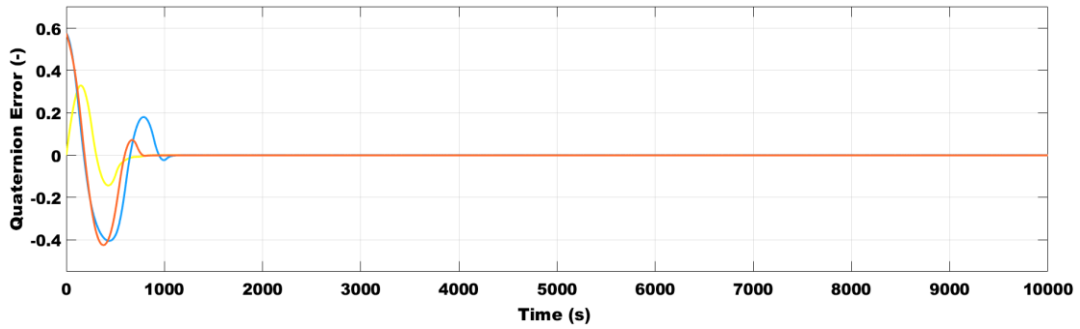


Figure 74 Quaternion Error vs time with Quaternion Error Control using gains:  $k_p=1200$ ,  $k_{qe}=60$

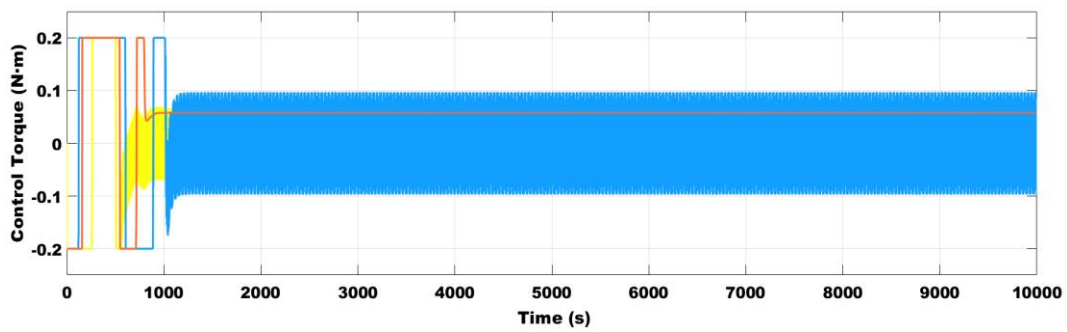


Figure 75 Control Torque vs time with Quaternion Error Control using gains:  $k_p=1200$ ,  $k_{qe}=60$

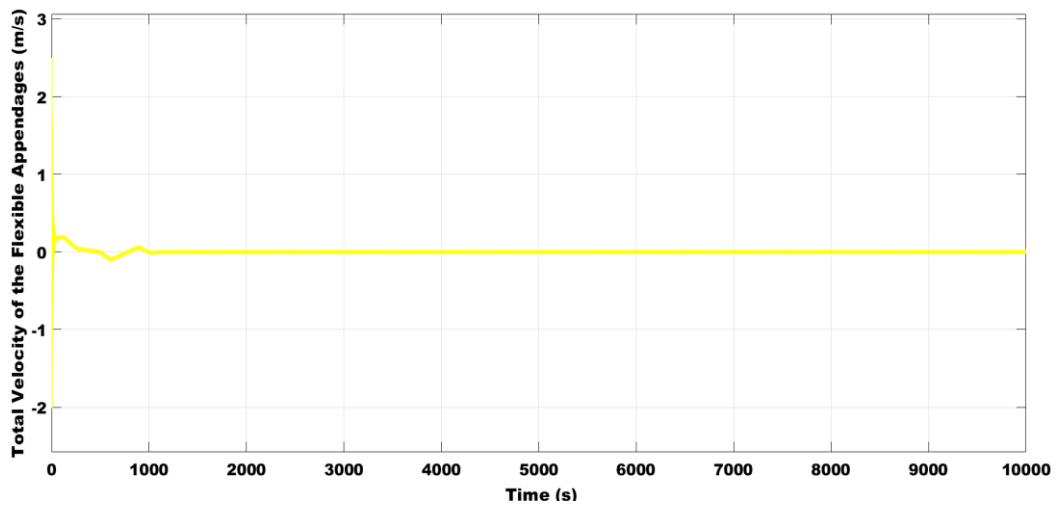


Figure 76 Total Velocity of the Flexible Appendages vs time with Quaternion Error Control using gains:  $k_p=1200$ ,  $k_{qe}=60$

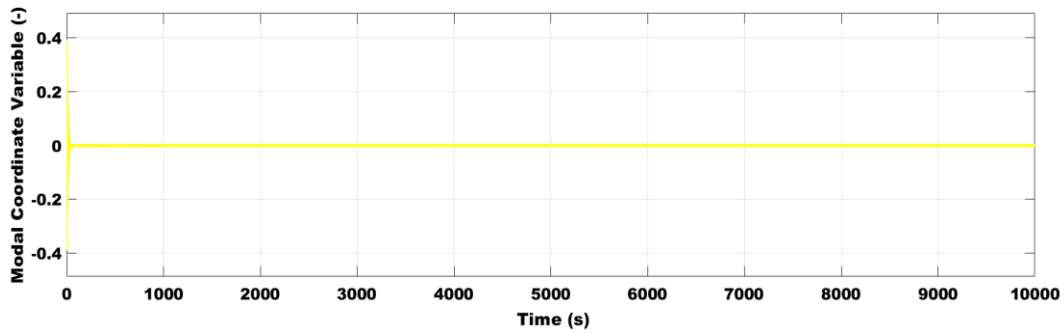


Figure 77 Modal Coordinate Variable vs time with Quaternion Error Control using gains:  $k_p=1200$ ,  $k_{q_e}=60$

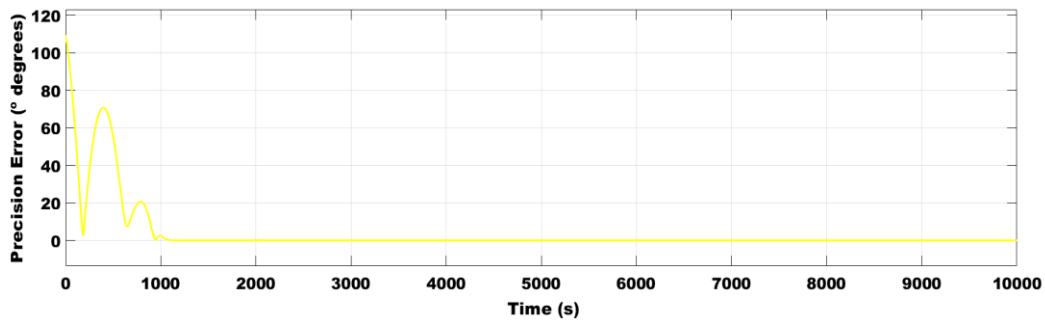


Figure 78 Precision Error vs time with Quaternion Error Control using gains:  $k_p=1200$ ,  $k_{q_e}=60$

Increasing the gains, the number of oscillations of the angular velocity and the quaternion error decrease, and its convergence is achieved in less time. This fact is high desirable when performing the control. In terms of the modal state variable and the total velocity of the flexible appendages the transient response is approximately the same. The main disadvantage is that the required torque to perform the control is higher during the implementation.

**Nonlinear state observer control (2), using gains:  $k_p = 1200$ ,  $k_{q_e} = 60$**

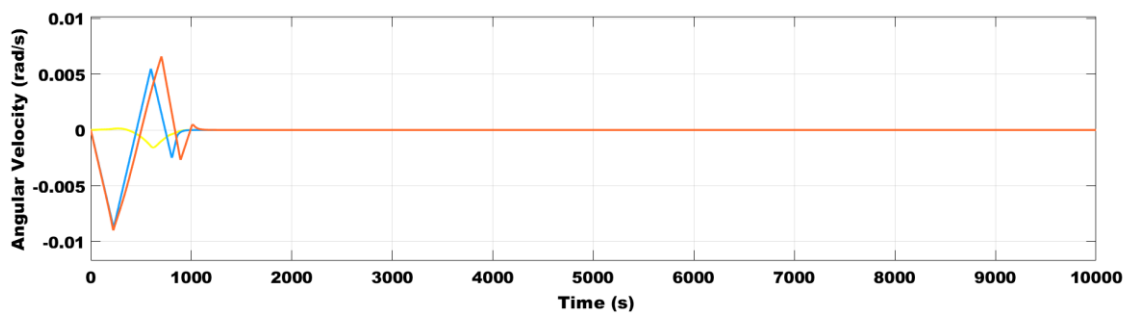


Figure 79 Angular Velocity vs time with Nonlinear state observer control (2), using gains:  $k_p=1200$ ,  $k_{q_e}=60$



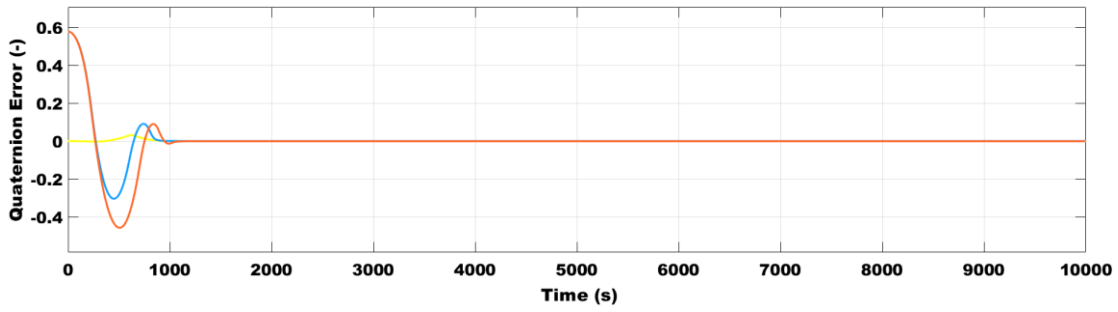


Figure 80 Quaternion Error vs time with Nonlinear state observer control (2), using gains:  $k_p=1200$ ,  $k_{qe}=60$

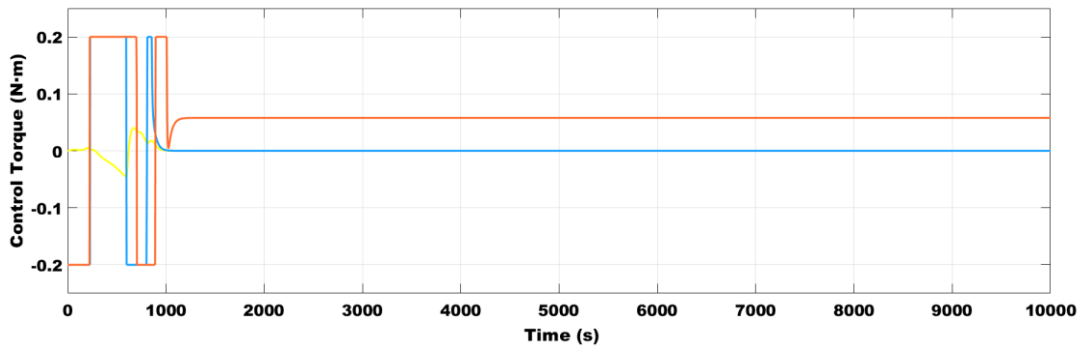


Figure 81 Control Torque vs time with Nonlinear state observer control (2), using gains:  $k_p=1200$ ,  $k_{qe}=60$

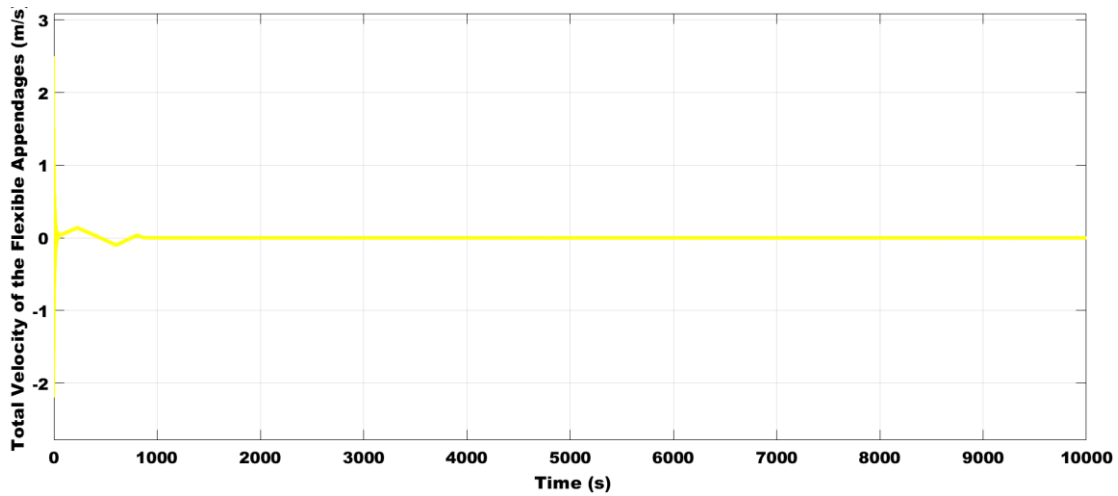


Figure 82 Total Velocity of the flexible Appendages vs time with Nonlinear state observer control (2), using gains:  $k_p=1200$ ,  $k_{qe}=60$

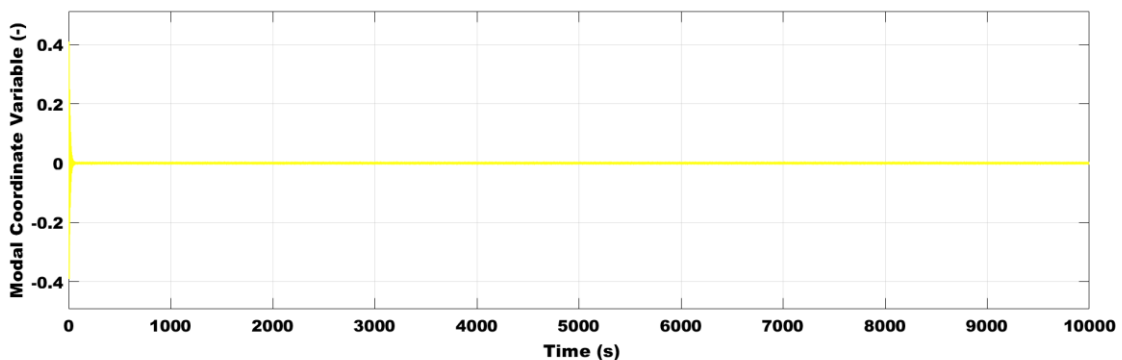


Figure 83 Modal Coordinate Variable vs time with Nonlinear state observer control (2), using gains:  $k_p=1200, k_{q_e}=60$

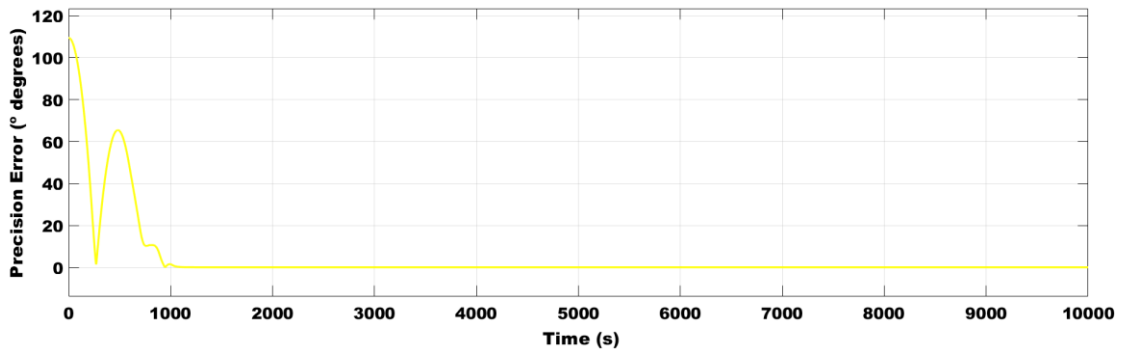


Figure 84 Precision Error vs time with Nonlinear state observer control (2), using gains:  $k_p=1200, k_{q_e}=60$

In comparison with the quaternion error control using gains:  $k_p = 1200, k_{q_e} = 60$ , the big difference is that the quaternion error performance has a high improvement. The number of oscillations of the second and the third component of the quaternion error reduce dramatically. The third component of the quaternion error has practically a constant behaviour. This quaternion error response of this selected control with those gains selected is the best one achieved considering all the controls implemented.

The required torque needed to perform this control becomes lower than using the same control but with lower gains. Also, the torque needed at the convergence has a constant behaviour. This circumstance is advantageous when performing the selected control.

Referring to the modal state variable and the total velocity of the flexible appendages there is not a big difference in the behaviour of the response.

**Flexible control estimation with output feedback controllers using gains:  $k_p = 1200, k_{q_e} = 60$**

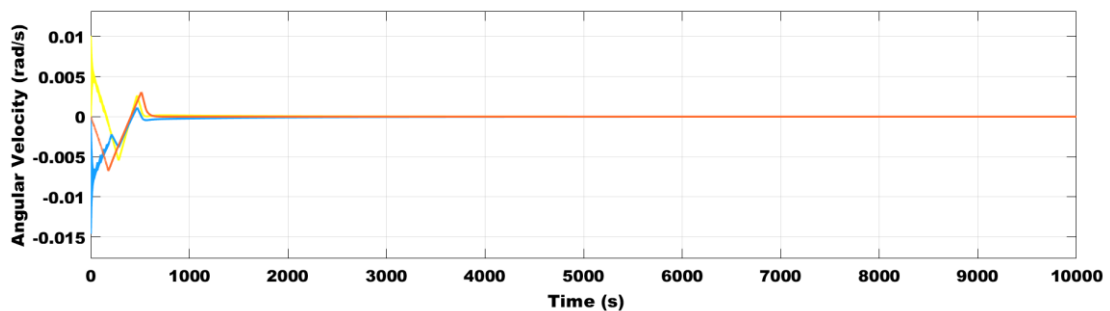


Figure 85 Angular Velocity vs time with Flexible control estimation with output feedback controllers using gains:  $k_p=1200, k_{q_e}=60$

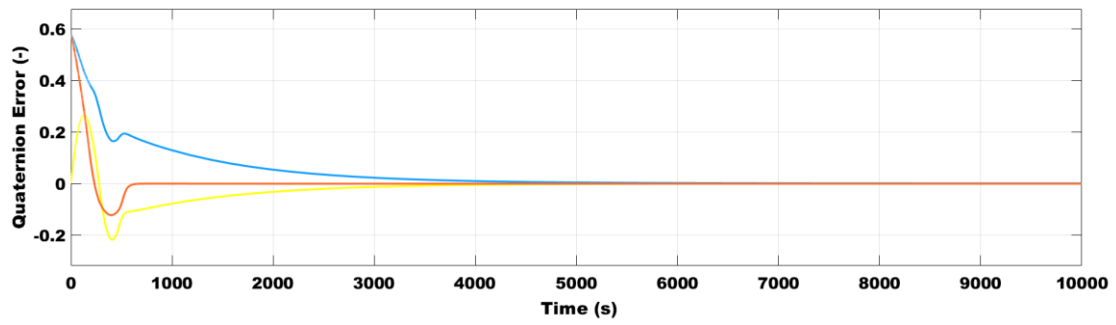


Figure 86 Quaternion Error vs time with Flexible control estimation with output feedback controllers using gains:  $k_p=1200$ ,  $k_{qe}=60$

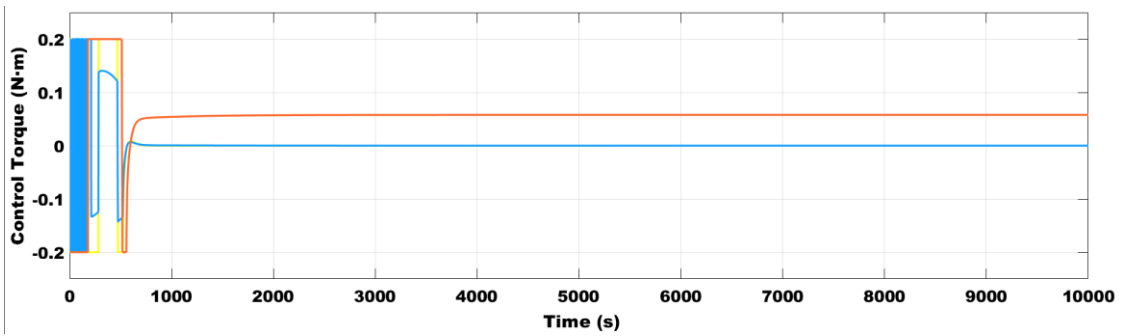


Figure 87 Control Torque vs time with Flexible control estimation with output feedback controllers using gains:  $k_p=1200$ ,  $k_{qe}=60$

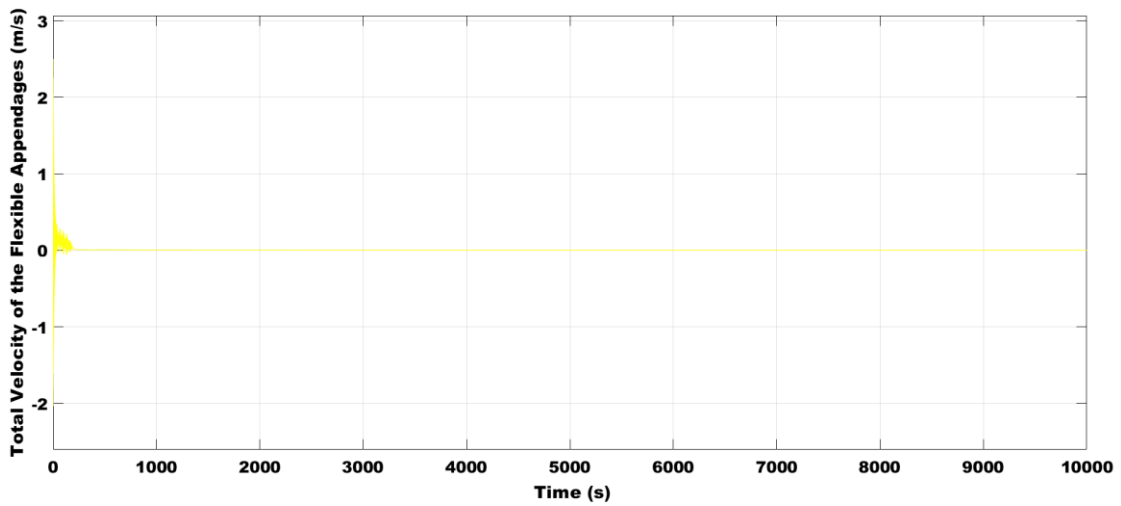


Figure 88 Total Velocity of the Flexible Appendages vs time with Flexible control estimation with output feedback controllers using gains:  $k_p=1200$ ,  $k_{qe}=60$

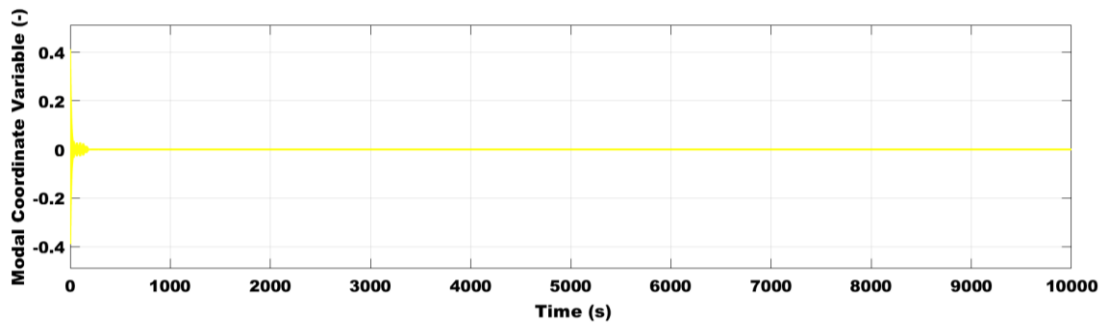


Figure 89 Modal Coordinate Variable vs time with Flexible control estimation with output feedback controllers using gains:  $k_p=1200$ ,  $k_{qe}=60$

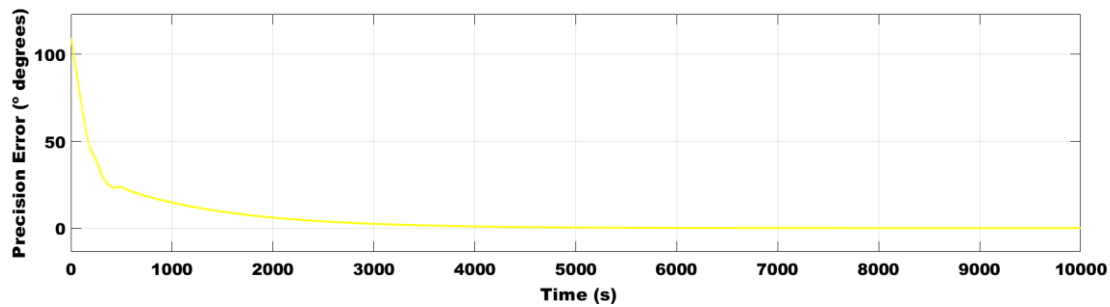


Figure 90 Precision Error vs time with Flexible control estimation with output feedback controllers using gains:  $k_p=1200$ ,  $k_{qe}=60$

The flexible control with output feedback controllers using gains:  $k_p = 1200$ ,  $k_{q_e} = 60$  has the best performance in terms of the angular velocity. The number of the oscillations are the same as the nonlinear state observer control (2), using gains:  $k_p = 1200$ ,  $k_{q_e} = 60$  however the amplitude of that oscillations is lower, having so a smoother tendency.

Referring to the quaternion error performance this control with those selected gains has the smoother response of the three components of the quaternion error. The second-best performance found of the quaternion error is the found using the flexible control estimation with output feedback controllers using gains:  $k_p = 50$ ,  $k_{q_e} = 4$ .

The modal state variable and the total velocity of the flexible appendages have a higher variance of the first implementation time, nevertheless both variables converge rapidly. Therefore, at a general view there is not a big difference implementing this control instead of the other controls.

In comparison with the quaternion error control using gains:  $k_p = 1200$ ,  $k_{q_e} = 60$  and the nonlinear state observer control (2), using gains:  $k_p = 1200$ ,  $k_{q_e} = 60$  there is an improvement of the required torque to control the spacecraft. The time when the maximum torque is required becomes lower and the global control required on the implementation is lower than the other two cases. Hence, this control with these selected gains is more cost effective, requiring less torque, and then less energy to perform its correct activity.

### 9.3. Ranking of the controllers and final selection

At this moment there is a knowledge of the results of each control in each configuration of gains. Also, a knowledge of the tendency of each of the variables during the transient. Therefore, to

do a proper comparison and a selection of the most appropriate control it is required to rank the controls according to different preferences. In the following table there is a ranking of all the configurations of the controls implemented. It has been decided to rank each control with each configuration considering the time of convergence of the angular velocity  $\vec{\omega}$ , the quaternion error  $\vec{q}_e$ , the modal state variable  $\eta$  and the total velocity of the flexible appendages  $\vec{\psi}$ .

Then also it has been decided to rank each control with each configuration considering the final error at its convergence of the time of convergence of the angular velocity  $\vec{\omega}$ , the quaternion error  $\vec{q}_e$ , the modal state variable  $\eta$  and the total velocity of the flexible appendages  $\vec{\psi}$ .

Moreover, it has been decided to rank each control with each configuration considering the final precision error  $\phi$ . And finally considering the time with maximum torque required  $t_{u_{maximum}}$  and the torque requiring constant per second  $\gamma$ .

Type of control	$k_p$	$k_{q_e}$	Time to converge				Error at the convergence					Torque requirement	
			$\vec{\omega}$	$\vec{q}_e$	$\eta$	$\vec{\psi}$	$\vec{\omega}$	$\vec{q}_e$	$\eta$	$\vec{\psi}$	$\phi$	$t_{u_{max}}$	$\gamma$
Quaternion Error Control	50	4	5	4	5	11	8	7	11	11	7	6	6
Sliding Mode Control	50	4	1	11	6	4	10	11	10	9	11	12	1
Nonlinear State Observer (1)	50	4	4	3	2	9	4	8	4	2	9	7	9
Nonlinear State Observer (2)	50	4	6	5	4	10	3	6	7	7	8	8	5
Flexible Control	50	4	12	12	12	7	12	12	5	4	12	11	11
Flexible Control													

with Output Feedback controllers	50	4	11	9	10	2	5	10	1	1	10	2	4
Flexible Control	450	125	9	7	11	8	9	3	6	6	1	10	12
Flexible Control with Output Feedback controllers	80	15	7	10	9	1	6	9	2	3	6	8	7
Quaternion Error Control	80	15	8	6	1	12	11	5	9	10	5	9	10
Flexible Control with Output Feedback controllers	1200	60	10	8	8	3	2	4	3	5	4	1	2
Quaternion Error Control	1200	60	2	2	7	6	7	2	12	11	2	4	8
Nonlinear State Observer (2)	1200	60	3	1	3	5	1	1	8	8	3	3	3

*Table 6 Global Rank of the Performance of each Control*

(1). Nonlinear state observer control obtaining data of the angular velocities from a Quaternion Error controller

(2). Nonlinear state observer control having an own calculation of the angular velocities

The ranking effectuated helps to do a fair selection of the most suitable control. There are three different scenarios. The first one is that is desirable to have a quick control. Therefore, the control would have a lower time of convergence of the state variables. The second one is to have a very precise control. In this case, the time of convergence will not have such importance.

It will be only considered the final error at the convergence. The third scenario would be having a low consuming control. Therefore, the required torque will be lower. Finally, considering the three scenarios it will be possible to select the most suitable control as a globally most desirable control.

In terms of the time of convergence, the most suitable control would be the Nonlinear State Observer control having an own calculation of its angular velocities and using gains:  $k_p = 1200, k_{q_e} = 60$ . It has the quickest convergence of the quaternion error and the third position out of twelve options in the quickness of the convergence in the angular velocity response and the modal state variable response. Then the time of convergence of the total velocity of the flexible appendages is not as good as the other variables. However, it is one of the quickest, being the fifth most rapid. Other controls, like the quaternion error control using gains:  $k_p = 1200, k_{q_e} = 60$  have a very fast convergence in the angular velocity and the quaternion error. Nevertheless, the time of convergence of the modal state variable and the total velocity of the flexible appendages is not that low.

In terms of the precision of the control, the most indicated control would be the Flexible Control with Output Feedback Controllers using gains:  $k_p = 1200, k_{q_e} = 60$ . In average has better performance than the other ones. In this case, the selection has been tough because there are other controls, like the Nonlinear State Observer control having an own calculation of its angular velocities and using gains:  $k_p = 1200, k_{q_e} = 60$ , that has also a very low error at the convergence in the angular velocity and the quaternion error. However, a lower error at the convergence of the modal state variable and the total velocity of the flexible appendages is achieved with the Flexible Control with output Feedback Controllers.

In terms of the consumption and torque requirement, clearly the best control would be the Flexible Control with Output Feedback Controllers using gains:  $k_p = 1200, k_{q_e} = 60$ . It is the control that requires less time using the maximum torque and the second best in terms of the torque requiring per second. It is a really low consuming control. It should be noted that the Sliding Mode control has the less torque requiring per second, that is caused because there are many seconds that the control is in off position, not consuming anything. However, the time required using the maximum torque is very high (all the implementation time). This fact shows the unfeasibility of this control, it will cause much consumption during the working life of the spacecraft.

Accordingly, having in mind the three different scenarios previously selected it can be stated that globally the best control for the implementation of a Solar Sail situated in the L1 point would be the Flexible Control with Output Feedback Controllers using gains:  $k_p = 1200, k_{q_e} = 60$ . It is averagely the most precise control and the less consuming control. As the Solar Sail it is situated in the L1 point orbiting around the Sun, there is not a big necessity to do a really fast control because its relative movement with the Sun is very slow. It is more interesting to have a more precise control because an accumulate error in that big amount of time of implementation will cause major problems. Also, as the life time of the Solar Sail is wished to be very large it is desirable to select a low consuming control because then it will lead to a saving in the required reserve of energy and a more efficient spacecraft.

## 10. Conclusions

The Solar Sail is a flexible spacecraft. During this work it has been shown that the effects of the flexibility are not negligible in the implementation of the control of the sail. The precision of the angular velocity decreases and the transient of the angular velocities and the quaternion error to stabilize becomes more abrupt. Therefore, the performed movement to achieve the final stable state is more precipitous. However, the time to stabilize is similar. Hence those results indicate that it is highly desirable to consider the effect of the flexibility in the simulation of the control in order to have a complete knowledge of the movement of the spacecraft to achieve the stabilization and avoid unexpected movements or disturbances appeared during the transient.

Also, during this work it has been intended to quantify the effects of causes the flexibility of the spacecraft in the control. The effects have been quantified as a flexible disturbance. It has been proved that concerning all the controls, the most appropriate to deal with the disturbance is the PD control with a term which considers flexible appendages with output feedback controllers. The main factor that has made this controller the most appropriate is its liability. It assures a final convergence of the angular velocity and the quaternion error. Hence, a final stabilization. Moreover, it works with the modal variables, so it allows to have a more precise knowledge of how the nature and the magnitude of the movement of the flexible appendages interfere in the control of the spacecraft. This knowledge will be very profitable to solve warning situations.

The final objective of this work is to find the most suitable control for the solar sail. To find the most proper control a deep comparison of the performances of all the controls implemented with different gains has been done. There are three important factors that are considered to do the comparison. The time of convergence of the state variables, angular velocity, quaternion error and the modal variables (total velocity of the flexible appendages and modal state variable). The precision of the control. And the consumption of the control.

In terms of the time of convergence of the state variables, the most appropriate control found is the Nonlinear State Observer control having an own calculation of its angular velocities and using gains:  $k_p = 1200$ ,  $k_{q_e} = 60$ . Having the quickest convergence of the quaternion errors and the third quick convergence of the angular velocity and the modal state variable. Then the fifth quickest response regarding the total velocity of the flexible appendages. It is a rapid control. However, due to it is a highly theoretical control it seems difficult to have a real implementation of this control.

In terms of the precision of the control, the most indicated control would be the PD control plus a term which considers flexible appendages with Output Feedback Controllers using gains:  $k_p = 1200$ ,  $k_{q_e} = 60$ . Averagely has better performance than the other ones. Other controls have very low error in a specific state variable. But regarding a global performance and considering all the variables it has the best behaviour.



In terms of the consumption of the control, the most efficient is the PD control plus a term which considers flexible appendages with Output Feedback Controllers using gains:  $k_p = 1200, k_{q_e} = 60$ . It is the control that requires less time using the maximum torque and the second best in terms of the torque requiring per second. It is the best cost effective consuming control from all the controls considered.

Thus, considering all the three factors explained before and focusing in a global performance it can be stated that the most suitable control is the PD control plus a term which considers flexible appendages with Output Feedback Controllers using gains:  $k_p = 1200, k_{q_e} = 60$ . As the solar sail will be placed in the L1 Lagrange point there is not a need to perform a fast control. It is more important to have a precise control, to avoid the accumulate error. Because the time of implementation of the solar sail will be very large and it is not desirable to have accumulate error in a big amount of time because it will rise. Another important factor is related with the implementation time of the spacecraft. The solar sail it designed to have a very long lifetime, therefore it is very interesting to have a low consuming control to avoid a very large reserve or use of energy. Then have a more efficient spacecraft.

This work is wished to be a proper background for future studies. It is important to note that it is achievable to have a most precise model of the spacecraft. Then being able to have a more precise control and have a more complete knowledge of the real movement and attitude of the solar sail. It would be useful to do a thermal study of the structure. And a study of the vibration movements of the flexible appendages that could create possible frequency resonance in the structure. Which could put in danger the solar sail.

## 11. Bibliography

- [1] Full Quaternion Based Attitude Control for a Quadrotor written by Emil Fresk and George Nikolakopoulos in the 2013 European Control Conference (ECC) July 17-19, 2013, Zürich, Switzerland.
- [2] Solar Sail Attitude Control and Dynamics, Part 1 by Bong Wie in the Journal of Guidance, Control and Dynamics. Vol.27, No.4, July-August 2004
- [3] Fault tolerant satellite attitude control using solar radiation pressure based on nonlinear adaptive sliding mode by S.Varma and K.D. Kumar in the Acta Actronautica, Volume 66, Issues 3-4, February-March 2010, Pages 486-500
- [4] Satellite attitude control using solar radiation pressure based on non-linear sliding mode control by T.R. Patel, K.D. Kumar and K. Behdinan written in Proceedings of the Institution of Mechanical Engineers Part G Journal of Aerospace Engineering 222(3):379-392. May 2008.
- [5] AACS Performance and Stability Validation for Large Flexible Solar Sail Spacecraft by Stephanie Thomas, Michael Paluszek, Bong Wie and David Murphy in the 41<sup>st</sup> AIAA/ASME/SAE/ASEE Joint Propulsion Conference & Exhibit 10-13 July 2005, Tucson, Arizona.
- [6] A nonlinear attitude control law for a satellite with flexible appendages by S. Monaco and S. Stornelli in Proceedings of the 24<sup>th</sup> Conference on Decision and Control, Ft. Lauderdale, FL-December 1985.
- [7] Passive Attitude Control of Flexible Spacecraft from Quaternion Measurements by S. Di Gennaro, communicated by M. A. Simaan written in the Journal of Optimization Theory and Applications: Vol. 116, No.1, pp.41-60, January 2003.
- [8] MONACO, S., and STORNELLI, S., *A Nonlinear Attitude Control Law for a Satellite with Flexible Appendages*, 24th Conference on Decision and Control, Ft. Lauderdale, Florida, pp. 1654–1659, 1985.
- [9] MONACO, S., NORMAND-CYROT, D., and STORNELLI, S., *Sampled Nonlinear Control for Large-Angle Maneuvers of Flexible Spacecraft*, Paper ESA SP-255, 2nd International Symposium on Spacecraft Flight Dynamics, Darmstadt, Germany, pp. 31–38, 1986
- [10] DI GENNARO, S., *Output Feedback Stabilization of Flexible Spacecraft*, 35<sup>th</sup> Conference on Decision and Control, Kobe, Japan, pp. 497–502, 1996.
- [11] Spacecraft Attitude Dynamics and Control, Attitude Representation and by James Douglas Biggs. Politecnico di Milano
- [12] Spacecraft Attitude Dynamics and Control, Attitude Kinematics-quaternions and Gibbs Vectors by James Douglas Biggs. Politecnico di Milano
- [13] Spacecraft Attitude Dynamics and Control, Momentum exchange devices by James Douglas Biggs. Politecnico di Milano

[14] Space Vehicles Dynamics and Control (book). AIAA Education Series. Second Edition.  
Written by Bong Wie

## Annex 1: Quaternion Error proportional control using CMG as actuator

This type of control uses a CMG (momentum exchange device) as the generator of the required torque to control the spacecraft. The CMG is a more efficient device than a RW or IW. Then it will be a more efficient control. However, the control algorithms are much more complex. Here there is a light explanation about how this control works and how it is implemented.

The control departs from a generic Quaternion Error control ideal. Then it is constrained by the maximum momentum and torque achievable by the real control device. Then it is implemented the real control law that is the following one:

$$\vec{u} = \dot{A}\vec{h}_r - \vec{\omega} \times A\vec{h}_r \tag{76}$$

-A is a matrix that defines the position of the CMGs respect to a point of reference. That is to say, how the CMGs are positioned in the space.

$-A\vec{h}_r$  corresponds to the angular momentum of the CMGs ( $h_{CMG}$ ).

$-\dot{A}\vec{h}_r$  corresponds to the derivative of the angular momentum of the CMGs ( $\dot{h}_{CMG}$ )

Also it is needed to recall that some configuration of angles between the CMGs have singularities, therefore it is needed to avoid them. For example:

$$[\delta_1 = 90^\circ \delta_2 = 0^\circ \delta_3 = -90^\circ \delta_4 = 0^\circ] \text{ or } [\delta_1 = 90^\circ \delta_2 = 180^\circ \delta_3 = -90^\circ \delta_4 = 0^\circ]$$

Block diagram

The block diagram differs from the two controls previously explained. For a more complete explanation of the implementation it is recommended to visit the bibliography [13].

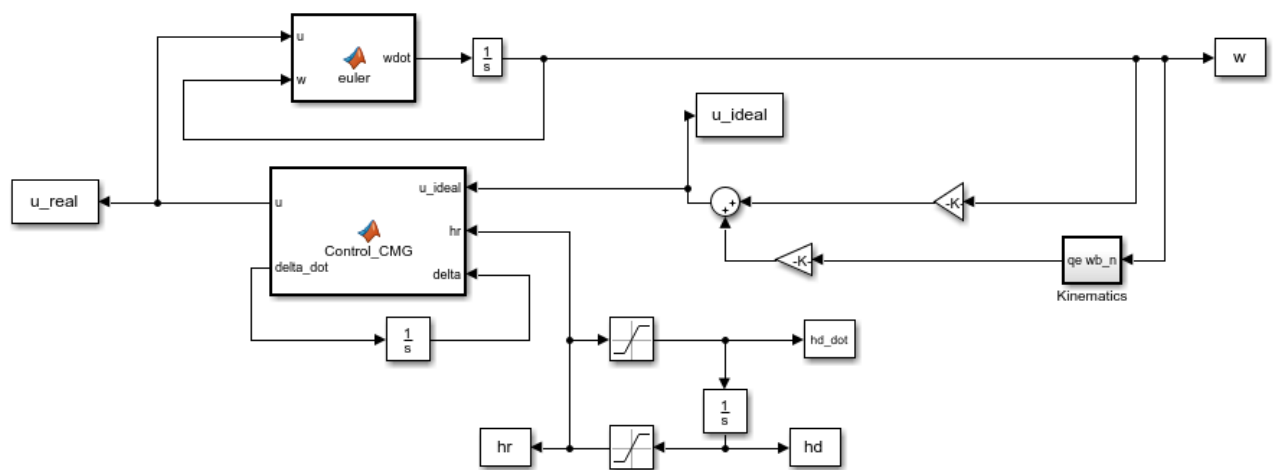


Figure 91 Block diagram of the Quaternion Error proportional control using CMG as actuator

The loop of the two saturation boxes of the lower part of the diagram is the implementation of the constraints to obtain the real values of angular moment.

